AN EXPERIMENTAL INVESTIGATION OF CONVECTIVE FLOWS ASSOCIATED WITH ROOM FIRES

Thesis by

Ernst N. Tangren

In Partial Fulfillment of the Requirements

for the Degree of

Aeronautical Engineer

California Institute of Technology

Pasadena, California

1978

ACKNOWLEDGMENTS

The author wishes to express his gratitude to Professor E. E. Zukoski for his guidance and encouragement during the course of this investigation. The experimental apparatus was developed and initial experiments were conducted by Mr. W. Sargent, whose efforts are gratefully acknowledged. The assistance given by Professor T. Kubota is also deeply appreciated. A word of thanks is owed to Dorothy Eckerman for the expert typing of this thesis.

This work was sponsored by the National Science Foundation and National Bureau of Standards, to whom the author is thankful.

ABSTRACT

This thesis presents an experimental investigation of the fluid dynamic aspects of a room fire and the applicability of a theoretical model. The model, developed by Zukoski, considers a single room containing a point heat source with or without an opening to the outside. For the case of an opening the interest is in the height and density of the ceiling layer of hot air and combustion products. The case without an opening concerns itself with the time required to fill a room with smoke.

Water was used as the fluid medium and a flow of salt brine represented the heat source. The experiments investigated the effects of fire strength, opening geometry, fire location and fire geometry for the open room case. For the closed room the movement of the ceiling layer interface and the general flow field were investigated.

TABLE OF CONTENTS

Section

Acknowledgments
Abstract
Table of Contents
Nomenclature

A. Introduction

B. Open Room Fire Model

C. Open Room Experimental Setup

D. Open Room Experimental Results

1. Fire Strength
2. Opening Geometry
3. Fire Locations
4. Fire Height
5. Fire Geometry
6. 2-Dimensional Room

E. Closed Room Model

F. Closed Room Experimental Setup

G. Closed Room Results

H. Summary and Conclusions

References

Figures

Appendix A

Appendix B

Nomenclature

A	- area
b	- opening span
C_o	- oriface coefficient
C_p	- specific heat capacity
f	- fuel to air ratio
g	- acceleration due to gravity
H	- opening height (fig. 1)
$\mathfrak{L}$	- length of 2-dimensional source
$\dot{m}$	- mass flow rate
p	- pressure
$\dot{Q}$	- rate of heat input
q^*	- dimensionless buoyancy factor, eqn. (4) and (9)
q^*_2	- dimensionless buoyancy factor, eqn. (12)
T	- temperature
$\overline{\Delta T}$	- mass averaged plume temperature difference
$\dot{V}$	- volume flow rate
$\dot{V}_o$	- volume flow rate of brine
Y	- height defined in fig. 1
y	- height above opening sill
y_o	- height defined in fig. 1
Z	- plume height
ρ	- density
$\overline{\Delta\rho}$	- mass averaged plume density difference

Subscripts

1 - fresh air or water

2 - ceiling layer

p - plume

H - quantity evaluated at Z = H

A. INTRODUCTION

In recent years, with the advent of large computers, attempts are being made to model the spread of fire in a burning structure. Until this time, the problem could not be solved due to its complex nature. But now there is the opportunity to utilize the computer to predict fire spread and to develop better ways of controlling it. In the past few years several theoretical models have been developed as elementary building blocks of a solution.

This thesis is a report on an experimental investigation carried out to support the development of two theoretical models. The first model considered concerns a single room with one opening and a point heat source. The second is concerned with a closed room containing a heat source.

Both models were developed at Caltech by Zukoski and are described and analyzed in references (1) and (6). A brief description of these models is included here for completeness.

The experiments were carried out in scale model rooms using water as the fluid medium. A salt brine introduced into the room represents a heat source and the flow field was inverted to account for the sign change in the density difference. This technique was chosen due to the ease of executing these experiments.

The experiments are intended to demonstrate the validity of the model and to test its limits. The main interests of the open room model are the height and density of the ceiling layer

of hot air and combustion products, while the closed room model is concerned with the time required to fill a room with smoke.

The two models and their experimental results are presented separately in this thesis.

B. OPEN ROOM FIRE MODEL

A model of an isolated fire in a room with a single opening was developed by Zukoski (1) and is summarized here for completeness. The elements which make up the model, illustrated in Figure 1, are a turbulent plume of hot gas, a ceiling layer, and a counter current orifice flow through the opening. The principal assumptions for this simple case are:

1) a single point heat source or fire is present in the room;
2) the plume is the only source of mass and energy flow into the ceiling layer;
3) the plume can be described usefully within the small density difference approximation, the Boussinesq approximation;
4) the ceiling layer is a constant density or temperature region;
5) no mixing occurs at the door between inflowing and outflowing streams;
6) the flow out the opening is the only stream carrying mass and energy out of the ceiling layer.

These assumptions appear to be reasonable on the basis of experiments reported later in this paper.

A plume of hot air is formed from the heat source and entrains fresh air as it rises to the ceiling. It has been observed to form a wall jet, after impingement on the ceiling, which spreads to the ceiling-wall corners and is deflected downward. Buoyancy

forces then turn this jet-like flow toward the horizontal direction and the plume axis. This process forms a highly turbulent and well mixed ceiling layer. However, the boundary between the ceiling layer and fresh air is often laminar with an extremely sharp interface.

At the opening to the room, the hot buoyant air flows out in a jet-like manner and is matched by an inflowing jet of fresh air. Both flows are suggestive of weir flow when the flow is steady. When we neglect any fuel flow, continuity arguments show that the plume mass flow is equal to that of the flow in through the opening and to that flowing out from the ceiling layer.

To model the flow through the opening we consider a wall separating two bodies of fluid - that on the right of uniform density, and that on the left separated into two regions of unequal density. Figure 2 illustrates this situation and the resulting pressure difference across the wall. Assuming that the flow through the opening doesn't influence the pressure difference, the flow rates of the two streams are calculated using the idea of orifice flow. The volume flow through an orifice of area dA is:

$$d\dot{V} = C_o \sqrt{\frac{2\Delta P}{\rho}}\, dA \qquad (1)$$

Here, C_o is a constant called the orifice coefficient. Given the conditions in figures 1 and 2 the pressure across the wall is

$$\frac{\Delta P}{\rho} = \frac{\rho_1 - \rho_2}{\rho}\, g\, (y_o - y) \quad \text{for } y > Y \qquad (2a)$$

$$\frac{\Delta P}{\rho} = \frac{\rho_1 - \rho_2}{\rho} g (y_o - Y) \qquad \text{for } y < Y \tag{2b}$$

The notation is illustrated in Figures 1 and 2. Note that $\Delta P \equiv 0$ at $y = y_o$. We can now carry out an integral of the velocity over the area of the opening using equations (1) and (2), to get an equation for volume fluxes:

$$V_1 = \left[C_{o1} \frac{2}{3} \sqrt{2} \right] \sqrt{\frac{\rho_1 - \rho_2}{\rho_1} g} (y_o - Y) (y_o + Y/2) b \tag{3a}$$

when $Y \geq 0$

$$V_1 = \left[C_{o1} \frac{2\sqrt{2}}{3} \right] \sqrt{\frac{\rho_1 - \rho_2}{\rho_1} g} (y_o)^{3/2} b \tag{3b}$$

when $Y \leq 0$

and

$$V_2 = \left(C_{o_2} \frac{2\sqrt{2}}{3} \right) \sqrt{\frac{\rho_o - \rho_2}{\rho_2} g} (H - y_o)^{3/2} b. \tag{3c}$$

The C_o's are flow coefficients with values near 0.6.

The flow of a buoyant plume has been the subject of a large number of studies, and is well understood in the Boussinesq limit, e.g. (2). The results of Yokoi's investigation (3) have been used by Zukoski (1) to characterize the plume in this case. He has expressed the plume results for Boussinesq case of very small density differences in terms of a nondimensional heat input parameter:

$$q^* = Q / (\rho_1 C_p T_1 \sqrt{g Z} \quad Z^2) \tag{4}$$

Using the values of several constants taken from the work of Yokoi (3) one gets for the mass averaged temperature and mass flow:

$$\frac{\overline{\Delta T}}{T_1} = \frac{\overline{\Delta \rho}}{\rho_1} = 5.26 (q^*)^{2/3} \tag{5}$$

$$m_p = \rho_1 \sqrt{g \frac{\overline{\Delta\rho}}{\rho_1}}\, 0.08056\ Z^{5/2} . \qquad (6)$$

These assume the density differences are small and the elevation above the fire is large compared to the fire diameter. We have the conservation laws of mass and energy:

$$m_p = m_1 \text{ and } m_1 = m_2 \qquad (7a, b)$$

$$m_p C_p \overline{\Delta T} = Q \qquad (8)$$

and if we assume the mass averaged plume flow temperature is equal to the ceiling temperature:

$$\overline{\Delta T} = \left(T_2 - T_1\right) \qquad (9)$$

Neglecting the difference between ρ_1 and ρ_2 which would appear in the denominator of the square root terms of equations (3), a Bousinesq approximation for the door flow, the following solution is formed from the above equations:

$$\frac{H}{y_o} = 1 + B\left(1 - \frac{Y}{y_o}\right)^{\frac{1}{3}} \left(1 + \frac{1}{2}\frac{Y}{y_o}\right)^{\frac{2}{3}} \quad \text{when } Y > 0 \qquad (10a)$$

$$\frac{H}{y_o} = 1 + B \quad \text{when } Y < 0 \qquad (10b)$$

$$\frac{Y}{H} = A(1 - y_o/H)^{3/5} - L/H \qquad (11)$$

where

$$A \approx 2.14\ (b/H)^{2/5} ,$$

$$B = \left[\frac{C_{o_1}}{C_{o_2}}\right]^{2/3} .$$

These equations can easily be solved by graphical or iterative methods.

The above equations lead to several conclusions con-

cerning the height and density of the ceiling layer. The ceiling layer height is a function of the opening geometry and the fire geometry. For the Boussinesq approximations used here the height does not depend on the fire strength; the ceiling layer density depends on the interface height, fire strength and the fire geometry.

The interface height is a complicated function of the sill height, soffit height (height to the top of the opening), and opening width. Generally the interface will go down as the door narrows or window area decreases. For the case of a rather small window, the interface may be below the level of the sill.

Although the model assumes a point fire source, the effect of the fire geometry on the interface height can be determined by modifying the equations for the plume. It is most easily demonstrated by comparison between a single fire source and two half strength fire sources. The development leading to equations (10) and (11) is only changed by the multiplication of the constant A by a factor $(0.5)^{2/5}$, 0.76. For a doorway with A = 1 and B = 1, Y/H is reduced from 0.55 to 0.47.

The geometry of the room opening directly influences the interface height which, in turn, influences the density or temperature of the ceiling layer. A change in the interface height will change the length of the plume and its corresponding

entrainment flow rate. The density difference of the ceiling layer decreases as 5/3 power of the interface layer height.

The only effect of the fire strength is on the density or temperature of the ceiling layer. The density difference increases as 2/3 power of the heat input.

The sensitivity of the calculated values of ceiling layer interface height and density difference ratio, $(\rho_2 - \rho_1) / \rho_1$, to changes in entrainment rate is shown in Figure 3. This calculation has been carried out for a room that is H high, with a door opening which is 0.813H by 0.375H wide and with $q^* = 10^{-5}$. Note that both parameters decrease as the rate of entrainment is increased. The density decrease is a result of the increase in dilution which overpowers the effect of the decreased ceiling layer height (which increases the density ratio by decreasing the area available for entrainment). The ceiling layer interface height decreases because an increase in area is required to drive the larger flow rate of ceiling layer gas through the door.

Variation in density ratio and layer height corresponding to $\pm 20\%$ changes in entrainment are shown below in Table 1.

Table 1

Entrainment Rate, Fraction of Standard	Y/H	$\frac{\rho_2 - \rho_1}{\rho_1}$
1.20	.554	.00545
1.00	.585	.00604
0.80	.617	.00690

Note that $\pm$ 20% change in entrainment rate produces about $\pm$ 10% change in density ratio and $\pm$ 5% change in interface height. These variations are greater than the experimental accuracies with which these parameters can be determined in the experimental work. In addition, for experiments in which the plume is undisturbed by interaction with walls or the door jet and in which no mixing occurred in the doorway, the agreement between predicted and experimentally observed values of ceiling layer interface height and density difference was within the bounds given above. Hence, we conclude that the proposed value of entrainment used in the present calculations (without origin shifts) is satisfactory for small fires (the Boussinesq approximation) of small geometrical extent, i. e. (fire diameter) << (ceiling layer height).

The dependence interface height and density of ceiling layer on flow coefficients is shown in Figure 4 and Table II for a number of examples. The door geometry and fire size or q^* values are the same as used above. If the coefficients are of equal value, the interface height Y, increases slowly and density difference decreases slowly as flow coefficients increase. If the coefficients are increased from 0.6 to 0.8, interface height increases by about 5% and density ratio decreases by about 8%. When the coefficients are different (see last two columns of Table II) the biggest changes occur when the cold side coefficient is changed.

For this door opening and q^* value, the effect of changing flow coefficients from 0.60 to 0.80 is just within our capabilities

of observing and hence we cannot distinguish values in range .6 to .7.

Simulation by Salt Water

The usefulness of the salt water modeling technique is critically dependent on the manner in which viscous and buoyancy effects on the flow field are modeled. One measure of the accuracy of the modeling of viscous effects is given by comparing the Reynolds number of a full scale flow with that of the corresponding model flow. Similarly the relative influence of buoyancy and dynamic effects must be compared for the ceiling layer flow and for flow through openings. A Froude or Richardson number will be used to compare the influence of these parameters. Finally, the fire-room flow model indicates that the heat input rate itself will influence the steady state and transient flow fields. The pertinent parameter here is the dimensionless heat input parameter, q^*.

The effects of these parameters and the degree of similarity achieved in the salt water model experiments is discussed in the following paragraphs.

Heat Input (Buoyancy Flux) Parameter

The parameter used to model the heat input rate, q^*, appears in the description of the buoyant plume. The parameter is defined by equation (4) for $Z = H$, the room height:

$$q_H^* = Q/\rho_\infty \sqrt{gH}\, Cp\, T_\infty H^2$$

When salt water is used to model the fire, this parameter is defined by equation (12):

$$q_H^* = \Delta\rho_o V_o / (\rho_1 \sqrt{gH} H^2) \quad (12)$$

Here:

$\Delta\rho$ = initial difference in density between brine and water.

V_o = brine volumetric flow rate

ρ_1 = undisturbed water density.

The influence of q_H^* on density in the ceiling layer and height of ceiling layer interface was calculated by the model described above but without assuming that $\rho_2/\rho_1 = 1.0$. The plume calculation was left as before. The results are shown in Figure 5 for the range, $10^{-5} \leq q_H^* \leq 3 \times 10^{-2}$. The most important effect of q_H^* is the change in the density of the ceiling layer fluid: At low q_H^* values, the ratio of ceiling layer density, ρ_2, to ambient density ρ_1 is very close to one. As q_H^* values increase, this ratio decreases, becomes appreciably less than one around $q_H^* = 10^{-2}$ and decreases rapidly for higher values of q_H^*. In the latter regime, the height of ceiling layer also decreases rapidly. Clearly, the value of q_H^* is very important in determining the height of the ceiling layer when $q_H^* > 10^{-2}$ and it is always important in fixing the density of the ceiling layer and the density difference ratio $(\rho_1 - \rho_2)/\rho_1$.

Values of q_H^* corresponding to a number of situations are shown in Table III. Example A corresponds to a fire in a 2.5m high room; fires with a 100 kw and a 100 w heat input rate are considered. The larger fire has a q^* value of 10^{-2} and the smaller, a value of 10^{-5}. Example B corresponds to a half

scale model with heat input rates picked to give the same q_H^* values. Example C corresponds to the salt water model tests with a salt water flow of 0.1 to 0.4 l/sec at a density difference ratio of $\Delta\rho/\rho_1 = 0.05$. For the water case q_H^* values are about 10^{-5}. Clearly, then, the salt water models can give exact q_H^* modeling of very small fires but cannot be used to give precise results for large fires. However (note from Figure 5) ceiling layer heights will be accurately modeled up to $q_H^* \approx 10^{-3}$.

Reynolds Number

In order to assess the effects of viscosity we must select a characteristic velocity and scale for the flow. We have chosen to use the properties on the centerline of a free buoyant plume at an elevation corresponding to the ceiling height. The rationale for this decision is our belief that other densities and velocities within the room will be proportioned to the values in the plume. The dependence of plume velocity and density on scale, and heat input rate is presented in Appendix A, taken from (3) and the corresponding Reynolds number dependence is:

$$Re^* = \frac{\rho_1 W_m H}{\mu_1} = \left(\rho_1 \frac{\sqrt{gH}\, H}{\mu_1}\right)\left(C_v C_1 (q^*)^{1/3}\right)$$

The velocity on plume axis at height H is W_m. μ_1 is the undisturbed gas viscosity, and the other parameters are as defined above. Note that Re^* depends weakly on q^* and more strongly on room scale, H.

Values of Reynolds numbers for the three examples

discussed above are shown in Table III. Again exact similitude for the small, full scale fire ($q_H^* = 10^{-5}$) can be achieved and the difference in Re^* between salt water modeling ($Re^* = 1.8 \times 10^4$) and large full scale fire ($Re^* = 8 \times 10^4$) is probably not large enough to cause important differences.

A Reynolds number computed for flow through the door will be proportional to Re^* and hence will scale between the various examples as Re^*.

Buoyancy

We again use W_m, the velocity on the centerline of a buoyant plume, and $\Delta\rho_m$ the maximum density difference in the plume to examine buoyancy effects. If we compare $\frac{1}{2}\rho_1 W_m^2$, a characteristic dynamic pressure, with ($\Delta\rho_m gH$) a characteristic buoyant pressure, we get a Richardson number parameter:

$$Ri^* = \frac{\frac{1}{2}\rho_1 W_m^2}{\Delta\rho_m gH} = \frac{1}{2}\frac{Cv}{C_\ell} \qquad (15)$$

Here Cv and C_ℓ are constants (see Appendix A) and hence, this ratio is independent of heat input rate and scale. Thus, as far as the ceiling layer is concerned, buoyancy effects should be scaled exactly in the salt water model.

In a doorway flow, buoyancy can affect the stability of the shear flow set up between the inflowing and outflowing streams. Although we may expect that velocity gradients will be similar in the full scale and model cases (because of Reynolds number similarity) density gradients may depend strongly on the Prandtl

number. The Prandtl number for air is about 0.7 and for water is about 10. Hence, we would expect that the gradient Richardson number would not scale in the same manner. Thus, the stability of the shear layers may not be the same for model and full scale examples.

Heat Transfer

The density of gas in the ceiling layer is affected when heat is transferred from ceiling layer gas to the walls or floor. In a fire situation up to 25% of the enthalpy flux in the plume can be transferred from the ceiling layer gas by conduction and radiation. In addition to changing the density and hence the buoyancy of ceiling layer gas, this process will generate a source of gas at an intermediate density in the thermal boundary layers over the surfaces of the walls and ceiling. This intermediate density gas may flow down to the interface between the ceiling layer and cool air and cause this interface to thicken greatly. Thus heat transfer can have several effects which cannot be produced in the salt water model.

Summary

The salt water experiments can produce exact Reynolds and Richardson number scaling for small room fires. For this example, q_H^* scaling is possible and the primary failure of the model concerns heat transfer effects. Failure to scale large fires, i.e., high q_H^* values, lies in effect of q_H^* on ceiling layer density. Reynolds number and Richardson number effects can still be

simulated properly, but the density changes cannot. In addition, heat transfer effects are still omitted in this case.

C. OPEN ROOM EXPERIMENTAL SETUP

To test the model, small scale tests were performed using water as the fluid medium. A flow of salt brine was used as the heat source and the flow field was inverted to account for the sign of the density difference. The dimensionless buoyancy factor and predicted ceiling layer density were modified to fit this situation:

$$q^* = \frac{\Delta\rho}{\rho_1} \frac{V_o}{\sqrt{g Z} Z^2} \tag{12}$$

$$\overline{\frac{\Delta\rho}{\rho_1}} = 5.26 \, (q^*)^{2/3} \tag{13}$$

The experimental set up is shown in Figure 6. It consisted of a rectangular transparent tank 235 x 115 x 60 cm partitioned on the inside by plexiglass walls. The room occupied approximately half the tank while the other half simulated an infinite reservoir of fresh water.

A fresh water flow of~2.4 ℓ/s entered through a sponge to enter the area outside the "room." The boxes and sponge were found to be necessary to produce a uniform flow. Several siphons located underneath the sponge carried off the brine once it left the room. A skimmer was used to maintain a constant water level.

Two basic overall room geometries were used. For most of the experiments the scale model room measured 100 x 50 x 50 cm with a door 41 x 19 cm. In a few experiments the room

measured 130 x 108 x 50 cm with a door 27 x 38 cm. In both cases the door was centered in the narrow wall with the fresh water supply in the area "outside the door." Pieces of plexiglass were used to block areas of the doorway to create the desired opening geometry.

The brine was introduced into the room through an inlet constructed to produce the desired source. Three different brine inlets were used in the experiments. One was a simple 2" PVC pipe which produced a 4.8 cm diameter round source. The second and most commonly used inlet was constructed such that its outlet geometry could be easily changed. It consisted of a 10 cm diameter chamber 38 cm high. The bottom, which was submerged about 1.5 cm below the water level, could be changed to produce any orifice geometry up to 10 cm diameter. For the experiments with a line fire, an inlet was constructed to produce a line source 0.038 cm wide and 50 cm long. The brine was stored in a 500 gallon tank and was supplied to the brine inlet through a constant head tank and rotometer type flow meter. Typically, the brine flow rates were between .03 and .25 liters per second.

Density of the salt-water mixture is a function of salt concentration and temperature. Measurements were made of the temperature by the use of thermocouples and of the salt concentration by use of conductivity probes. The density was computed from tabular listings of density as a function

of salinity and temperature.

Both the thermocouple and conductivity probes could be traversed throughout the tank and time dependent density profiles were measured throughout the room. However, those presented here were obtained in regions free from major disturbances such as the plume and the door.

The conductivity probe consisted of two short (1.5 mm) platinum wires supported close (1 mm) together. The impedance between these wires was a function of the salinity and was measured by a Sanborn carrier amplifier and demodulator, a system similar to that used with strain gauges. Before each experiment the conductivity probe was cleaned, recoated with an oxide of platinum, and calibrated by use of solutions of known salt concentration.

All measurements in the open room experiments were made at least 15 minutes after the start of the tests to insure that a steady flow had been established.

D. OPEN ROOM EXPERIMENTAL RESULTS

A large number of experiments were conducted and the flow fields in many different configurations were examined. In this section we will discuss in depth a typical experiment in which the configuration is identical to that assumed by the theoretical model. This discussion will demonstrate the agreement between the theory and experiments, and will also aid the reader in understanding and interpreting other results presented in this thesis.

For this particular experiment the room measured 50 x 100 x 50 cm deep; the door was 18.8 x 41.7 cm high; and the brine inlet used was the 2" PVC pipe. The nozzle was located 75 cm from the door and was centered between the side walls. The rest of the details are noted below:

Flow rate: 0.119 litre/s; ρ_{brine}: 1.048

ρ_1: 0.99884; ceiling layer density; 1.0049.

Door jet flow rate, in: 1.1 ℓ/s, out: 1.2 ℓ/s.

Figures 7 and 8 illustrate the flow field for this particular experiment and this flow field is representative of that observed in most of the experiments. The photograph was produced by adding aluminum dust to the brine and illuminating it from the side with a thin slit of light.

The dense brine in the plume sinks to the bottom and in this process entrains a flow of fresh water which is about 10 times larger than the brine flow. After impinging on the bottom

this plume flow spreads out to the wall-bottom corners, turns up at the corners, and flows back towards the plume. This process produces a turbulent well mixed "ceiling layer" as demonstrated in the photograph.

Fluid from the dense ceiling layer flows out the door and the pressure field set up by the stratification within the room produces a corresponding inflowing jet of fresh water at the door. As the flow in the ceiling layer leaves the area near the plume the turbulence tends to dampen out. Note that there is no visual evidence for mixing across the interface.

The inflowing stream at the door produces a well defined door jet which blows against the plume, and causes the plume to bend back and mix more vigorously with fresh water. The plume-doorjet interaction was not significant except for a few cases which are discussed later. The door jet also set up circulation in the separated regions near the corners next to the door but this flow was never observed to cause any significant disturbance.

Figure 9 shows a density profile for this typical experiment. Our main interest lies in the height of the interface between ceiling layer and fresh water and in the density difference between the fluid in these regions. Note that the vertical direction has been inverted such that the ceiling layer will be on top, the normal situation in a fire. This and all later density profiles are plotted as a density difference (density of fluid minus fresh water density) normalized by the

predicted density difference for the ceiling layer based on the theoretical model. Thus on the plots presented here, fresh water will appear as zero and a density difference equal to that predicted will be shown as one. Predicted values are shown as a solid line. The height was scaled as a fraction of the total room height. (Predicted values of the density difference are listed on each figure so that absolute values can be calculated if needed.)

One can recognize from this density profile that the experimental data were accurately predicted by the model for this example. Both the ceiling layer interface height and density difference agree well with the theoretical values.

From this example it appears that the assumptions made in the development of the theoretical model are valid in this experiment. These include the assumptions that:

1) The brine source diameter is small compared to the room height and can be considered a point source.
2) There is no mixing along the ceiling layer interface so the plume is the only source of mass flow into the ceiling layer.
3) The density difference is small everywhere so the Boussinesq approximation does hold.
4) The ceiling layer is well mixed and is a region of constant density.
5) Except for a few cases which will be noted later, there

is no mixing between the incoming and outflowing streams at the opening.

6) The only stream carrying mass out of the ceiling layer is that going out the opening.

The good agreement between the predictions derived from the model and experimental results indicates that the two layer model is a useful tool when these assumptions are satisfied. We are interested in examining the accuracy of the model with regard to several parameters contained in the theory and also want to determine the effects of violating several of these assumptions.

The effects of the following parameters on the flow field inside a room with a single opening to "fresh air" were investigated experimentally:

1) Fire Strength
2) Opening Geometry
3) Fire Location
4) Fire Height
5) Fire Geometry
6) Two-Dimensional Geometry

Experiments made to determine the effects of these parameters are discussed below.

1) Fire Strength

There were two series of tests performed to examine the effects of fire strength. One series had a 2" diameter source and the other had a 1" diameter source. The results are shown

in Figures 10 and 11.

The fire strength was varied by a change in the brine flow rate and in one of the 2" diameter tests, the brine density. Values of q^* (for Z = Y) covered the range, 1/2 to 5 x 10^{-5}. Data agree reasonably well with model predictions except for the two lowest flow rates in the 2" tests and the two high flow rates in the 1" tests. For the 2" case the flow is so weak that at the lower flow rates the inlet pipe is not fully filled with brine and additional mixing occurs within the inlet. For the 1" case the plume at the higher flow rates has a significant amount of momentum due to the high velocity. This changes the plume characteristics from that of a pure buoyant plume. A discussion concerning this aspect will be found later when the plume geometry is analyzed.

Other than the discrepancy pointed out above, the model does accurately predict both the ceiling layer height and density, and these series of tests confirm the fact that ceiling layer height is independent of the fire strength.

2) Opening Geometry

Door Width: The first geometric effect to be investigated was that of the opening height to width ratio and three fully open doors of various widths were tested. The density profiles are shown in Figure 12. In each case the ceiling layer density and height followed the theory with reasonable accuracy. As expected, the interface level went down as the door was

narrowed.

Door Interference: In the model we assume that all openings are simple openings in a plane wall. If we consider a doorway with a partially opened door, we would expect that the door will have an effect beyond that produced by reducing the open area because the door will also change the direction of the inlet jet. To investigate this case, we studied the effect of a door-like opening with a door opened outward at a 30° angle. (An angle of 0° corresponds to a closed door.) These data are also shown on Figure 12. In addition, the flow field of the fresh water for this case is shown in Figure 13. A strong door jet enters at a large angle, and after impinging against the side wall, flows down the side of the room. This causes the fresh water to mix with the ceiling layer. The entire room has a large scale swirl which breaks down the sharp interface and affects the plume entrainment. The ceiling layer falls from the predicted 57% down to 40% of the room height and the ceiling layer density difference is about 90% of the predicted value.

Clearly a strong swirl can have an appreciable effect on entrainment of the plume and a partially open door can produce such a swirl.

Mixing in the Opening: For a given inflow rate, the velocity of the flow through a small window is high due to the smaller area of the opening. Considerable mixing can take

place in the window under these conditions and this added source of entrainment is not covered in the model.

The conditions under which mixing in the doorway occurs have not been well established in the present studies. However, mixing of this type was always observed when the ceiling layer interface lay below the sill of the opening. To illustrate this phenomenon consider the data taken from the most severe window test, i.e., the smallest window, presented in the sketch of the flow field of Figure 14 and several density profiles of Figure 15. The circular data points were obtained by a probe located close to the window. The neutral buoyancy point in the window is close to 0.53H at which the density decreases rapidly. The density at this location rises again at about 0.4H as the probe moves below the window sill (see dotted line on Figure 14) and falls again as the interface is passed. For this example, mixing in the window is large enough to cause the density in the entire region below the interface to be contaminated. In this example the density change in this region is about 12% of that in the ceiling layer. The second profile, square points in Figure 14 and 15, was taken away from the window and shows the usual profile shape. Note close agreement of two profiles for $Y > 0.6H$ and for $Y < 0.35H$. Therefore the portion of the room normally containing fresh water now contains water contaminated by the salt water ceiling layer.

Window Openings: Density profiles for experiments with windows of the same width but varying height are compared in

Figure 16. In these tests, a door-like opening is progressively closed off from its bottom to form window-like openings with decreasing area. Because the plume entrainment does not similarly decrease, the inflow velocity must also increase to supply the required plume mass flow ratio. The largest window is predicted accurately by the model but the other two cases deviate from the model due to the door-jet mixing discussed above. The ceiling layer rises and the density difference decreases as the window becomes larger, as predicted in the theory. Clearly, effects of mixing in the door must be modeled when interface height approaches the sill of the opening.

3) Fire Location

The model does not take into account the location of the fire in the room. The effect of fire location was experimentally determined to have no effect except when the plume was influenced by the door jet or a wall.

Fire-Door Interaction: When the door jet blew strongly on the plume, it produced a region of mixing in the wake behind the plume, and increased the plume entrainment. This effect is illustrated in Figure 17 where the density profiles for different fire locations are shown. This blowing effect was most marked when the fire was near the door and was particularly marked when plume was in the mixing region in the corner next to the door. See sketch of Figure17. In this case, the door jet-plume interaction caused a large scale swirl around the plume and

greatly enhanced entrainment, the flow field is shown in the sketched Figure 18. This process caused the ceiling layer density difference to decrease, and broke up the sharp interface.

Fire-Wall Interaction: When the fire is placed near a wall or corner the plume will attach itself to the wall(s). This reduces the entrainment rate of the plume and raises the ceiling layer. Figure 19 compares the density profiles for our standard case with those of both a wall and corner fire. For both the wall and corner fires the density difference increased greatly and the interface, was higher. This is apparently due to greatly reduced entrainment as a result of wall interaction. However, it has been found that the model can still give us accurate predictions in these cases. The plume in the corner can be thought of as one quarter of a plume, four times as strong, placed in a room four times as large and with four doors (see Figure 20). Likewise, a wall plume can be thought of as half a plume, twice as strong. Figure 20 illustrates this idea of plume reflectivity about the wall or walls in order to account for the wall effects. Note that the opening is also reflected. If we multiply the fire strength and opening span by four for a corner fire and two for a wall fire and also increase opening area by the same factors, the model gives a good prediction for density difference and interface height. This comparison is shown in Figure 21. This result indicates that entrainment on the unobstructed surface of the plume is not strongly affected by the wall. This is an interesting

result which is not reproduced for the line fire discussed later.

Wall interference effects can be very large. Note, in Figure 19, that ceiling layer density difference can be increased by a factor of 2 and interface height by a factor of 1.1 when the "fire" is moved from the center of the room into a corner. This effect is the most significant observed result of fire location.

4) Fire Height

The vertical location of the fire will have a major consequence due to its effect on the length of the plume below the ceiling layer and hence on entrainment. A fire close to the ceiling will have a short plume, small entrainment rate and will produce a dense and thin ceiling layer.

To verify the effects, tests were made in which the brine inlet was lowered into the tank. Figure 22 shows three tests in which the fire was on the floor, 1/4 the total room height above the floor, and halfway between the floor and ceiling. In all cases the model accurately predicted both the ceiling layer height and density difference. However, in an actual fire situation the model may be less accurate for such cases due to the failure of the far field approximations made in the plume model. We expect that the entrainment model will become much less accurate as the level of the fire approaches the interface.

5) Fire Geometry

A series of tests were performed in which the effect of fire geometry on the ceiling layer was investigated. These tests

were designed to analyze two different effects. The first effect concerned the source momentum. In an actual fire situation the plume is purely buoyant without any initial momentum. Because brine is being added in these experiments, the source will always have an initial velocity. Tests were done to measure the signif - icance of this effect. The second effect concerned the cross-sectional shape of the source. It is obvious that the relative surface area of the plume is an important factor in fixing the entrainment rate, so several rectangular sources of various aspect ratios were tested.

Source Momentum: As noted above the effect of initial momentum in the plume can have a significant effect on the entrainment rate. To analyze this effect, consider the non-dimensional parameter F which is the ratio of the momentum flux per unit area to the pressure produced by buoyancy effects over a depth equal to the nozzle diameter:

$$F = \frac{\rho_b V_o^2}{2\Delta\rho_o g d} \tag{17}$$

Here ρ_b is brine density, $\Delta\rho_o$ is the difference between the density of the injected brine and fresh water, V_o is the initial plume velocity at the inlet, and d the diameter of the brine inlet. For the majority of the experiments F = 0.50 and only in a few cases it was as high as 1.0. Although it is felt that this is sufficiently small, tests were made with high initial plume velocity to verify this assumption.

As mentioned before in the section of this thesis concerning fire strength, tests were made with a 1" diameter source and compared with the usual 2" diameter source. This smaller opening results in F = 4.0. Figure 23 compares the data for the two cases. For the higher plume momentum the ceiling layer has risen slightly and the density is 15% larger. If this difference is due totally to changes in F, the small change in ceiling layer parameter suggests that momentum effects are not large for $F < 1$. The change is in agreement with other experimental results which indicate that the entrainment rate of a buoyant plume is larger than that in a jet.

Cross-Sectional Shape: In this series of tests, rectangular nozzles of aspect ratios 2:1 and 5:1 and of the same area as the 2" source (and hence the same F) were compared to the axisymmetric case. Figure 24 shows the data for these cases.

The ceiling layer height for the 2:1 case was within .05H of the value predicted for an axisymmetric nozzle and the density difference was 15% low. This increase in entrainment was expected due to the larger surface area of the rectangular plume.

The orientation of the 5:1 rectangle was found to be of some importance. When its major axis was perpendicular to the door jet, the jet blew against it and greatly enhanced the entrainment. See sketch below. A similar effect was observed when the nozzle axis was parallel to the door jet but its magnitude was reduced. Compared to an axisymmetric plume, the 5:1 parallel-

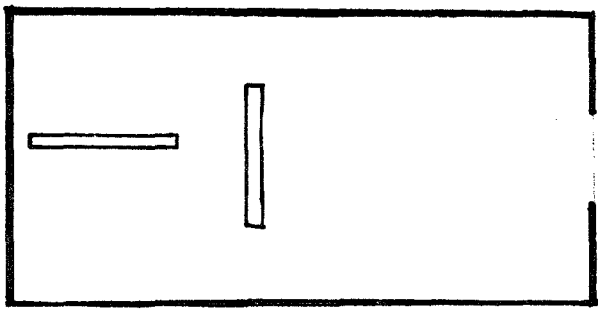

perpendicular

to the door jet had a ceiling layer density difference 20% below the value for the axisymmetric case and when this nozzle was orientated perpendicular to the door jet, the difference was 40%. In both cases of the 5:1 rectangle, the ceiling layer was substantially lower.

Yokoi (3) has also studied the two dimensional line fire and Zukoski (1) has put his results in a form convenient for use here. Those results have been used to analyze this 5:1 rectangle. The line plume is characterized by the following equations:

$$\dot{m}_p = \rho_1 \sqrt{\frac{\Delta P}{\rho_1}}\, g(0.3604)\ (Z^{3/2}\ \mathcal{L}) \tag{18}$$

$$\frac{\Delta T}{T_1} = 1.975\ (q^*_2)^{2/3} \tag{19}$$

$$q^*_2 = \frac{\Delta\rho}{\rho_o}\ \frac{V}{\sqrt{g\mathcal{L}}\ z\mathcal{L}} \tag{20}$$

In Figure 25 the data for the 5:1 rectangle are compared to this line fire theory. When the nozzle was parallel to the door jet (minimized interaction between plume and door jet) the data fit the theory very well. However, agreement is poor for the case with the strong plume-door jet interaction. Evident

from a simple circular nozzle to rectangular nozzles of aspect ratio 2:1 will not greatly affect entrainment rates. However, changes produced in going to 5:1 aspect ratio can not be ignored.

Line Fire: Several tests were done with a line fire (50 cm long and with an aspect ratio of 1400) which could span the entire room, and hence was a better model for the 2-dimensional plume described above. This line fire was tested in three positions: A. spanning the center of the tank; B. placed against the wall opposite the door; and C. in the center of the room such that fresh water could reach both sides. See sketch below.

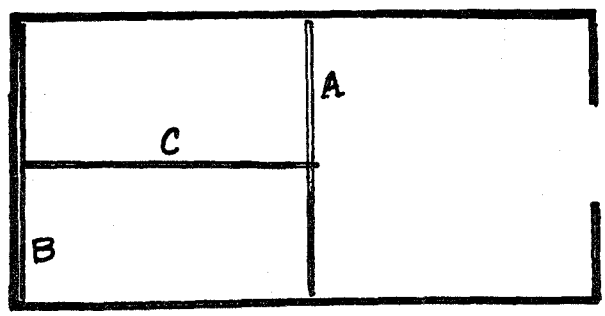

Figure 26 shows the data for the above three cases and a sketch of the flow field for case A is shown in Figure 27. In each case the data were taken between the plume and the door. A profile taken behind the plume showed that this was a region of constant density. In this example, case A, the flow field is very different from the one depicted for the model. The door jet was strong and entrained ceiling layer fluid along the ceiling layer interface from the plume to the door. Large waves such as those depicted in Figure 27 were observed on the interface. The plume

was blown back strongly by the door jet and entrained fresh water only on the side facing the door. Considering this complex flow field, it is probably fortuitous that the ceiling layer density profile shown in Figure 26 is still close to the predicted values.

For case C, the test in which the line fire was put in the center of the room, the source was placed parallel with the long (100 cm) direction of the room. This source was as long as the room width (50 cm) and thus reached from the back wall to the center of the room. Hence it was not a true 2-dimensional flow. This configuration reduced greatly the door jet effect and the plume was able to entrain fresh water on both sides. Agreement between the data for this case, which follows the assumptions of the model more closely, is shown in Figure 26 and it is a reasonably good agreement with model predictions. The ceiling layer was somewhat higher and much more diffuse, and the density difference was 10% more than predicted.

When the line fire was placed against the back wall, the flow field was similar to that assumed for the model except that the plume can entrain fresh water on only one side and was itself strongly influenced by the wall. The data are shown in Figure 26 The ceiling layer was very high and the density difference 50% larger than expected from the simple line fire model.

Figure 28 shows the data replotted for the cases in which the line fire spanned the center and for the line fire against the back wall. In this figure the two cases are compared to a theory

similar to the one employed for an axisymmetric plume on a wall (and discussed earlier in this thesis). The plume is thought of as half a plume in a room twice as large. This worked well for the axisymmetric plume but doesn't for this two-dimensional case. This negative result was expected because the two-dimensional plume attached to a wall has been shown to entrain substantially less than half that entrained for an unconfined plume of twice the buoyancy. See reference (4) for example.

Distributed source: A test was made in which the source was composed of many small holes over a 4" diameter area. The total area of these small sources equaled the same area as the 2" diameter source used in the other tests and thus had the same momentum flux.

A large swirl in the tank dominated the flow in these tests which complicates the analysis due to both effects taking place.

The data for this case are shown in Figure 29. The ceiling layer density difference is about 20% lower and the interface is low by about 10% of the total room height.

Figure 30 illustrates the general shape of the plume. It initially necks down as each individual plume entrains the surrounding fluid. After the individual sources joined together the plume then acted as a single source and spread as expected.

The interpretation of these experiments was complicated by the presence of swirl in the room. In addition, for this example, the ceiling layer interface height to source diameter ratio was only

about $2\frac{1}{2}$. Hence, all three effects - distributed source, swirl in the room and small height to source diameter - probably contribute to the observed increase in entrainment. More work on this type of source is needed.

6) Two-Dimensional Room

The fire research group at the University of Notre Dame, under the guidance of K. T. Yang and J. R. Lloyd, is in the process of developing a finite-difference calculation procedure to predict the fire and smoke spread in a situation similar to that investigated in this thesis Ref. (5). The calculation is much more elaborate using a set of first-principle differential field equations with several approximations to model turbulent flow.

Preliminary results have been published for a two-dimensional room case in which the fire is near the wall opposite the door. Since the room geometry could be easily changed in the experimental apparatus, a test was made which matches their configurations. A full width line fire was placed in the room and the opening widened to the full width.

Figures 31 and 32 show the data for the two-dimensional configuration compared to the theory presented in this thesis for a line source. The experiments in Figure 31 are for a case in which the door height hasn't been changed from the previous experiments, and Figure 32 is a case in which the door is half as tall as the total room height. The Notre Dame results are for a configuration like the latter case where the door is half the room height. Each

figure shows a case for the fire spanning the center and a case with the fire against the back wall.

As with the line fire results reported earlier, the data do agree surprisingly well with the theory even though the flow field doesn't follow the assumptions. For the standard door height and fire in the center, the ceiling layer height is a little high and the density difference almost exactly as predicted. For the door half as high and the fire in the center, both the ceiling layer height and density difference are accurately predicted. In both cases of the fire against the back wall the ceiling layer height is much higher and the density difference 50% and 70% stronger. This may be caused by a reduction in entrainment of the plume due to interaction with the wall.

These results cannot be directly compared to the Notre Dame results because their theory takes into account the heat transfer effects and they did not publish any numerical data regarding the temperature or density. But as a rough comparison the published results show a ceiling layer height between 25% and 30% of the room height and the test reported here had a height of 35%. No conclusions can be made concerning any agreement between their theory and these experiments due to the significant differences in the underlying assumptions.

E. CLOSED ROOM MODEL

The mathematical model describing the closed room is summarized here. The model flow field, illustrated in Figure 33 is made up of a turbulent hot plume feeding a ceiling layer. As the plume entrains fresh air, the interface falls and eventually the ceiling layer fills the entire room. We want to predict the motion of this interface and determine the time required to fill the room with combustion products.

The assumptions made are: the fire can be treated as a point heat source, the plume can be treated in the Boussinesq manner, and there is a leak in the room which makes the transient pressure term in the energy equation negligible. Under these conditions, it can be shown that the enthalpy flux from the room equals the heat addition (6). If we are interested only in the interface height we need not make any assumption concerning the mixing in the ceiling layer.

The concept of keeping the dP/dt term negligible is an important assumption and is justified by the idea that most structures contain the leaks necessary to keep this term small enough to be negligible. A detailed discussion concerning this argument appears in reference (6). The position of the leak is important and the analysis has been simplified by assuming that it is either at the ceiling or floor level. These two cases are discussed separately.

1) Floor Leak

We consider the mass balance in the cold region and obtain:

$$\rho_o HS \left(\frac{dy}{dt}\right) + \dot{m}_e + \dot{m}_p = 0 \tag{21}$$

$$\dot{m}_e = Q/C_p T_o \tag{22}$$

If we use our usual nondimensional heat-input parameter:

$$q^*_H = Q/\rho_1 C_p T_1 \sqrt{gH} H^2 \tag{23}$$

then:

$$\dot{m}_e = q^*_H \rho_o \sqrt{gH} H^2 \tag{24}$$

Previous analysis has geven a reasonable estimate of the plume flow rate as:

$$\dot{m}_p = (q^*)^{1/3} (\rho_o \sqrt{gH} H^2) \alpha \bar{y}^{5/3}, \quad \bar{y} = y/H \tag{25}$$

Where α is a collection of constants whose value is about 0.185

We rewrite eqn. (21) as:

$$\frac{dy}{d\tau} + q^*_H + \alpha (q^*_H)^{1/3} y^{5/3} = 0 \tag{26}$$

where τ is a nondimensional time defined as

$$\tau = t (\sqrt{g/H}) (H^2/S) \tag{27}$$

The integration of (26) is easily accomplished by numerical techniques when q^* is a constant. Thus:

$$\tau = \int dy / (q^* + \alpha (q^*_H)^{1/3} y^{5/3}) \tag{28}$$

Values of τ are plotted for several values of q^*_H in Figure 34.

2) Ceiling Leak

The case of the ceiling layer leak is more easily solved for equation (26) reduces to:

$$\frac{dy}{d\tau} = - \alpha (q^*_H)^{1/3} y^{5/3} \tag{29}$$

This is easily integrated to give:

$$y = \left[1 + (2\alpha/3)\,(q^*)^{1/3}\,\tau\right]^{2/3} \qquad (30)$$

This result is also plotted in Figure 34. Note that for very weak fires, (i.e., $q^* < 10^{-3}$) the two cases above will converge and yield almost identical solutions. The interface height is calculated here as a function of time without requiring the density field in the ceiling layer to be specified.

A paper by Baines and Turner (7) contains a discussion of turbulent buoyant convection from a point source in a confined region. The problem of the motion of the interface in the case of a very small heat input is analyzed. Their results are identical to those presented later by Zukoski in (6) and quoted above. Baines and Turner (7) also present an approximate calculation for the density profile in the ceiling layer after the interface has moved very close to the floor. Their analysis ignores the leak and again it involves use of the Boussinesq approximation. Hence, it is only useful for very small fires for which the location of the leak becomes unimportant and density differences are small.

In the model of these authors, entrainment is assumed to be given by

$$\frac{d\dot{m}_p}{dZ} = (2\pi \ell_v W_m)\ \alpha$$

Here ℓ_v is the Gaussian half width for the velocity profile. This equation is equivalent to the assumption that fluid is entrained by the plume at a radius ℓ_v and with a radial inflow velocity which is equal to α times the centerline velocity of the plume, W_m. In terms

of our description of the plume, α can be shown to be given by

$$\alpha = \frac{5C_1}{6} \approx \frac{5}{48} = 0.104$$

The value of $C_1 = 1/8$ was derived from the measurements of Yokoi (3). This value of α is almost exactly equal to the value 0.10 which Baines and Turner (7) found best fit their experimental data.

F. CLOSED ROOM EXPERIMENTAL SET UP

The experimental setup for the closed room case was the same as used for the room fire experiments discussed previously except that the door was closed off and there was no need for the recirculating fresh water. The water level was kept constant by allowing water to flow out over the walls of the room (i.e., a floor leak case due to our inverted geometry.)

The density data were taken by the conductivity probe as described before. The probe was mounted on a motorized mechanism such that it could traverse the entire tank vertically in about 10 seconds. This mechanism also provided an electrical signal indicating the position of the probe. The probe was continuously moved up and down in the tank while data were recorded on a two pen strip chart recorder, thus conductivity, position, and time were simultaneously recorded. The data were then reduced to give density vs time for various heights, density profiles for various times, and the interface vs time.

A new brine inlet was constructed such that it could be turned on and off very rapidly.

To study the flow field of the ceiling layer more clearly, a flow visualization technique was developed using aluminum powder. The powder was mixed with the brine before injection and was illuminated by a sheet of light produced by a vertical slit. This enabled the motion in any vertical plane to be observed visually and to be photographed.

G. CLOSED ROOM RESULTS

For the closed room case three different results were analyzed as a function of time; these were the interface position, density profiles, and a qualitative study of the flow field. The interface position was of primary concern in these tests and the density profiles, which were obtained as a consequence of measuring the interface height, also were of interest but their analysis is not pursued here. The flow visualization photographs presented in the following discussion clearly showed the complex nature of the flow field. They indicate that a turbulent region exists near the ceiling and that the flow patterns in the remaining region become laminar. This closed room case has also been studied by Baines and Turner (see reference (7)) and the following discussions will also compare their observations with those obtained in these preliminary experiments.

This closed room was tested with the plume in three locations: in the center of the room, against one wall, and in a corner. It was assumed that the idea of reflection mentioned in the open room discussions and shown in Figure 20 would be equally valid in this case. For example, we assume that an axisymmetric plume placed against a wall acts like half a plume of twice the buoyancy in a room twice the size. Thus, by placing the fire in the latter two locations, the effective room size has been doubled and quadrupled.

To aid the reader in analyzing the quantitative results, the first discussion will concern itself with the flow visualization.

1) Flow Visualization

Consider the development of the flow with time for the example with the plume in the center of the 100 x 50 cm room. At the beginning of the experiment, (see (a) of sketch in Figures 35) the spreading action of the plume, after impinging on the ceiling, causes a circular wave suggestive of a ring vortex to flow outward to the wall. The buoyant fluid in this wave impinges on the corner, moves down the wall and slightly overshoots its final level. (See b) The front of this flow then turns and moves, in a horizontal direction, back toward the plume. During this process the plume continues to supply new buoyant fluid to maintain the outward flow next to the ceiling. When the returning front reaches the plume, it turns again and flows out toward the walls. The volume flow rate in this front is greatly reduced as compared to the first reflection due to entrainment by the ceiling jet and plume.

The front continues to move back and forth between the plume and the wall. However, at the next wall reflection, the second reflection at the wall, a laminar layer is produced whereas the flow described above, in the region next to the ceiling is turbulent for all of the conditions we examined. See Figure 36.

The laminar fronts continue to move horizontally back and forth and gradually fill up the room. They give the appearance of leaving a number of distinct flow paths behind the propagating fronts through which flows the ceiling layer fluid generated by the plume. The flow field at two later times is illustrated in Figures 36 and 43.

The thickness of the turbulent region next to the ceiling quickly grows to 35 to 50% of the room height and then remains constant while the rest of the room is gradually filled with the laminar layers.

2. Interface Height

The dependence of the ceiling layer interface position on time is shown in Figure 34 for both the theory developed in an earlier section and the experimental results. The experiments were carried out with q^* between 3 and 5×10^{-6} and thus should be compared to the ceiling leak theory despite the fact that the leak was at floor level.

The growth of the ceiling layer thickness for the plume located in the center of the room is accurately predicted by the model after the initial waves have damped out. Considering the complex nature of the flow described in Figures 35 and 36, the agreement is remarkable. Note that no adjustable constants are available in the calculation except the plume entrainment constant which was selected before the present experiments were carried out. Good agreement between this same model and a similar experiment was also reported by Baines and Turner (7) who used q^* values in the range 3×1^{-7} to 5×10^{-6}. Hence, the model does lead to accurate predictions for small fires; no data are available for larger fires.

Interface height data are also shown in Figure 34 for a plume located against the wall (center of the 100 cm wall of a tank 50 x 100 cm) and in a corner of the tank. The data were reduced by

using the reflection principle discussed earlier. Hence Q^* values were 10^{-5} for the wall interference case and 2×10^{-5} for the corner example. If the reflection idea had not been used, the wall and corner values of $\tau(q^*)^{1/3}$ would be moved to the right by factors of 1.28 and 1.59 respectively. Agreement with predicted values is within about 10 to 15% and the data were overcorrected by use of the reflection idea. This suggests again that entrainment is affected by the presence of the walls and that the reflection ideal is a useful but not precise approach.

3) Density Data

The transient density data for the closed room experiments are shown in Figures 37 through 42. For each experiment, a set of density histories and density profiles is presented. The density on both types of plots is a density difference (density of fluid measured locally minus fresh water density) normalized by the fresh water density. The density history is presented as a plot of the nondimensional density difference against time in minutes.

The density gradient of the lower portion of the ceiling layer becomes sharper in time due to the plume entraining fluid from these areas and this process produces rather "full" profiles. After about 5 minutes, the shape of the upper portion of the profile doesn't change shape but translates to the right as time increases. This result is particularly clear in Figure 40. This behavior was suggested by Baines and Turner but appears to start at a much

earlier time than they expected. The density profiles in this steady state regime were compared to those produced by Baines and Turner and agree very well. In all cases profiles near the floor do change in shape. The profiles have slight discontinuities which remain at the same height throughout the experiment. In Figure 44, for example, we compare a density profile with a photograph taken at the same time. The slight discontinuity in the density profile near the center of the room approximately coincides with the center of a distinct pair of breaks in the density profiles. Hence it may be related to the interface between the turbulent and laminar region. Note in Figure 40 that these breaks persist over a period of 10 minutes.

The dependence of the thickness of the turbulent region on system parameters has not yet been determined satisfactorily. Baines and Turner (7) observed a similar turbulent region and believed that its thickness depended on the ratio between the plume length H and an effective floor radius. This has not been found to be true in our study. Excluding the wall and corner plumes, the turbulent region thickness has been found to be about 55% of room height regardless of the plume length to floor radius ratio, see Table IV.

For the cases of the plumes placed next to a wall in a corner the turbulent region thickness did decrease, but this was not observed for a plume in the room center with the same effective H/R ratios. Further study of this phenomenon could yield interesting results.

H. SUMMARY AND CONCLUSIONS

Presented in this thesis is the experimental verification of two theoretical models which characterize the behavior of the hot air and combustion products in some room fire situations.

The first model concerns a room containing one opening and a single heat source. It is based on current knowledge of buoyant plumes and a few basic assumptions concerning the flow through an opening. Scale model tests were conducted, using water as the fluid medium, to test the validity and limits of this model.

Another room fire situation, the case in which there is no opening, was also modeled and tested due to its similarity with the open room case. The main interest with this problem is to determine the time required to fill a room with smoke.

The experiments resulted in the following conclusions:

1) The theoretical model described for the open room gave a reasonably accurate prediction for the simple cases in the salt water experiments. There is some question as to the model's validity for full scale room fires. The theoretical model and the experimental modeling of the flow neglect heat transfer completely and both correspond to extremely weak fires. But the Reynolds number and buoyancy parameters achieved in the experimental work do correspond to full scale fire situations.

The salt-water experiments are very useful in the qualitative study of the flow field characteristics. The results can be used

to identify those fluid dynamic aspects of the room fire which should be studied in full scale experiments. In addition, the experiments give a good qualitative picture of various interactions.

2) The geometry of the fire plume was noted to be of significant importance. Plumes arising from rectangular and line sources had entrainment rates which produced ceiling layer densities as much as 25% lower than those of the axisymmetric plume. This is important because in an actual fire situation the source may assume a variety of geometries.

3) The interaction between the plume and wall will be important when the fire is near a wall. The entrainment will only be half as much for a plume against a wall or one quarter as much for a corner plume. However, if the walls are burning also, heat will be added throughout the plume and the present model will not be applicable.

4) It was noted that for small openings mixing can occur between the inflowing and outflowing streams. A complete study of this phenomenon was not made but results for the narrow door and windows suggest that mixing is significant for most windows but is not as much for the door cases. In the window cases the area usually containing fresh air obtained as much as 20% of its air from the ceiling layer.

5) Swirl in the room was found to be an important detail in the flow field. A nonsymmetry in the room configuration

would usually produce a large swirl around the plume which changed its entrainment rate. Its effect on the ceiling layer was noted as a decrease in ceiling layer density and a thickening of the interface region, (i. e. weaker density gradients.)

6) The door jet was an important flow field feature which was neglected in the model. For the simple cases it was negligible but the door jet could blow against the plume, mix with the opening outflow, or set up swirl in the room. Each of these effects were shown to be significant in some configurations.

7) The theoretical model developed for the closed room accurately describes the motion of the ceiling layer interface for very weak fires. Other features concerning flow field and density profiles were analyzed but no conclusions have been made pending further study.

References

(1) E. E. Zukoski, "Convective Flows Associated with Room Fires," June, 1975, California Institute of Technology.

(2) B. R. Morton, G. I. Taylor, and J. S. Turner, "Turbulent Gravitational Convection," Proc. Royal Society of London Vol. 234, March, 1956, 1.

(3) S. Yokoi, "Study on the Prevention of Fire Caused by Hot Upward Current," Report No. 34, Building Research Institute, Japanese Government, Nov. 1960.

(4) J. J. Grella, and G. M. Faeth, "Measurements in a Two-dimensional Thermal Plume Along a Vertical Adiabatic Wall," J. of Fluid Mechanics, Vol 71, 701.

(5) K. T. Yang and J. R. Lloyd, "Fire and Smoke Spread", October 1, 1976, University of Notre Dame.

(6) E. E. Zukoski, "Development of a Stratified Ceiling Layer in the Early Stages of a Closed Room Fire," February 1, 1977, California Institute of Technology.

(7) W. D. Baines and J. S. Turner, "Turbulent Buoyant Convection from a Source in a Confined Region," J. Fluid. Mech., Vol. 37, 1, pp. 51-80, (1969).

TABLE II

Hot Side Coefficient	0.6	0.7	0.8	1.0	1.0	0.6
Cold Side Coefficient	0.6	0.7	0.8	1.0	0.6	1.0
(Y_1/H)	.585	.600	.612	.633	.590	.625
$(100\ \Delta\rho_o/\rho_o)$	.604	.578	.558	.520	.595	.530

$q_H^* = 10^{-5}$ Door Soffit = .813H

Door Width = .375H

TABLE III

Example	Buoyancy Source	Q or $\frac{\Delta\rho_o}{\rho} V$	H	q_H^*	Re^*
A	Fire in Air	100 kw 0.1	244 cm	10^{-2} 10^{-5}	7.9×10^4 0.8
B		17.7 kw. .018	122 cm	10^{-2} 10^{-5}	2.8×10^4 0.3
C	Salt Water in Water	20 cc/sec 5 cc/sec	50 cm	4×10^{-5} 10^{-5}	1.8×10^4 1.1

TABLE IV

Case	1	2	3	4	5	6
$\Delta\rho_o$	.05	all examples				
V_o cc/sec	100	100	60	100	60	60
H cm	50 cm	25	25	25	25	50
D cm	2.22	2.22	2.54	2.54	2.54	2.22
Ht cm	27 1/2	13 1/4	13 3/4	13 3/4	13 1/4	27
L x W	100x50	100x50	100x50	50x50	50x50	50x50
Re	40	40	40	28	28	28
H/Re	1.25	.625	.625	.886	.886	1.772
H/D	22.5	11.3	9.8	9.8	9.8	22.5
q^*	0.9×10^{-5}	5×10^{-5}	5×10^{-5}	5×10^{-5}	3×10^{-5}	$.5\times10^{-5}$
Ht/H	.55	.53	.55	.55	.53	.54

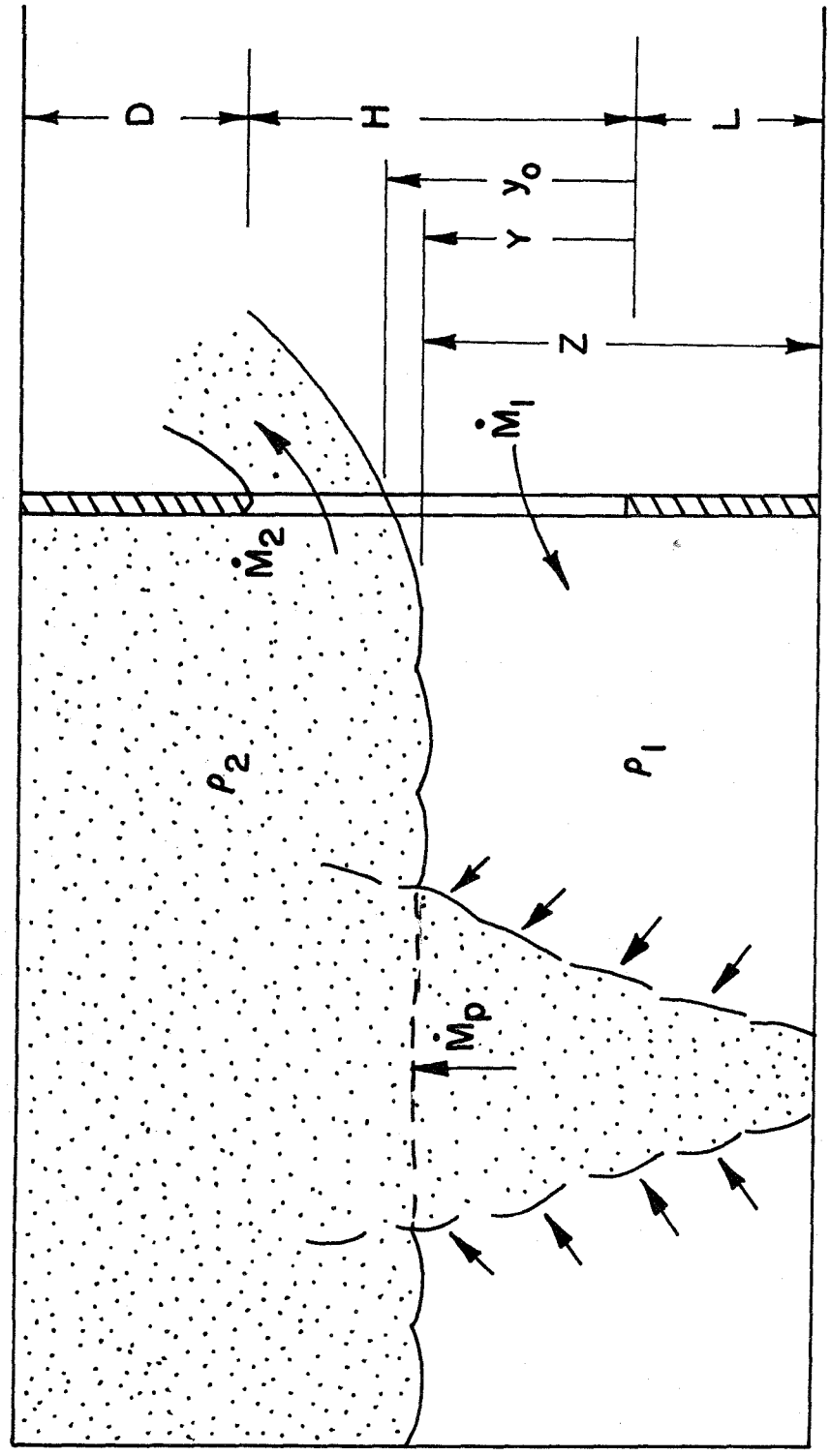

FIG. I GENERAL SKETCH ILLUSTRATING MODEL

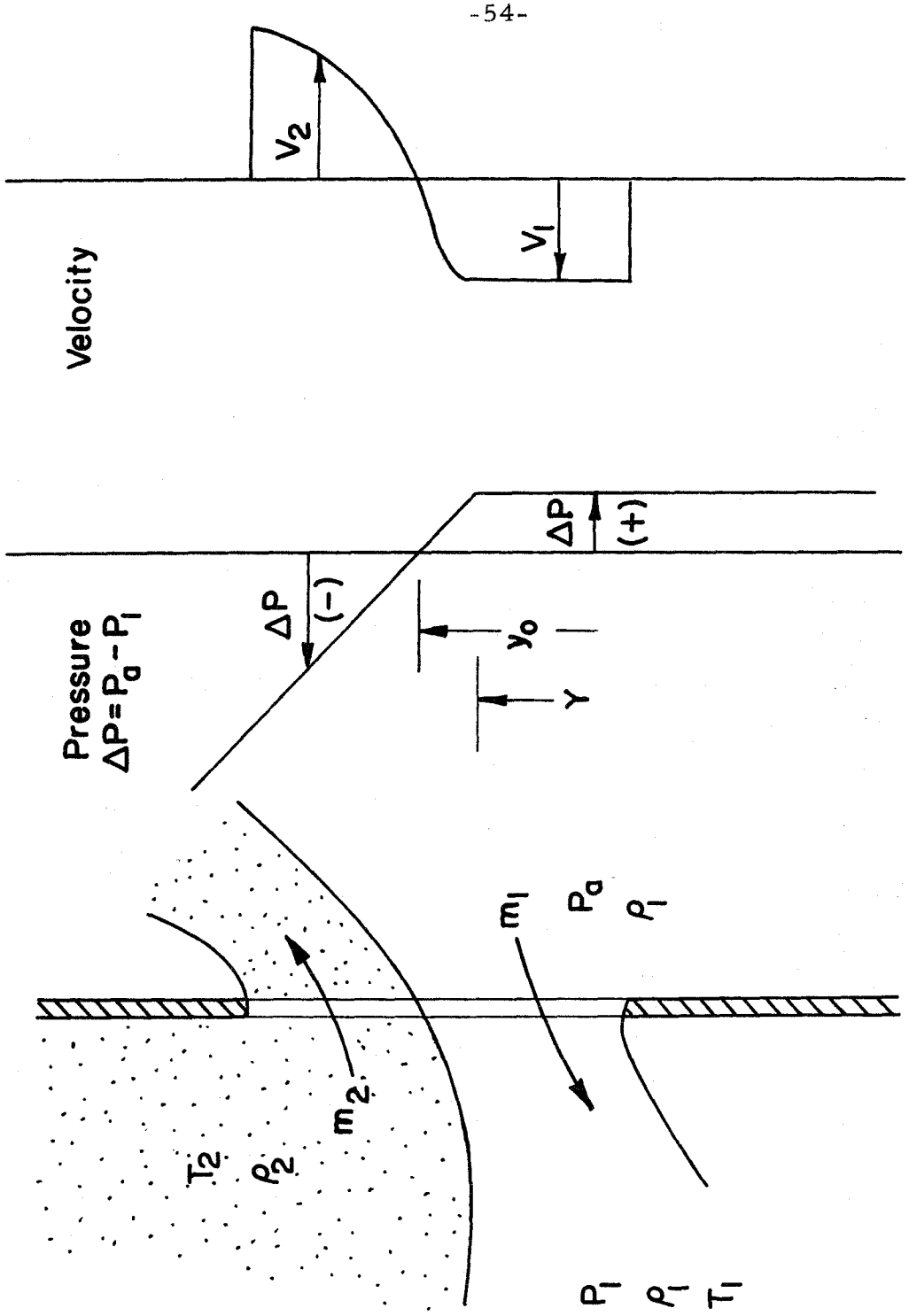

FIG. 2 OPENING COUNTER FLOW MODEL

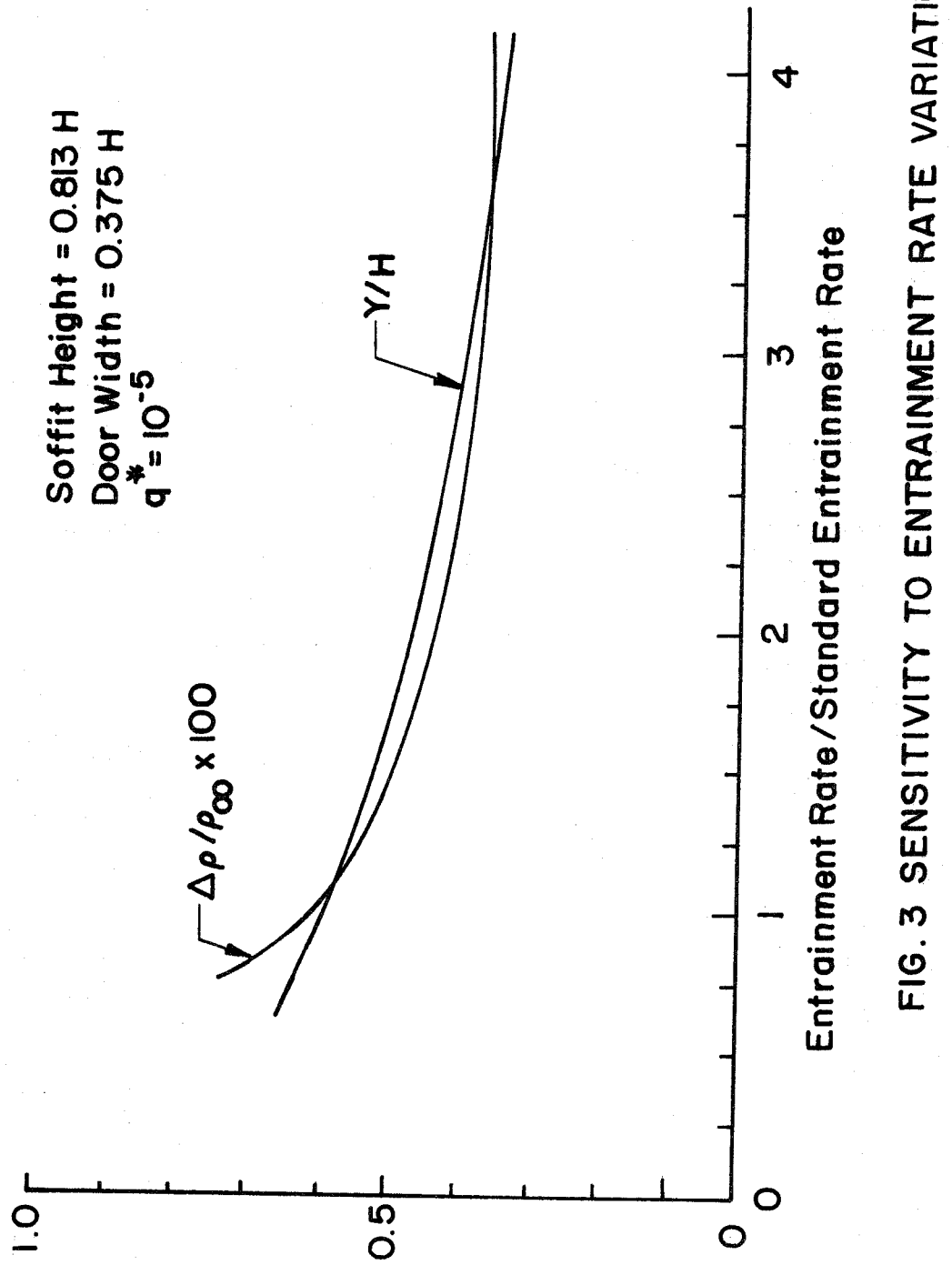

FIG. 3 SENSITIVITY TO ENTRAINMENT RATE VARIATION

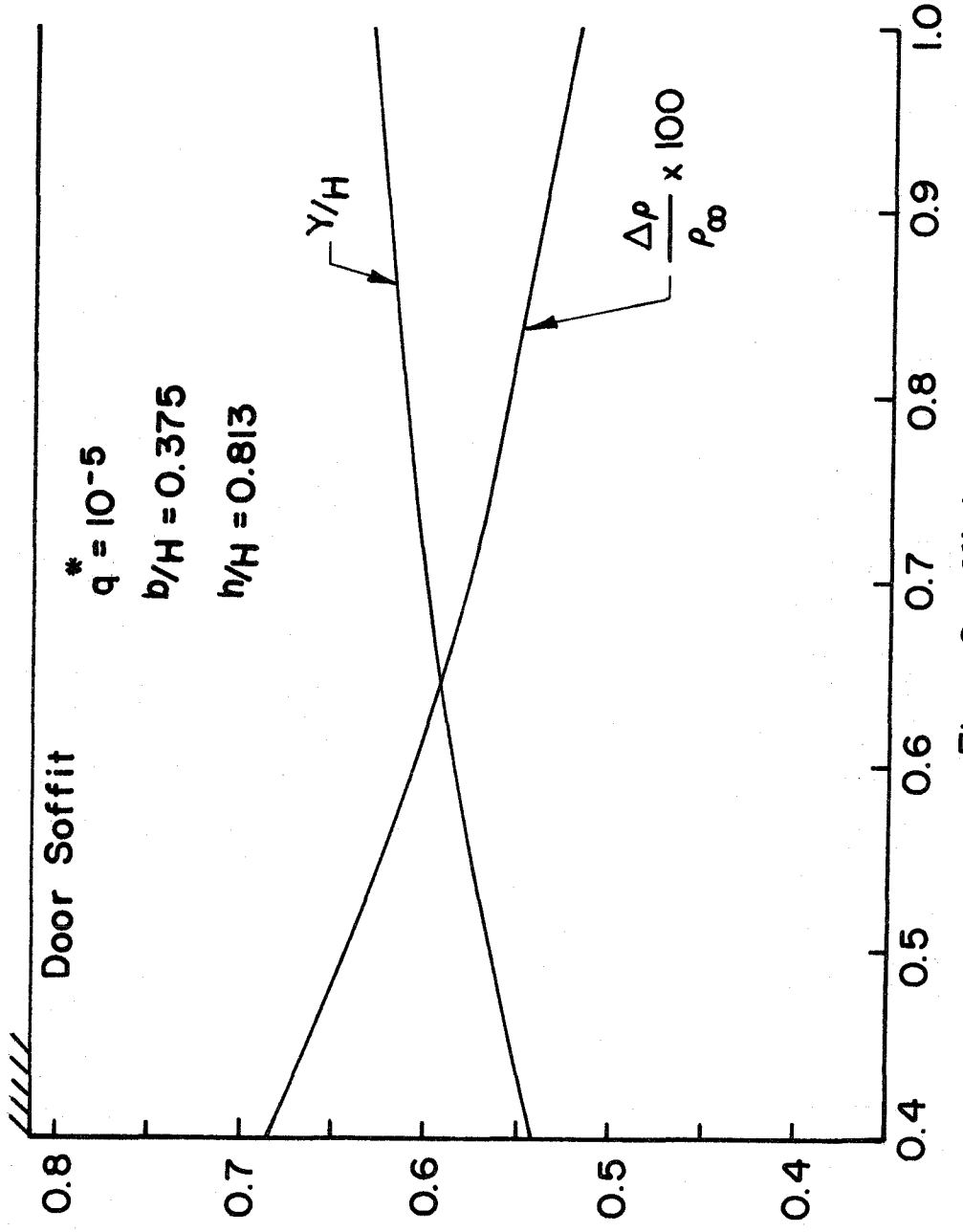

FIG.4 SENSITIVITY TO ORIFICE COEFFICIENT VARIATION

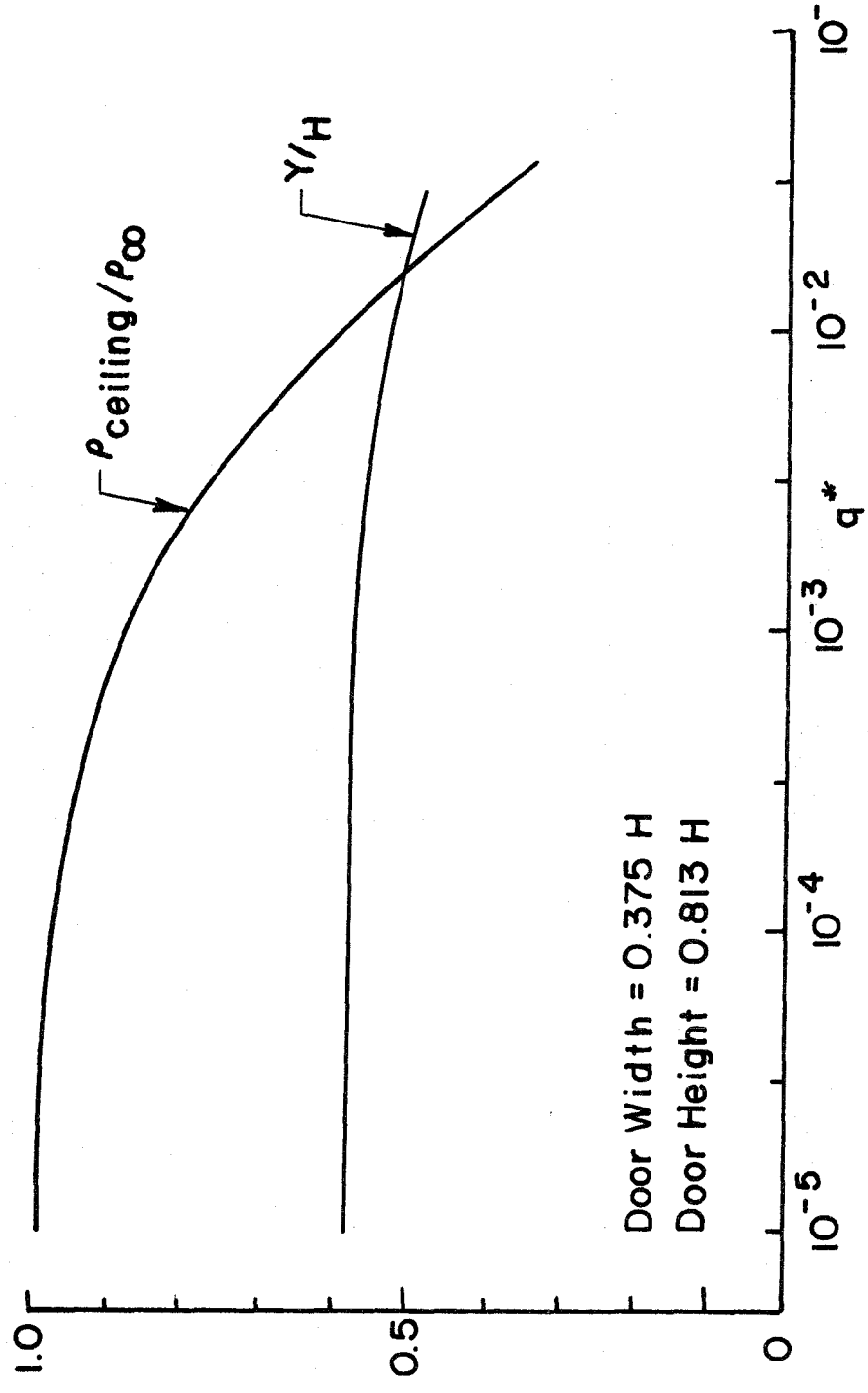

FIG. 5 SENSITIVITY TO q^*_H VARIATION

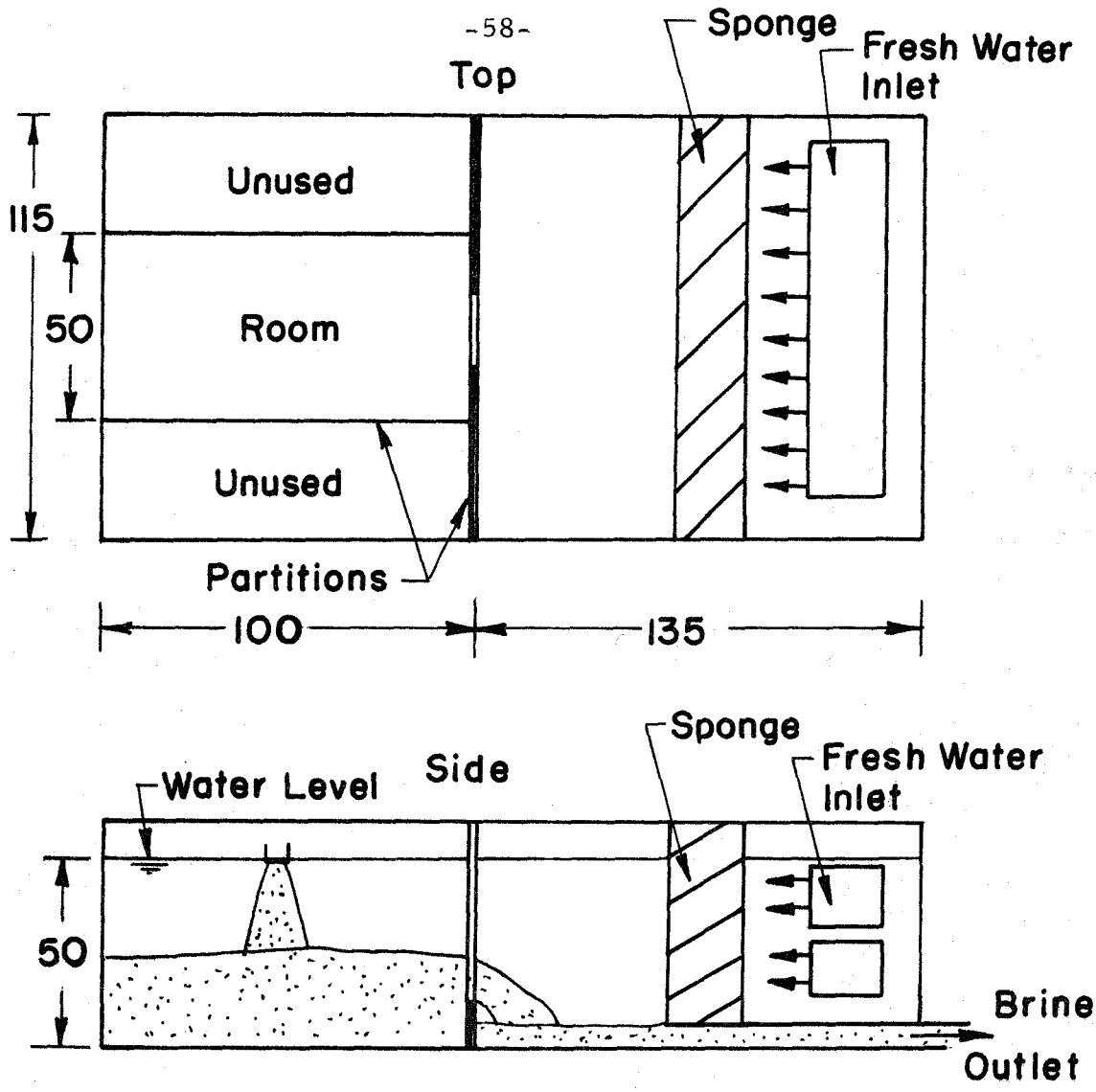

FIG. 6 GENERAL LABORATORY LAYOUT

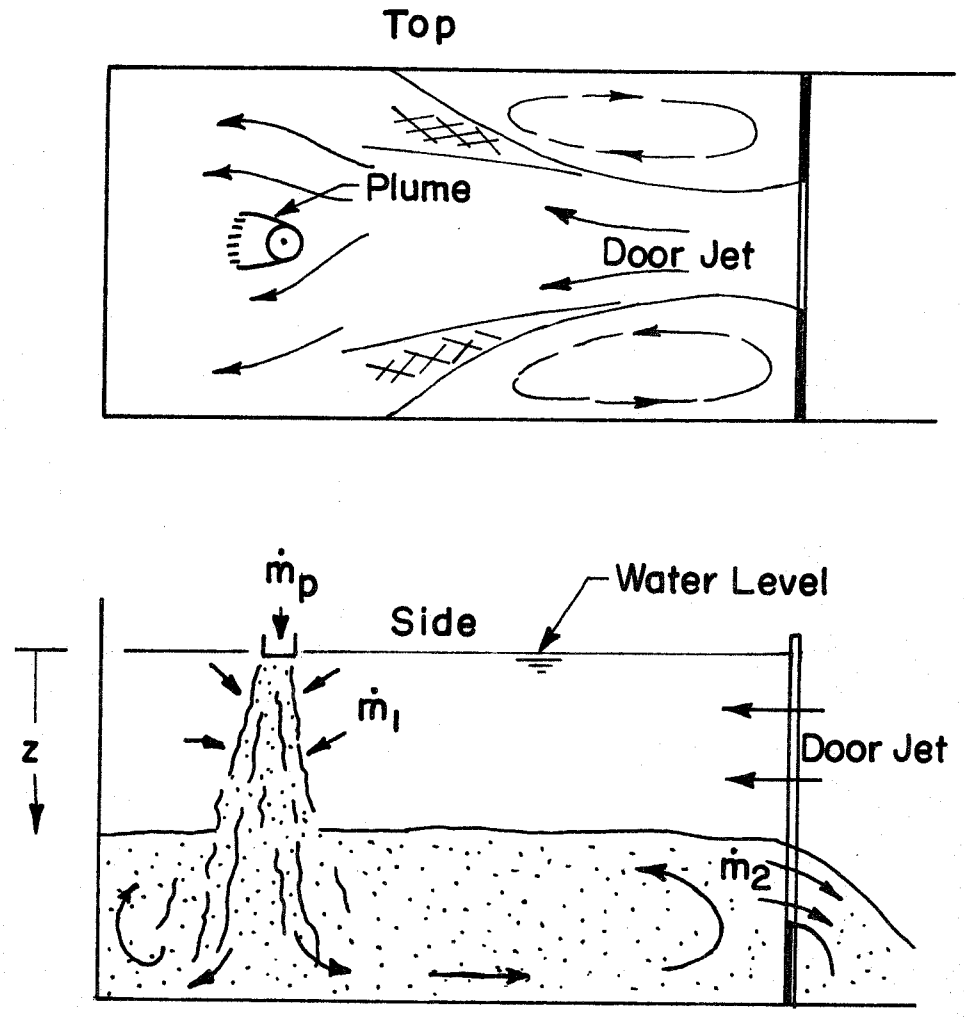

FIG. 7 FLOW FIELD IN OPEN ROOM

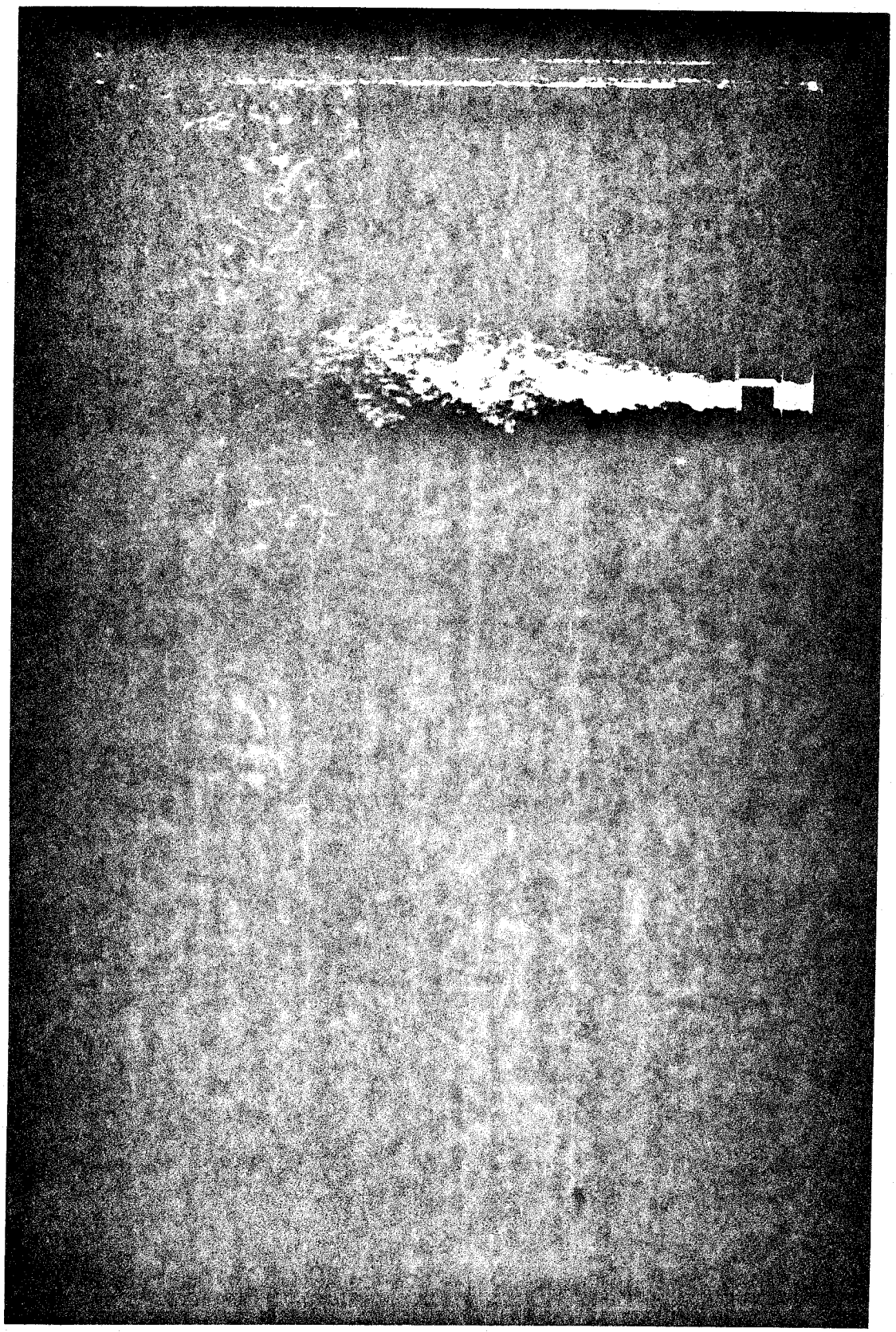

FIG. 8 OPEN ROOM FLOW PHOTOGRAPH

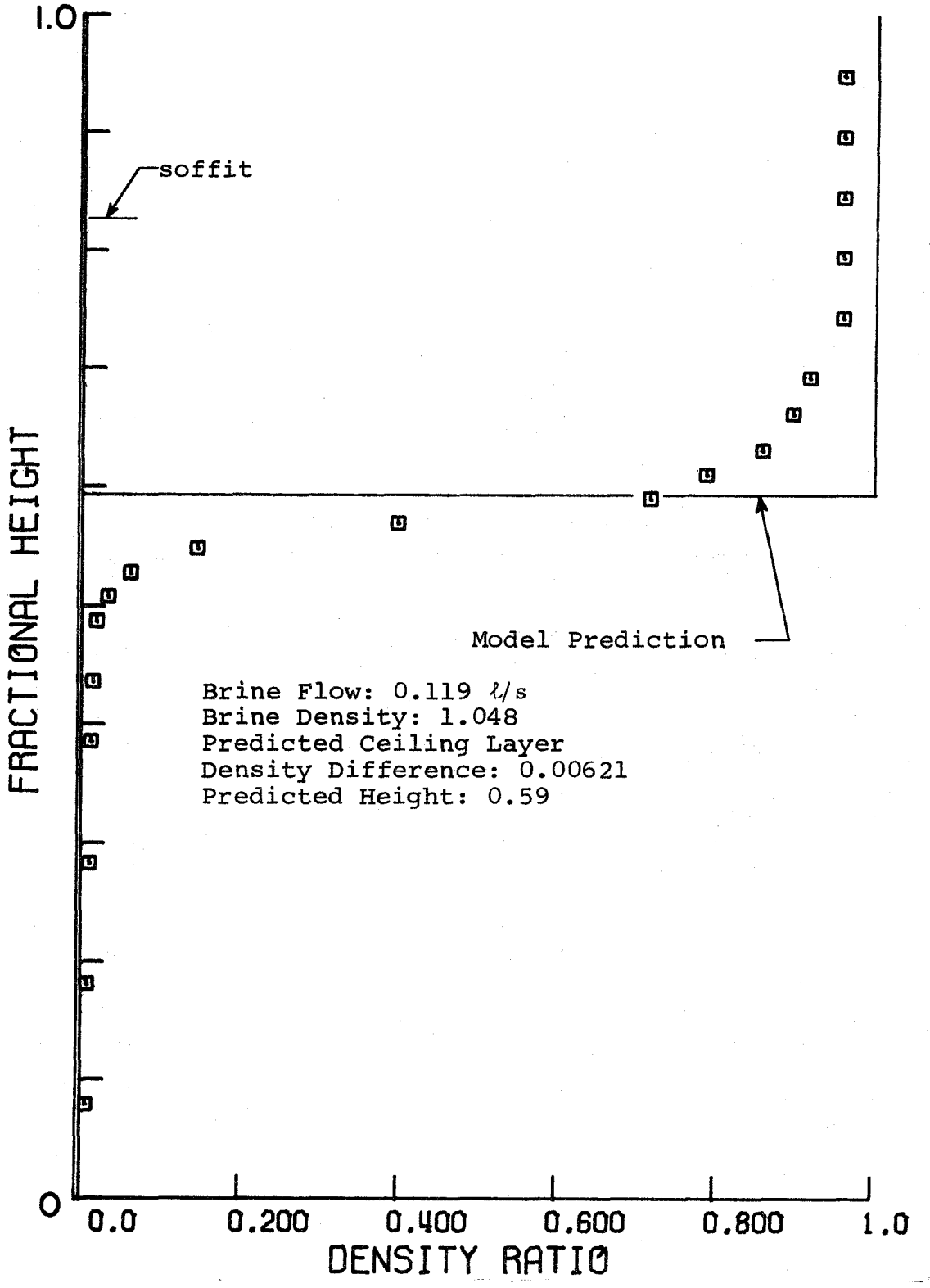

Figure 9 Data From Typical Experiment

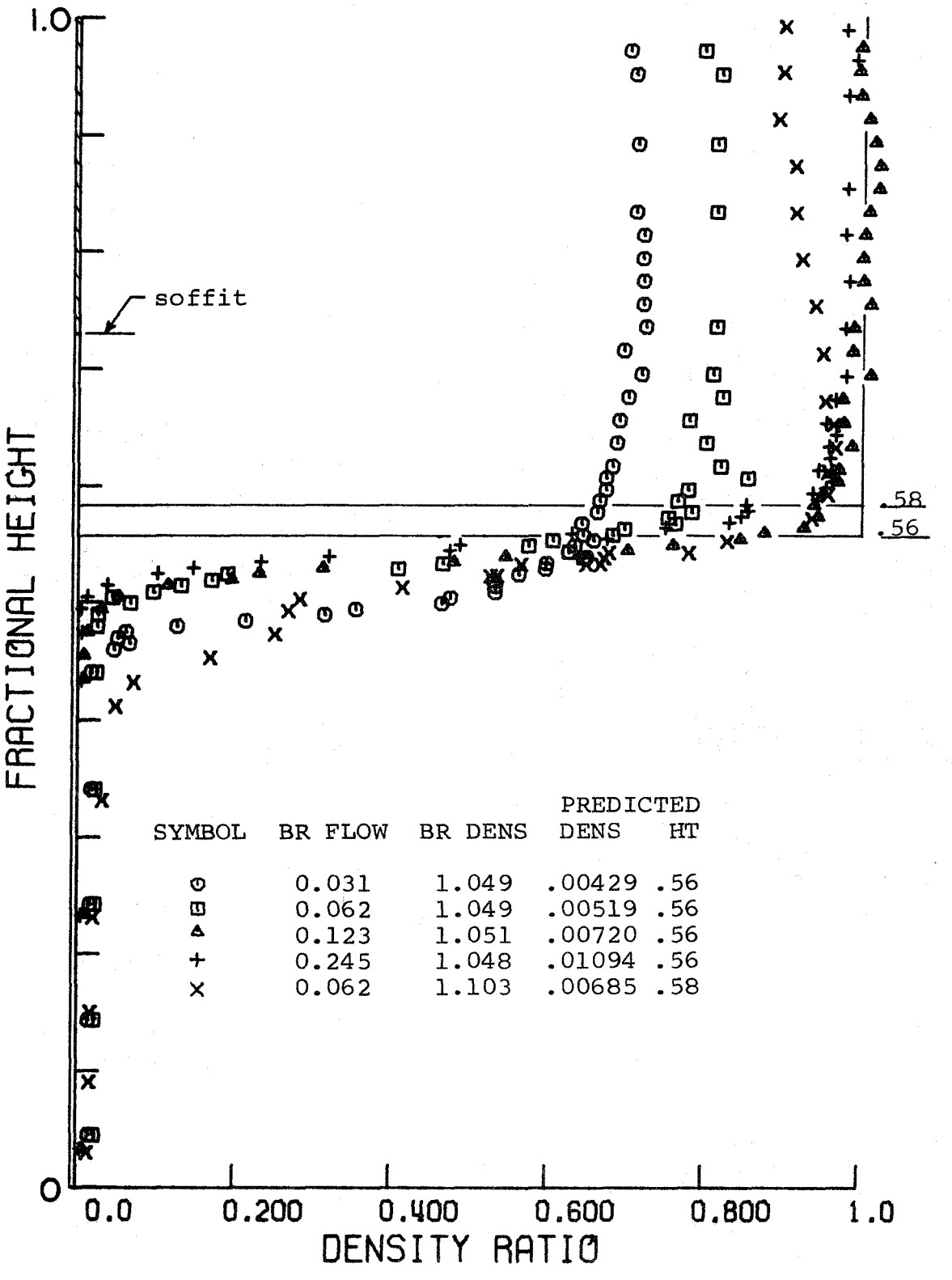

Figure 10 Effect of Fire Strength With 2" Source

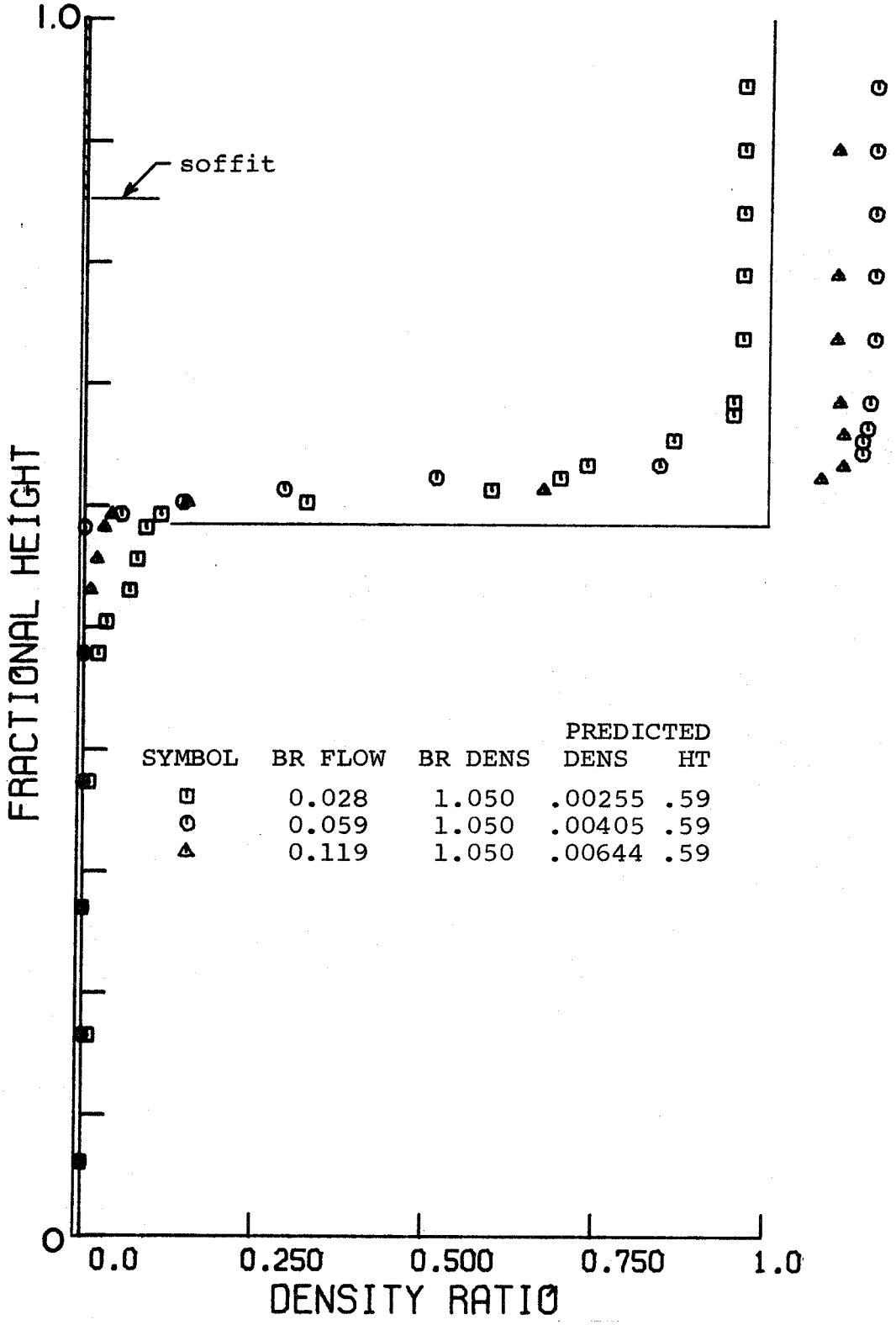

Figure 11 Effect of Fire Strength With 1" Source

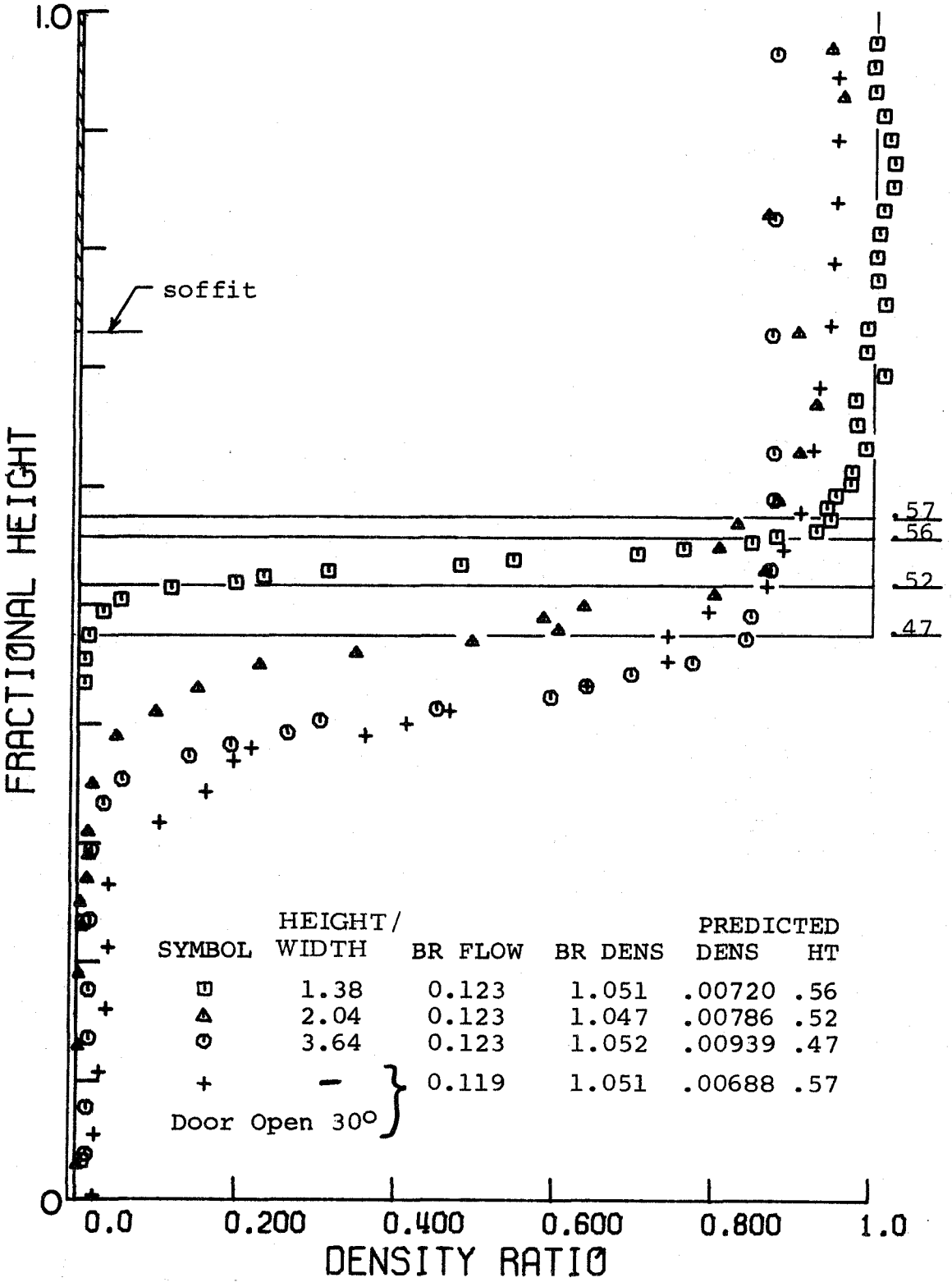

Figure 12 Effect of Door Geometry

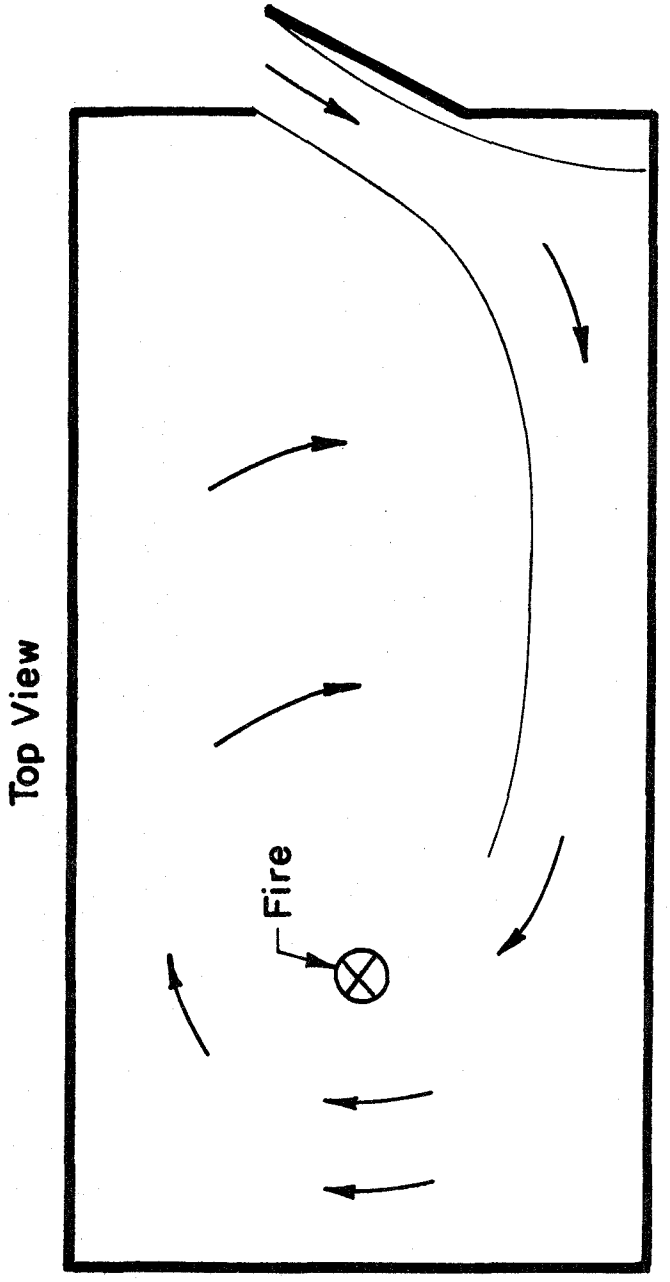

FIG. 13 FLOW FIELD FOR A PARTIALLY CLOSED DOOR

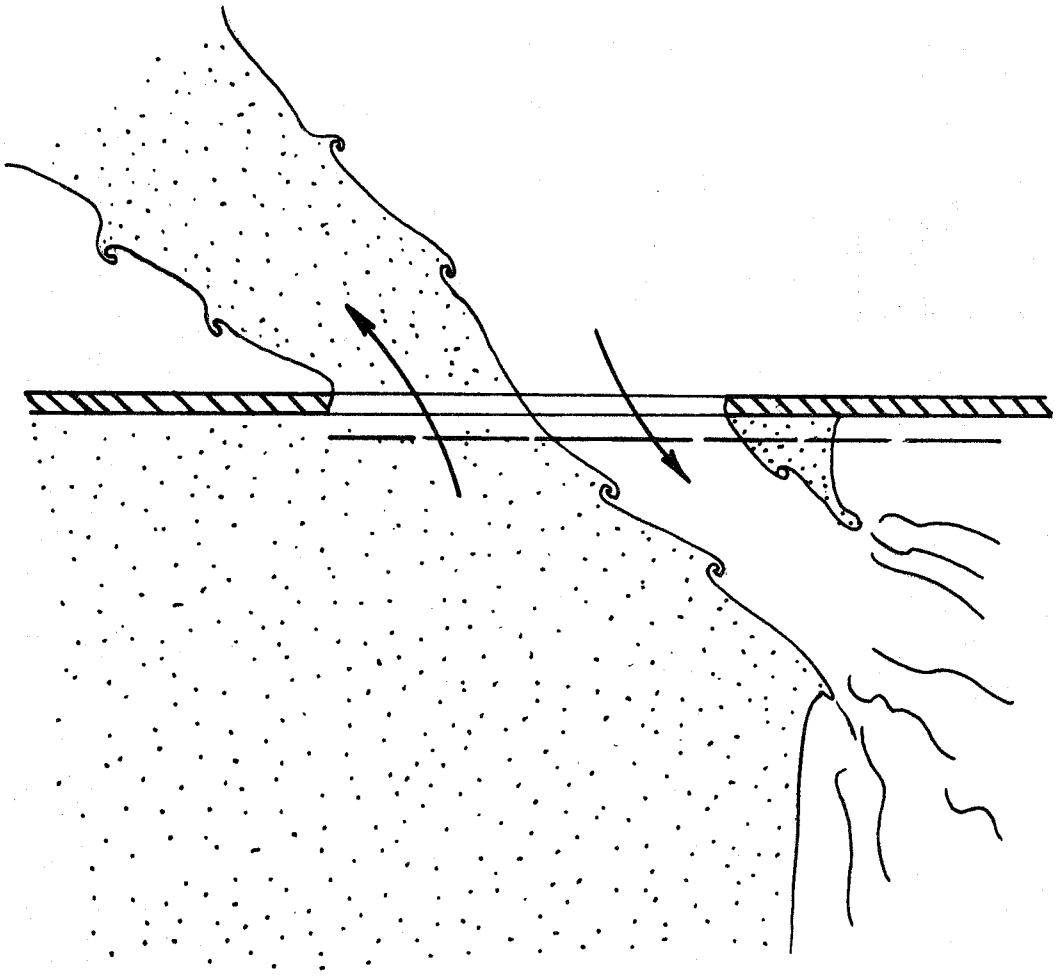

FIG.14 EXAMPLE OF FLOW THROUGH A SMALL OPENING

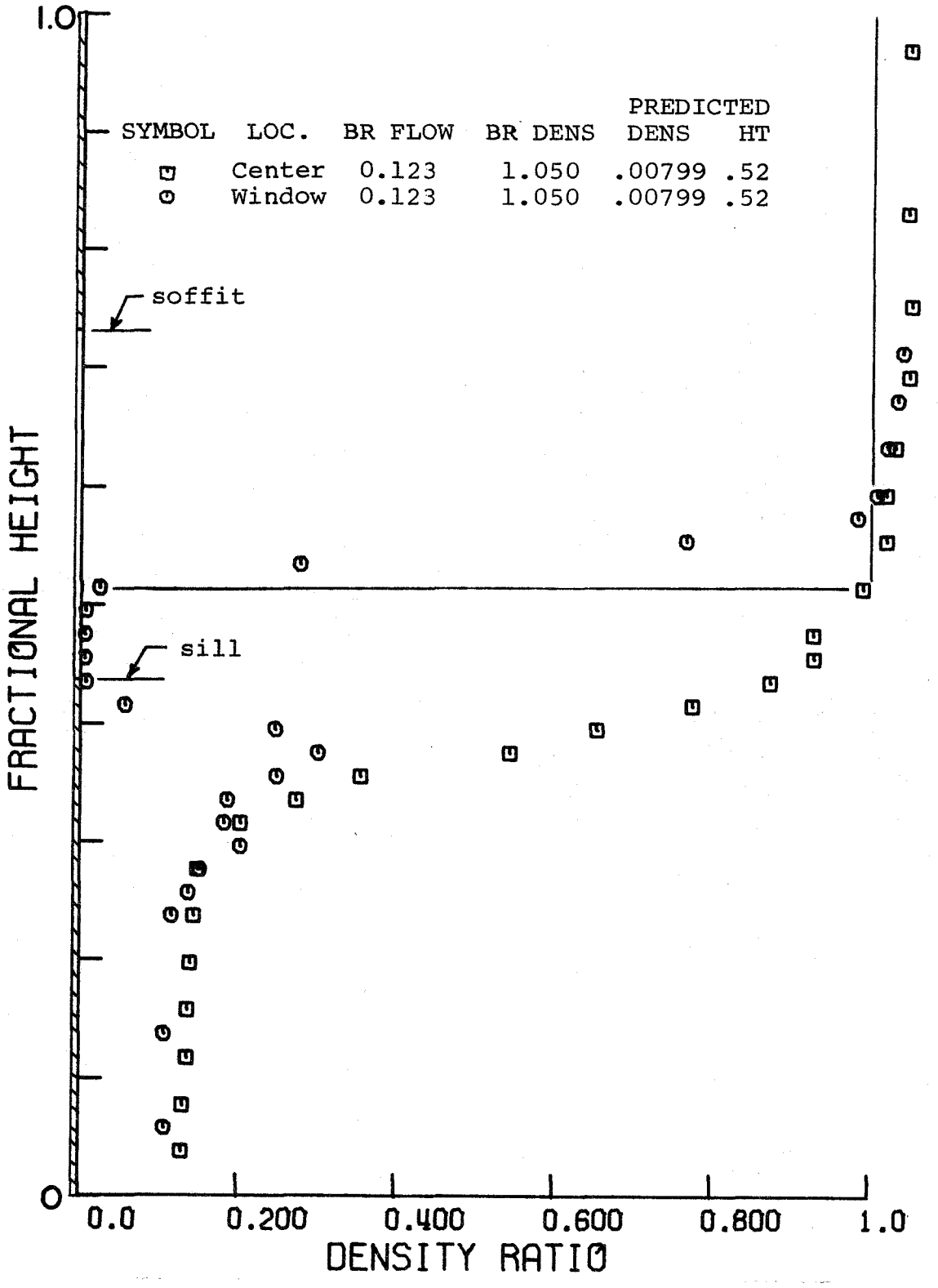

Figure 15 Small Window

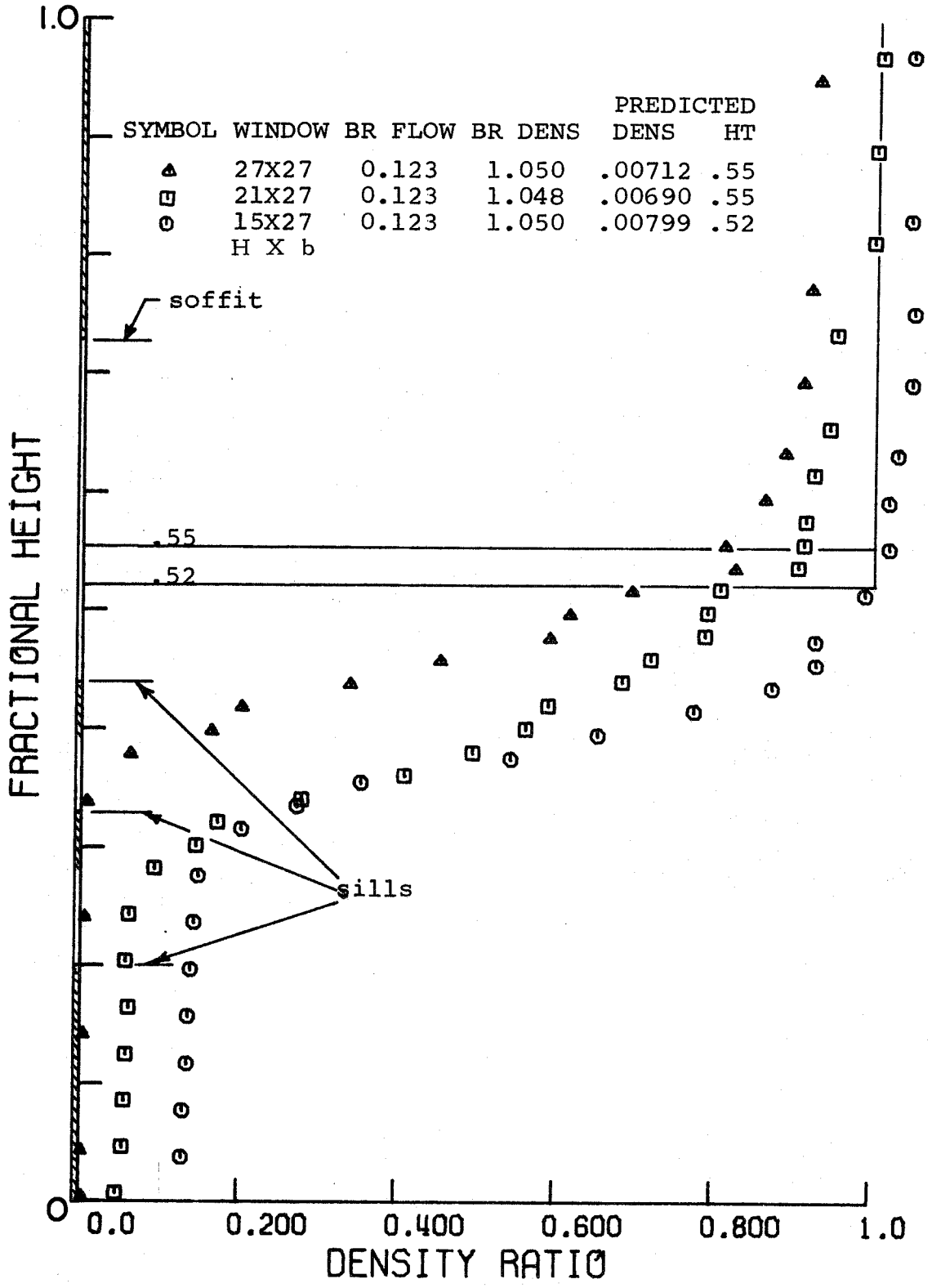

Figure 16 Effect of Window Geometry

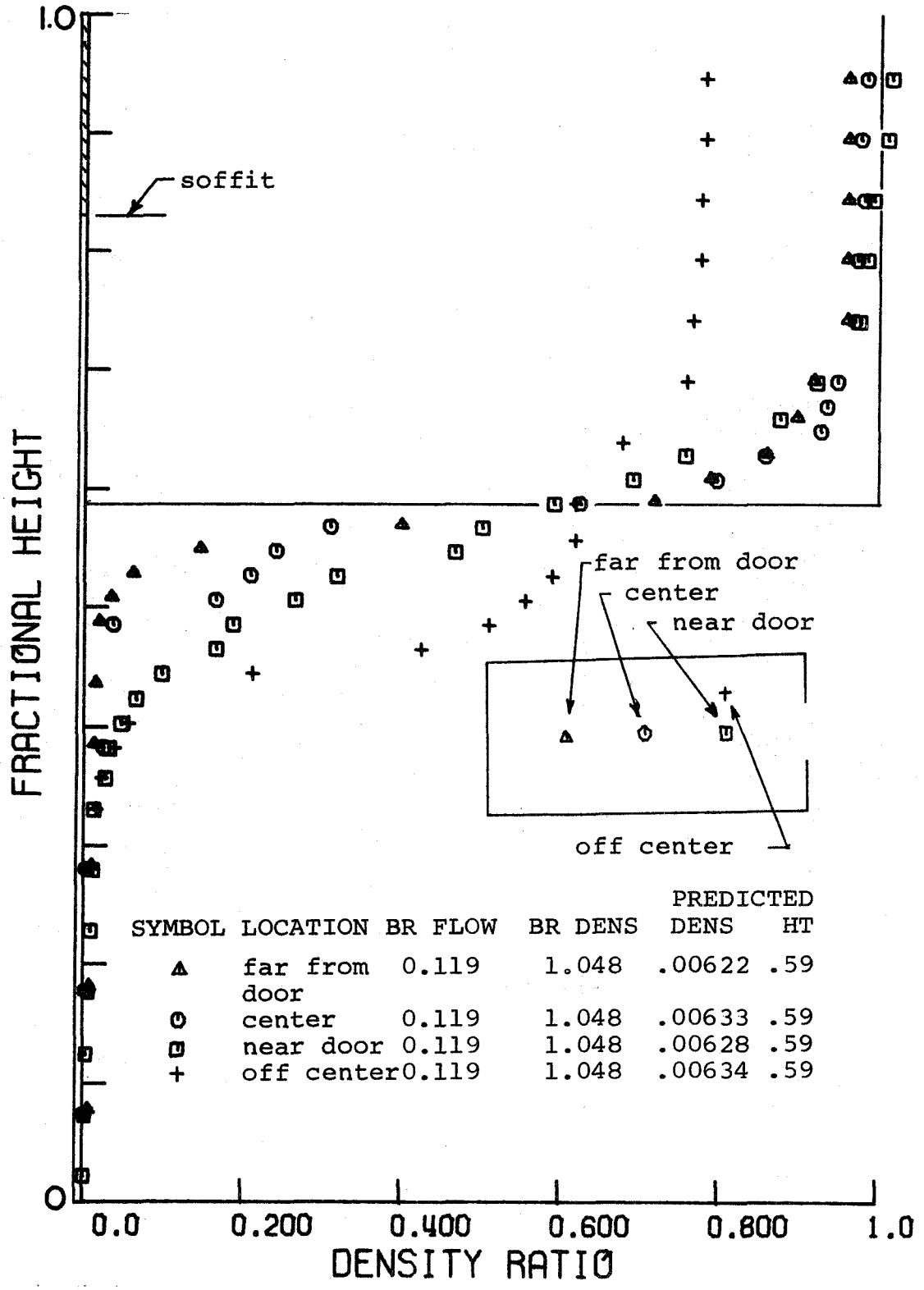

SYMBOL	LOCATION	BR FLOW	BR DENS	PREDICTED DENS	PREDICTED HT
▲	far from door	0.119	1.048	.00622	.59
⊙	center	0.119	1.048	.00633	.59
▣	near door	0.119	1.048	.00628	.59
+	off center	0.119	1.048	.00634	.59

Figure 17 Effect of Fire Location

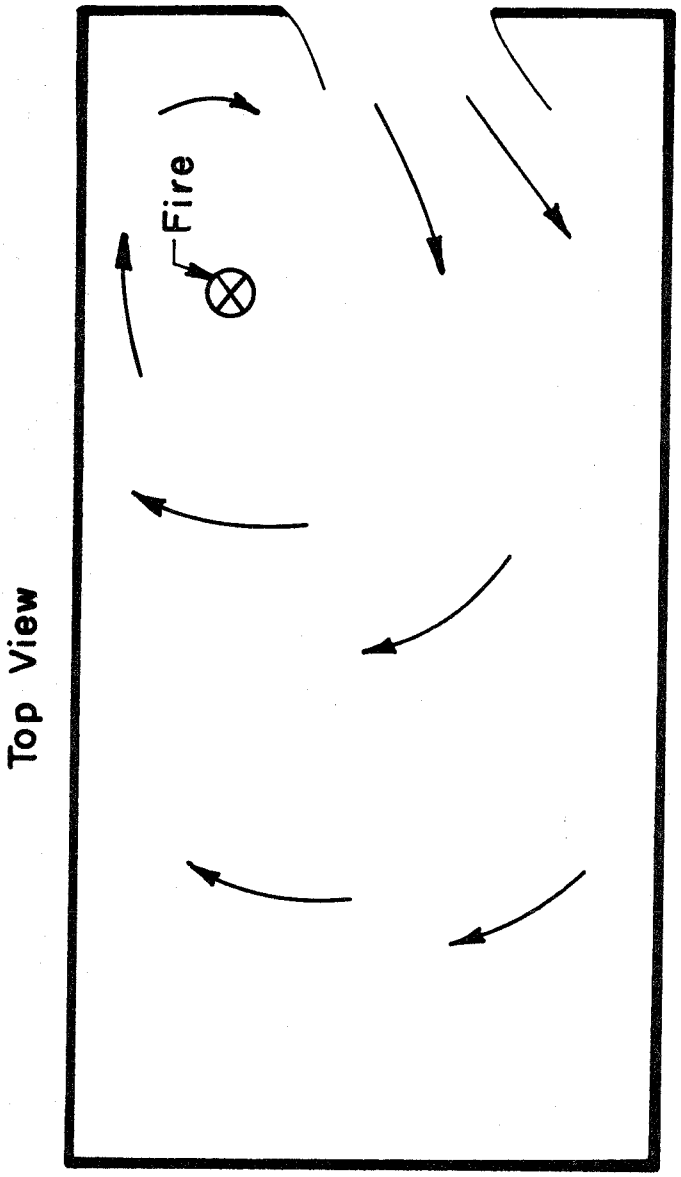

FIG. 18 FLOW FIELD FOR AN OFF CENTER FIRE

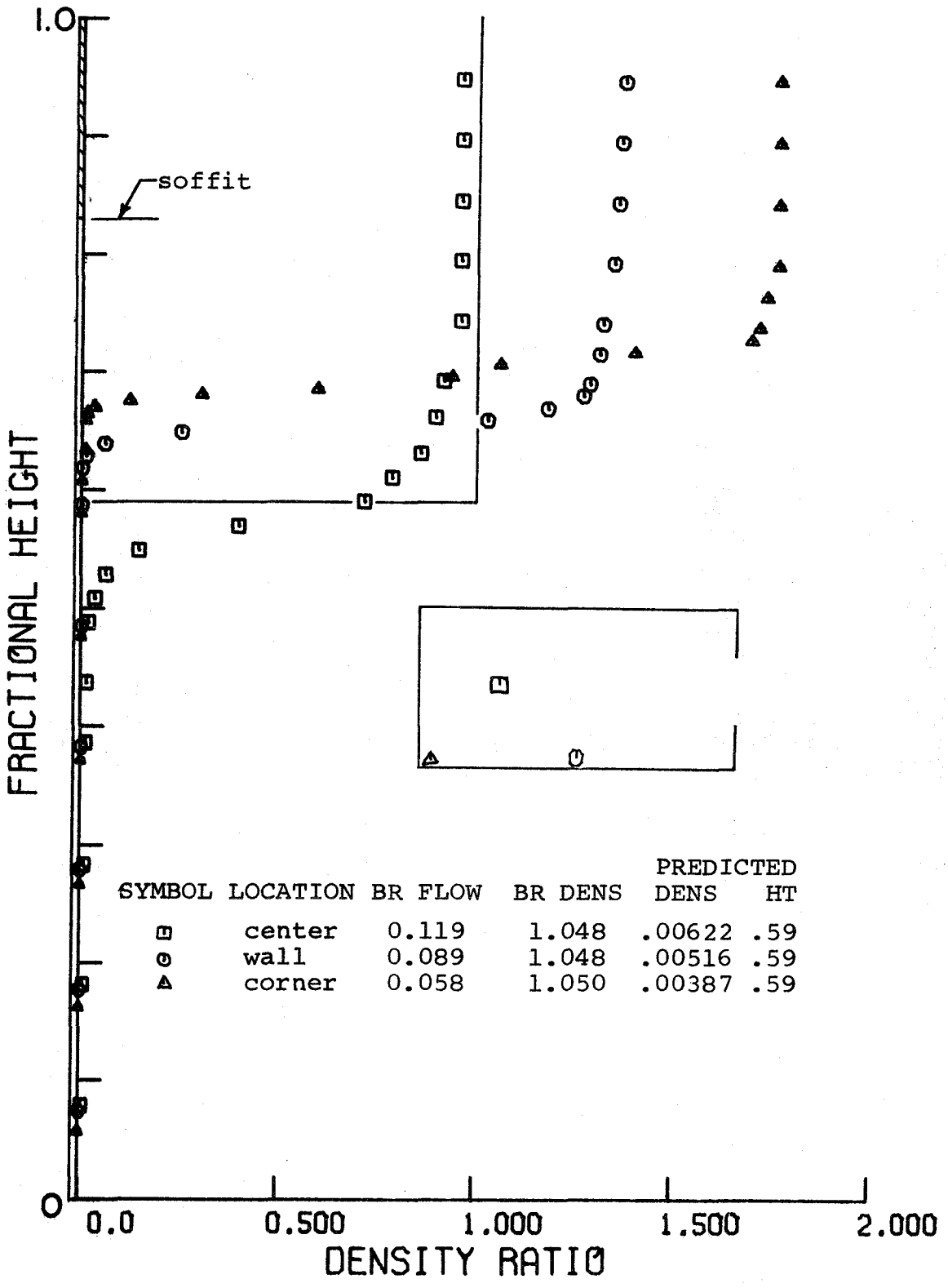

Figure 19 Effect of Fire Location Near Walls Compared to Simple Theory

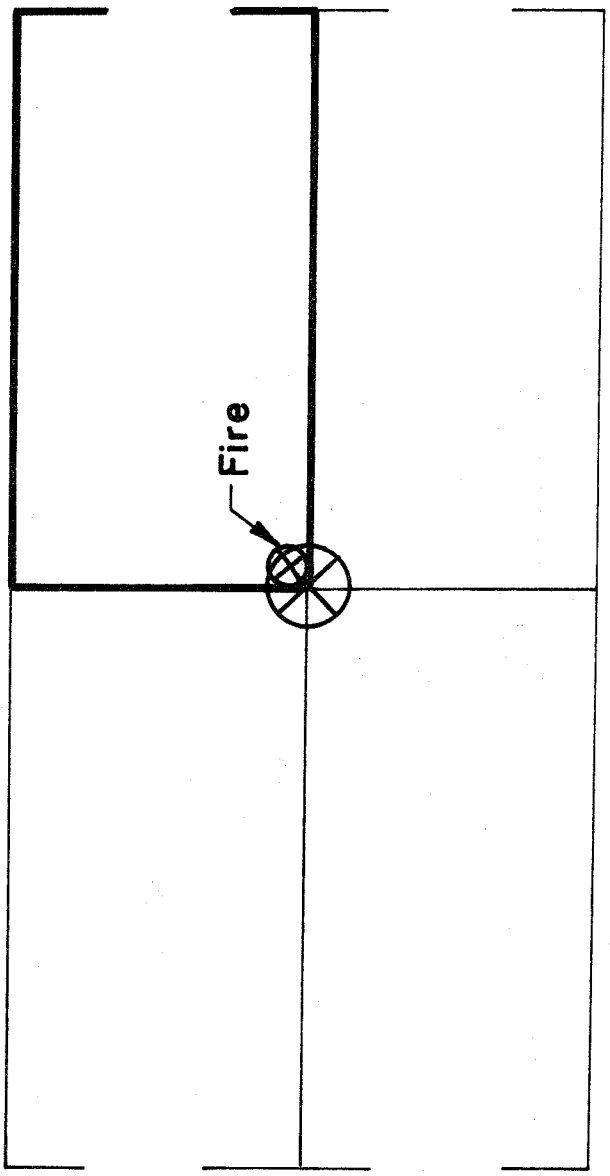

FIG.20 MODEL FOR A CORNER FIRE

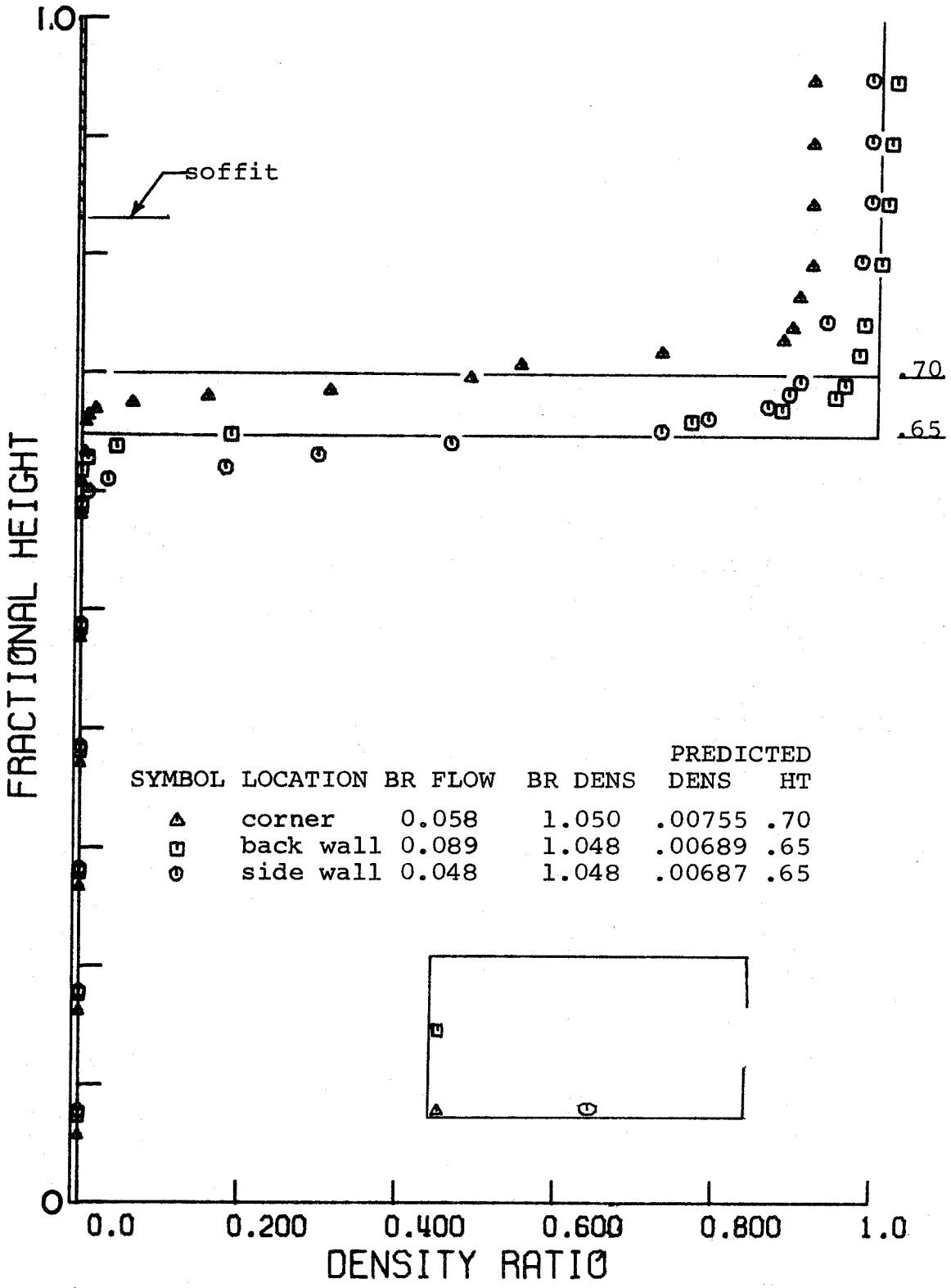

Figure 21 Effect of Fire Location near Walls Compared to Reflection Theory

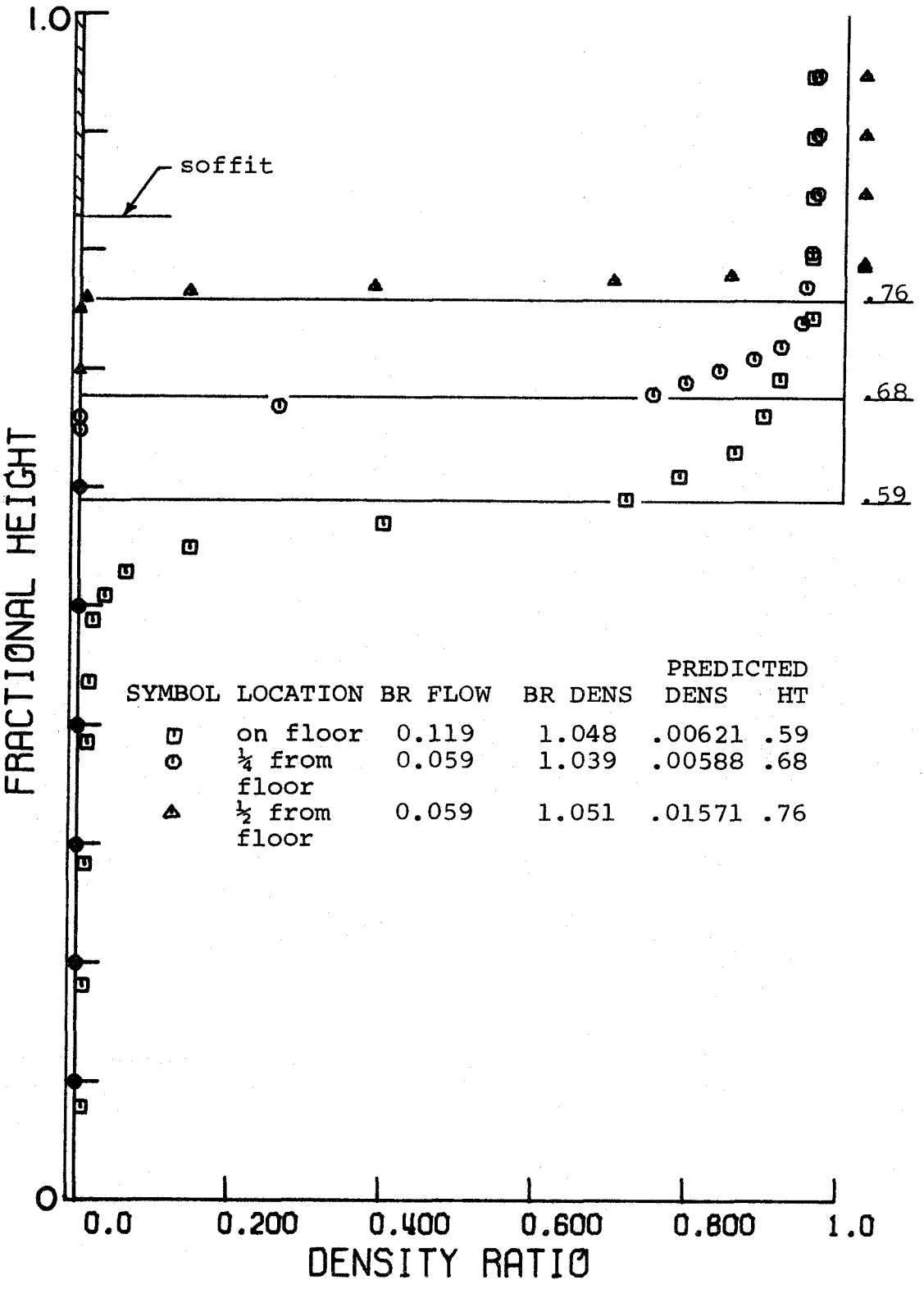

Figure 22 Effect of Fire Vertical Location

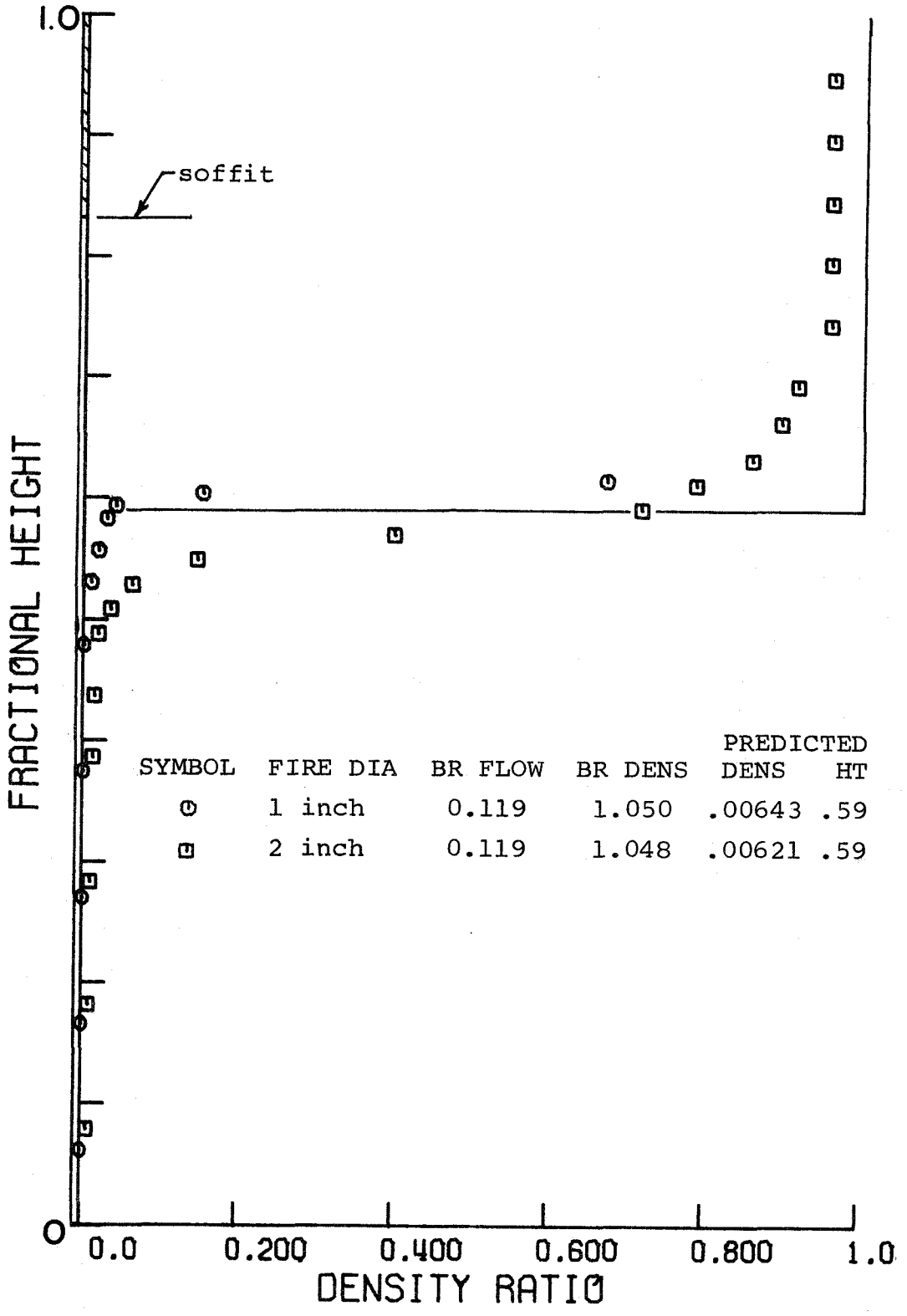

Figure 23 Effect of Fire Diameter

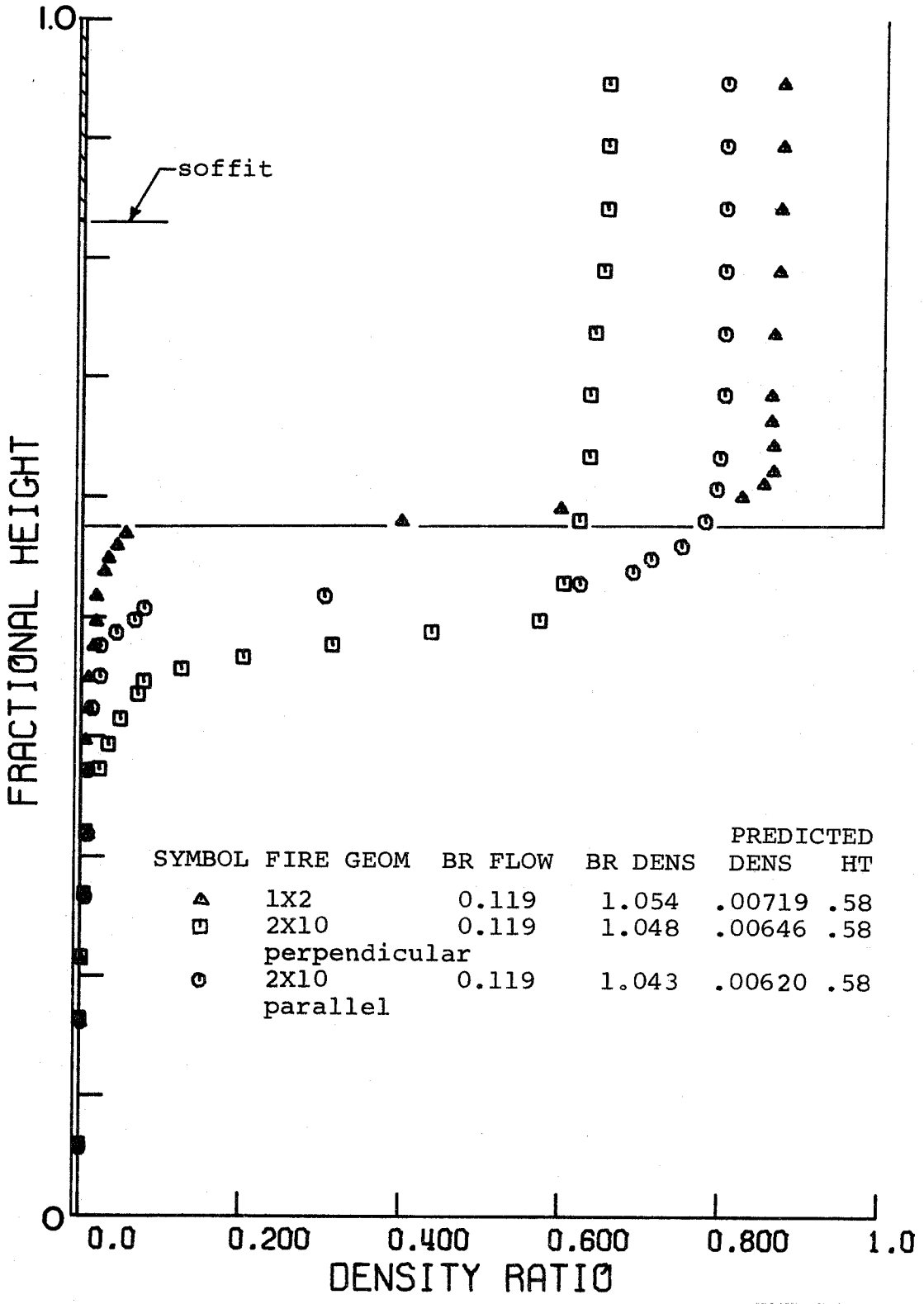

Figure 24 Effect of Fire Geometry

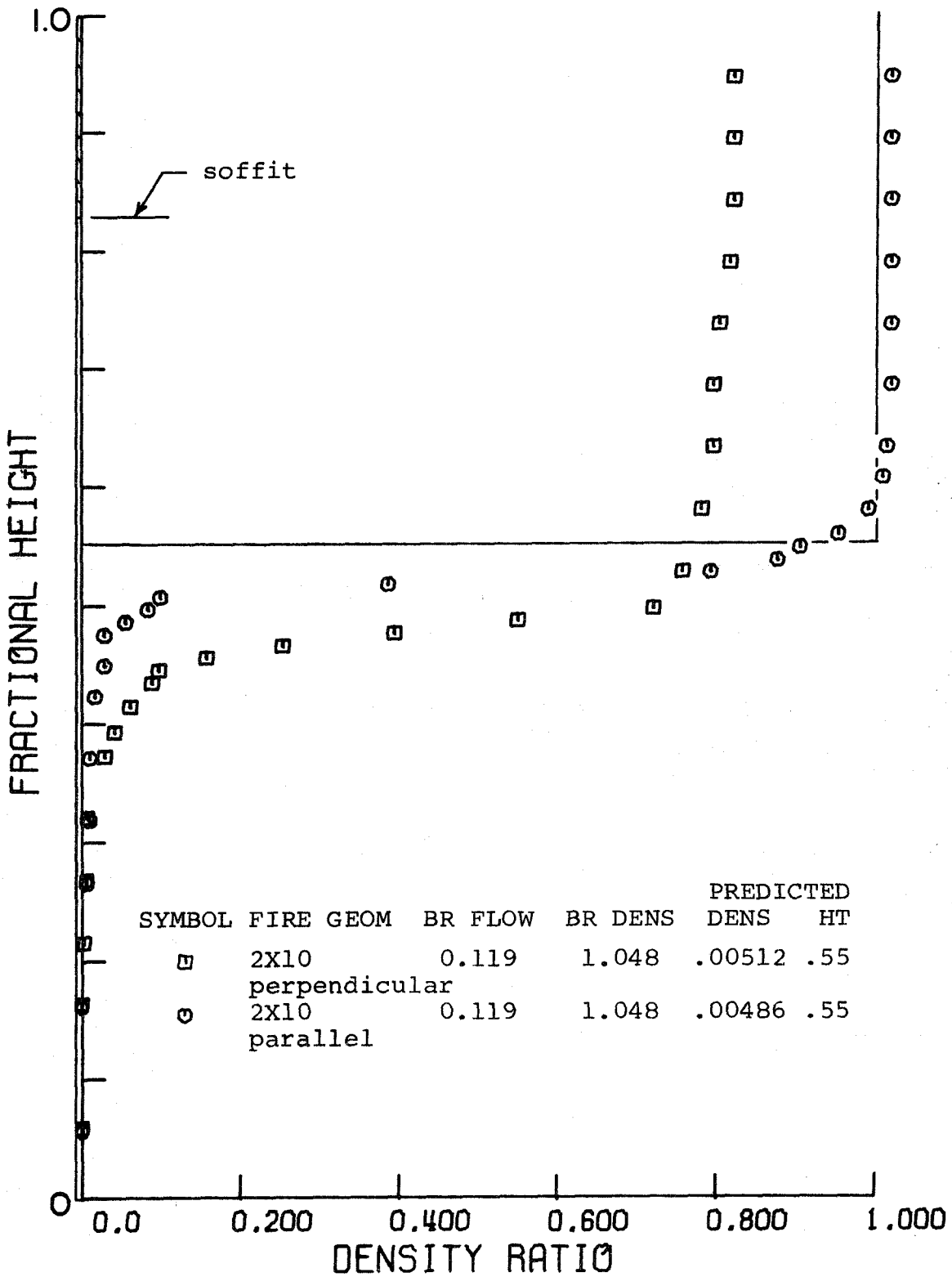

Figure 25 Effect of Rectangular Source Compared to Line Theory

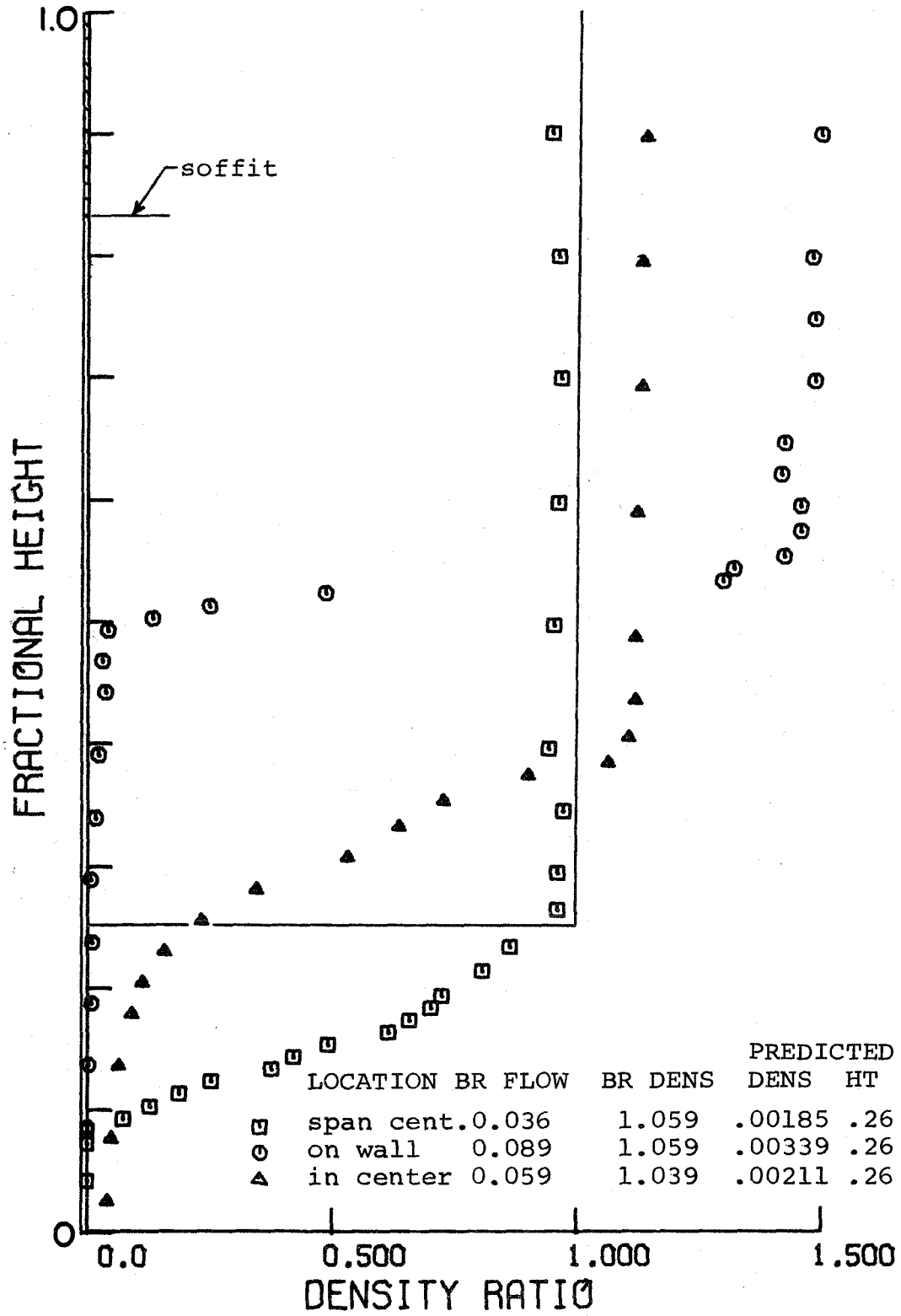

Figure 26 Line Fire

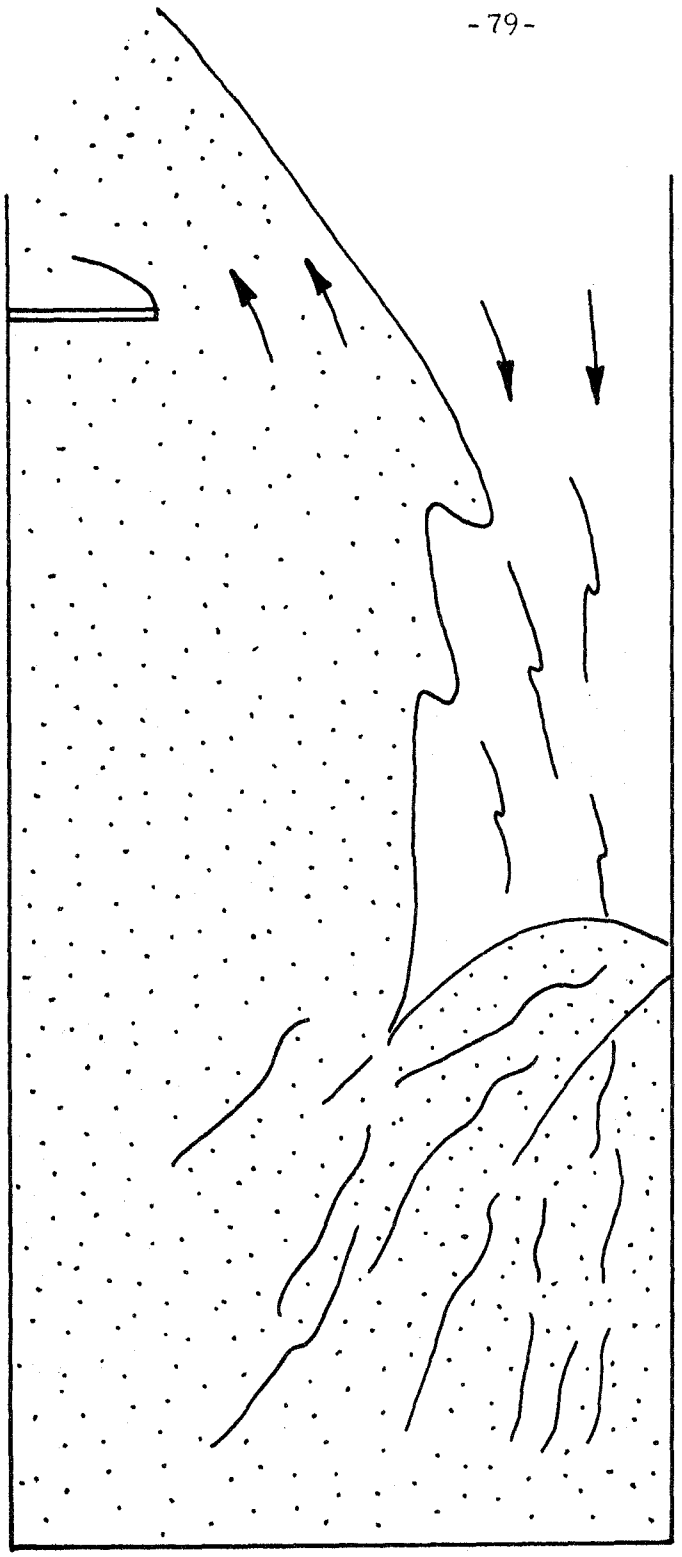

FIG. 27 LINE FIRE ACROSS CENTER OF ROOM

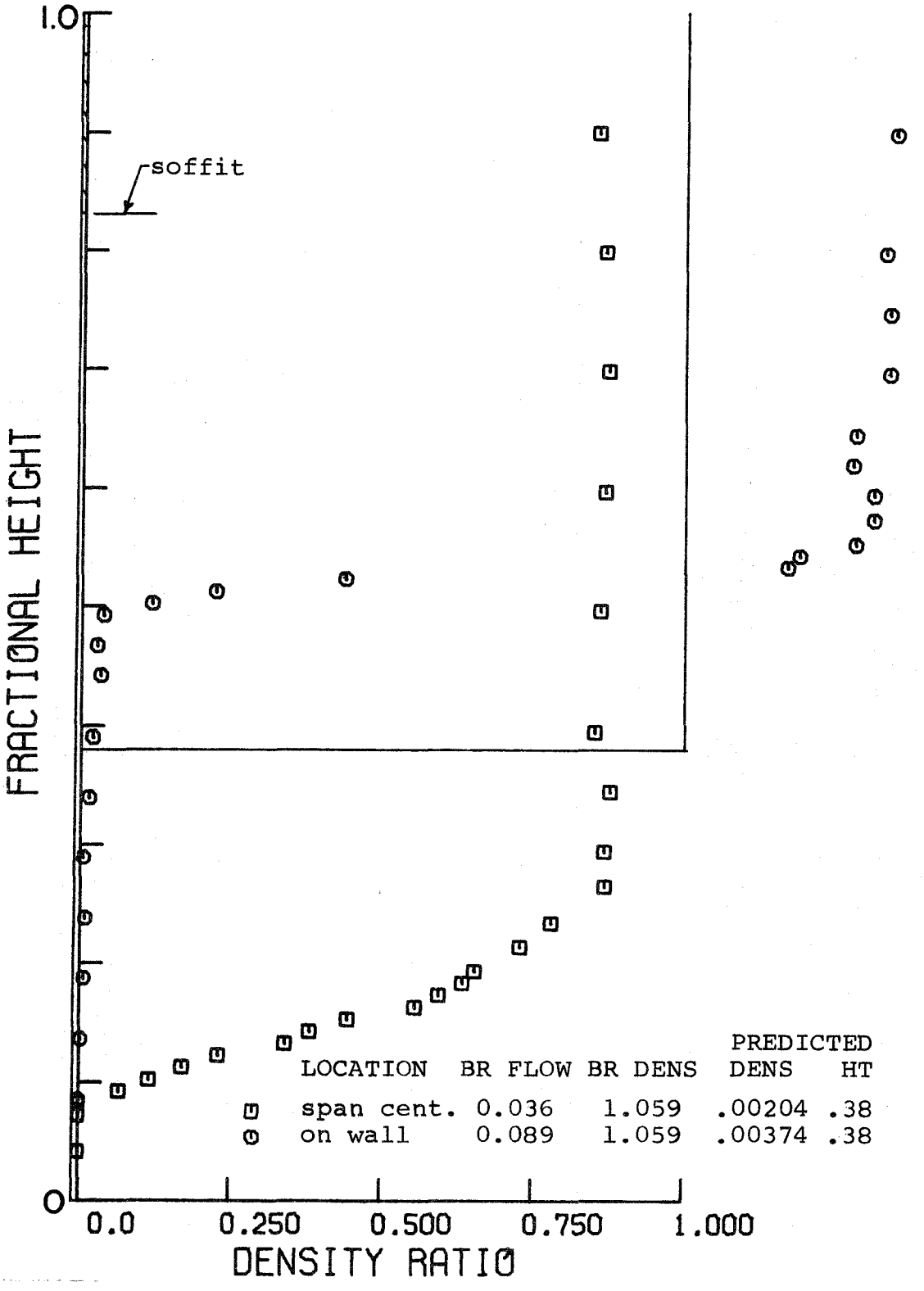

Figure 28 Line Fires Compared to Reflection Theory

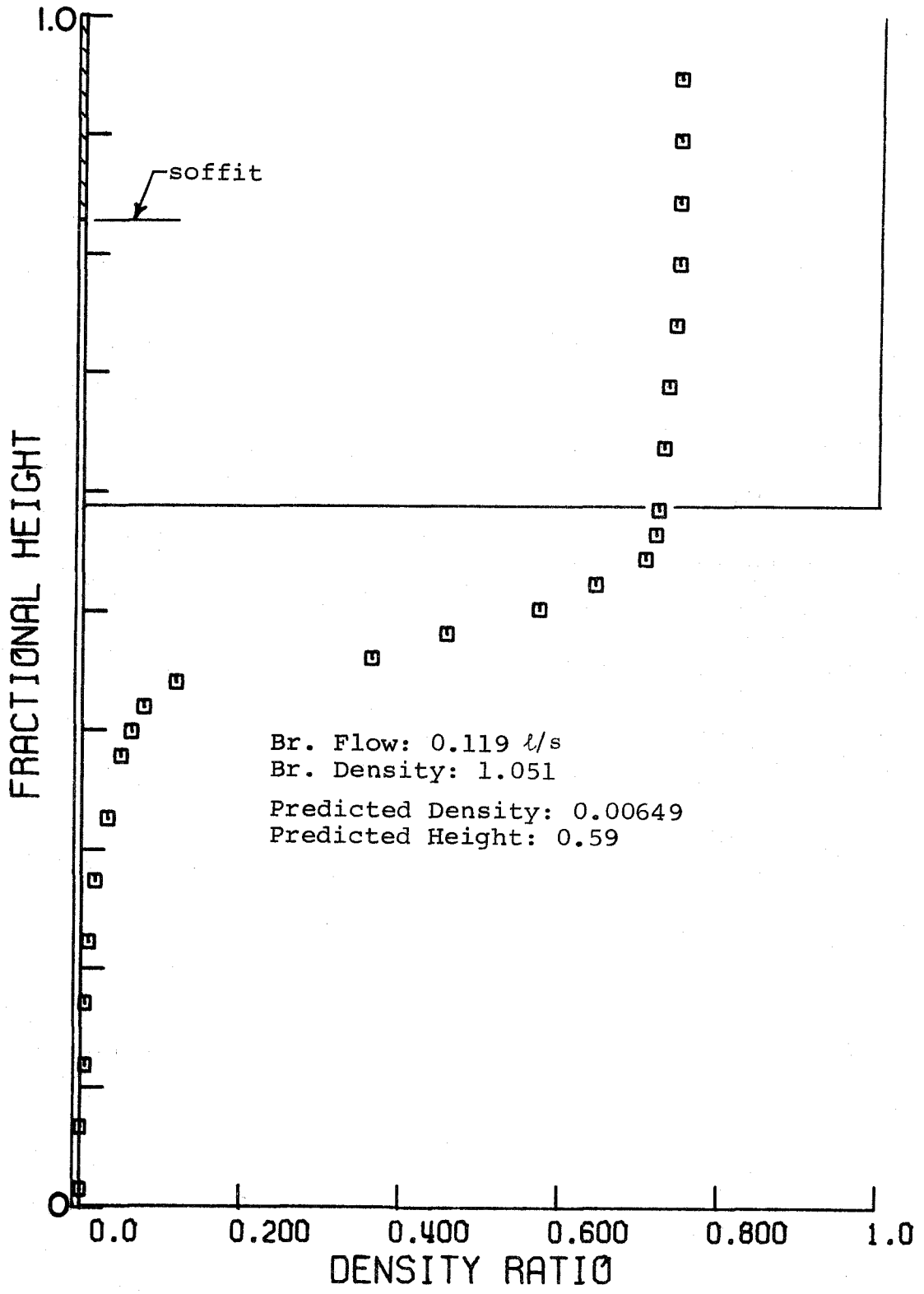

Figure 29 Distributed Source

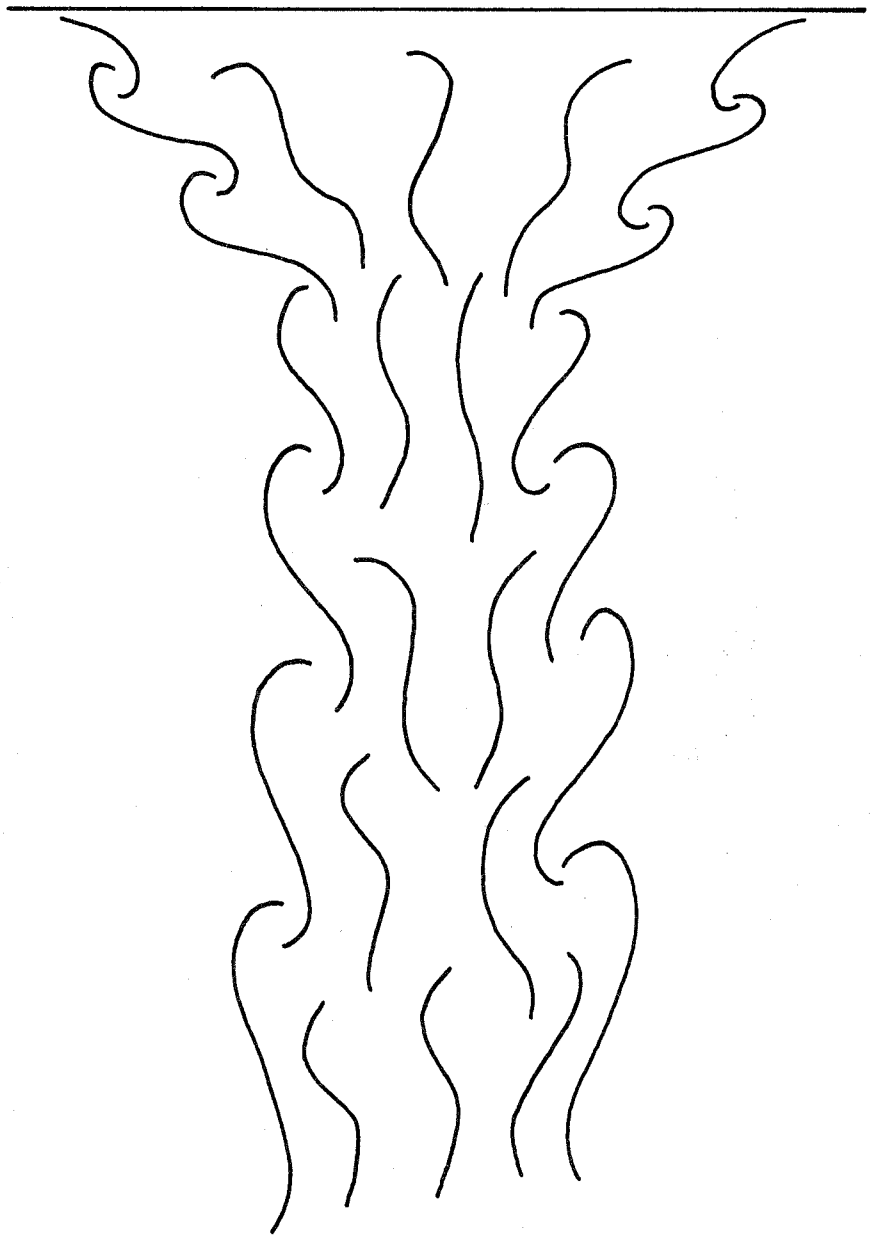

FIG. 30 DISTRIBUTED SOURCE PLUME

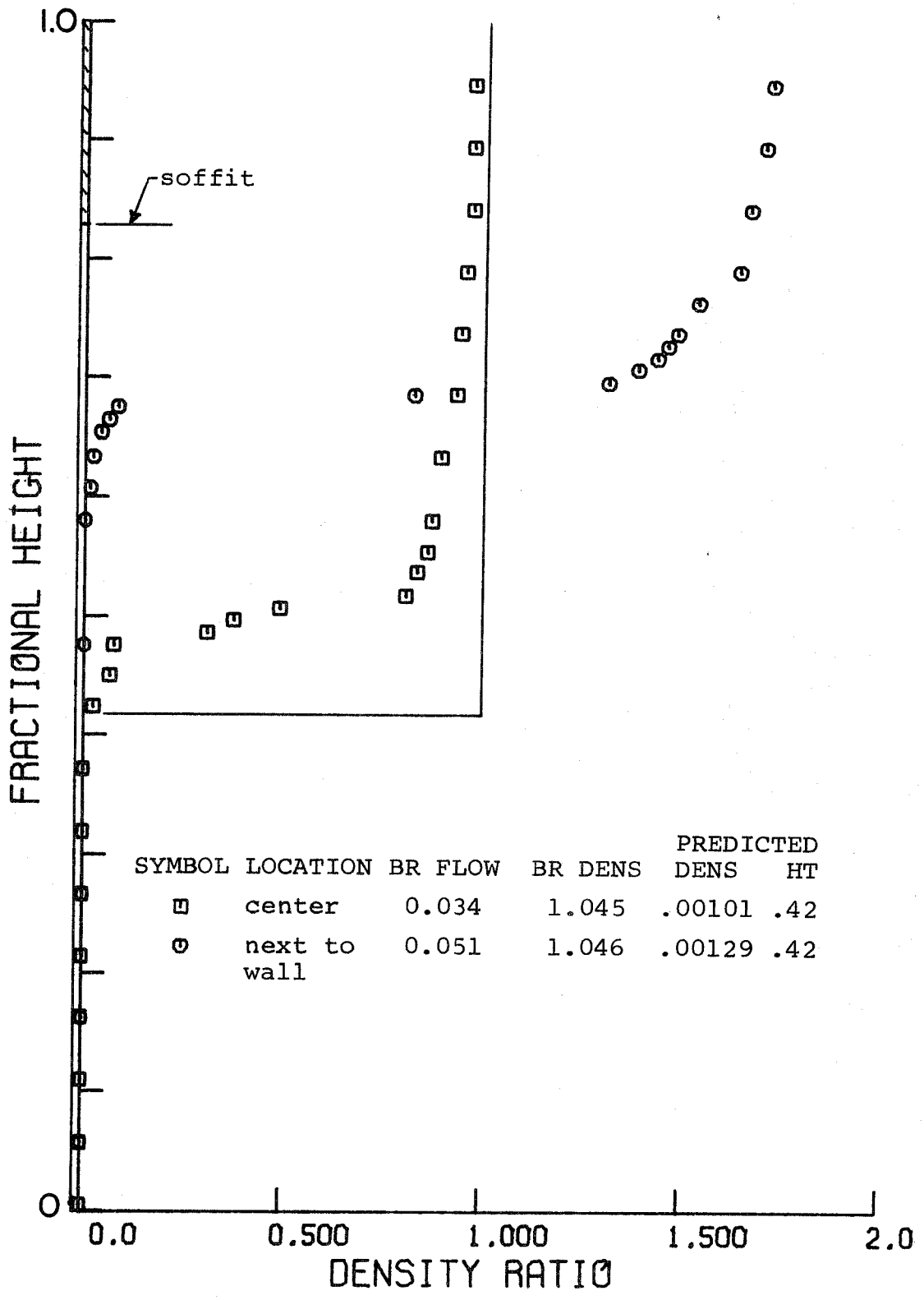

Figure 31 Two-Dimensional Standard Door

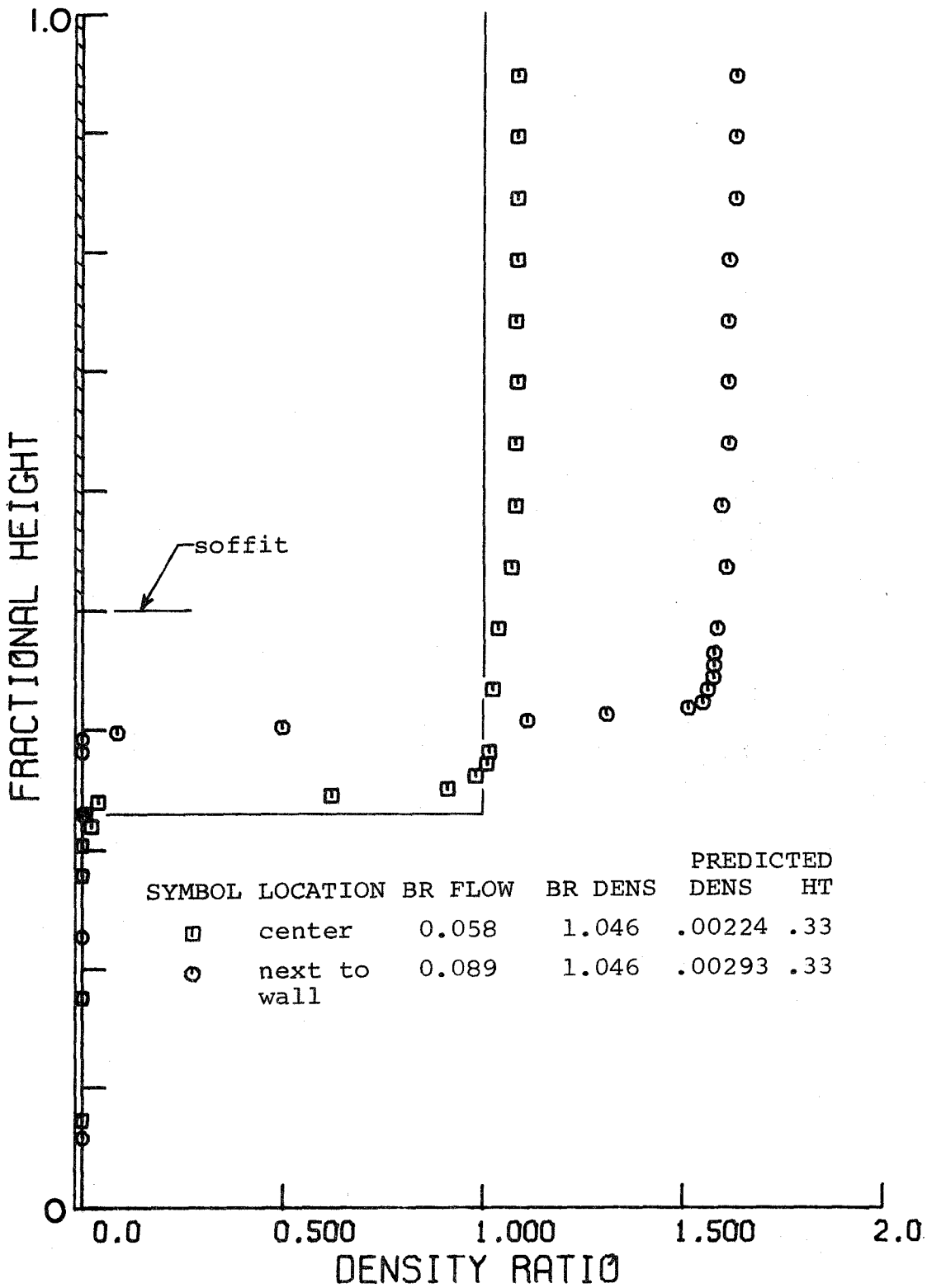

Figure 32 Two-Dimensional Low Door

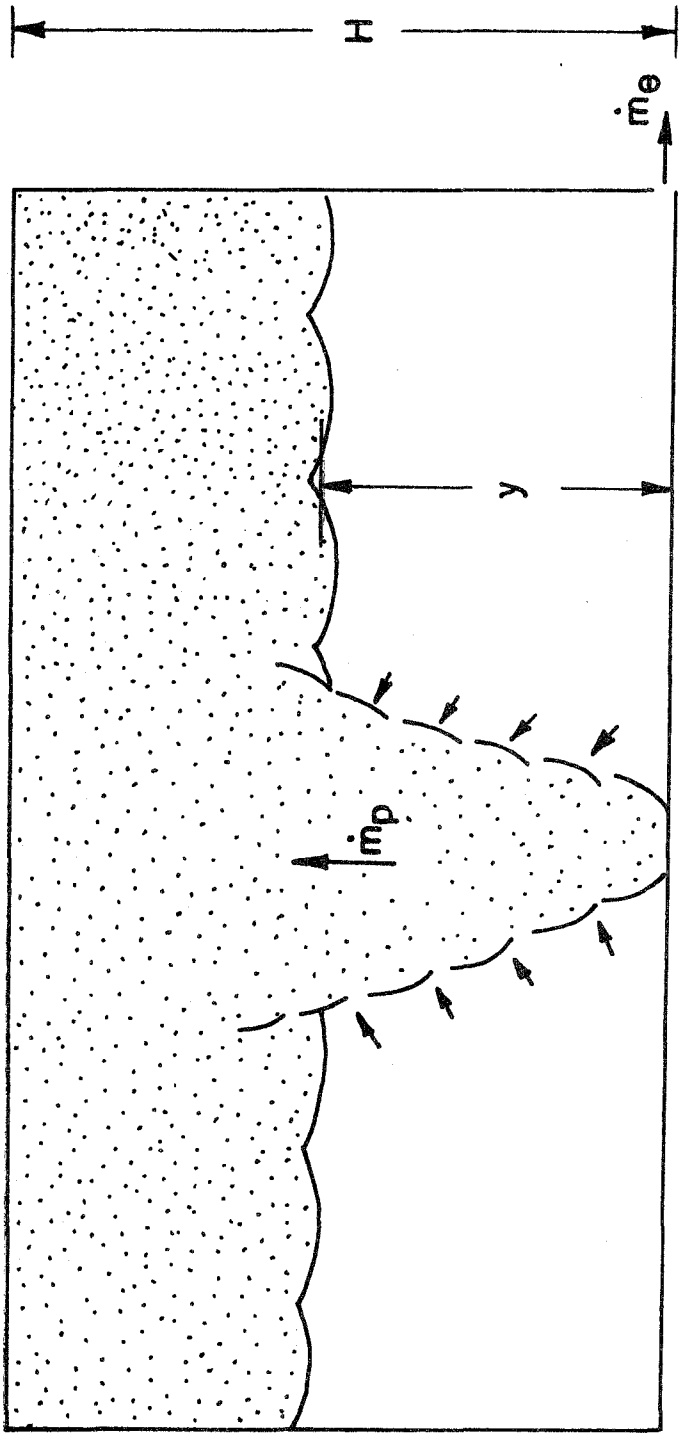

FIG. 33 CLOSED ROOM MODEL

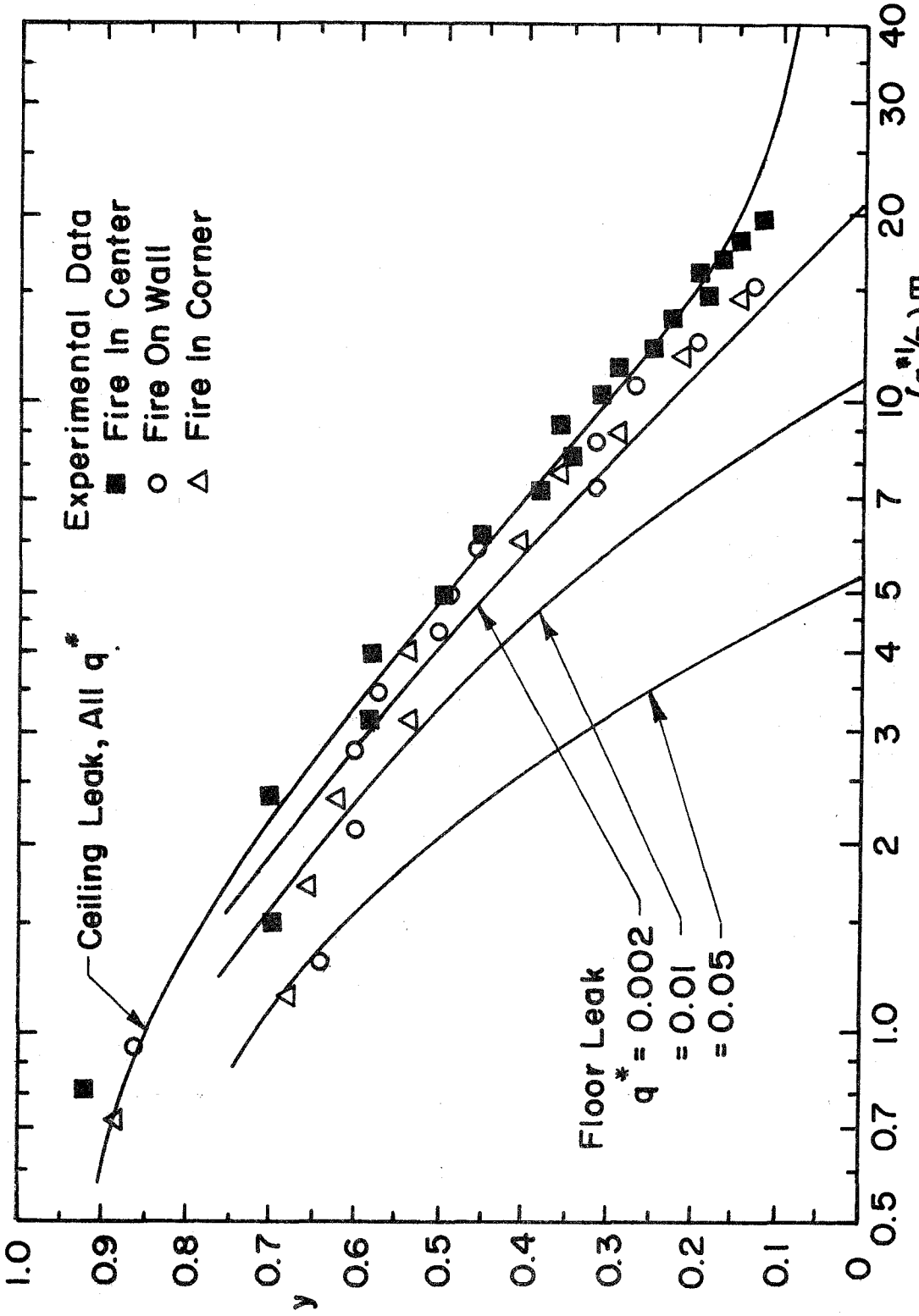

FIG. 34 DEPENDENCE OF y ON $(q^*_H)^{1/3}T$

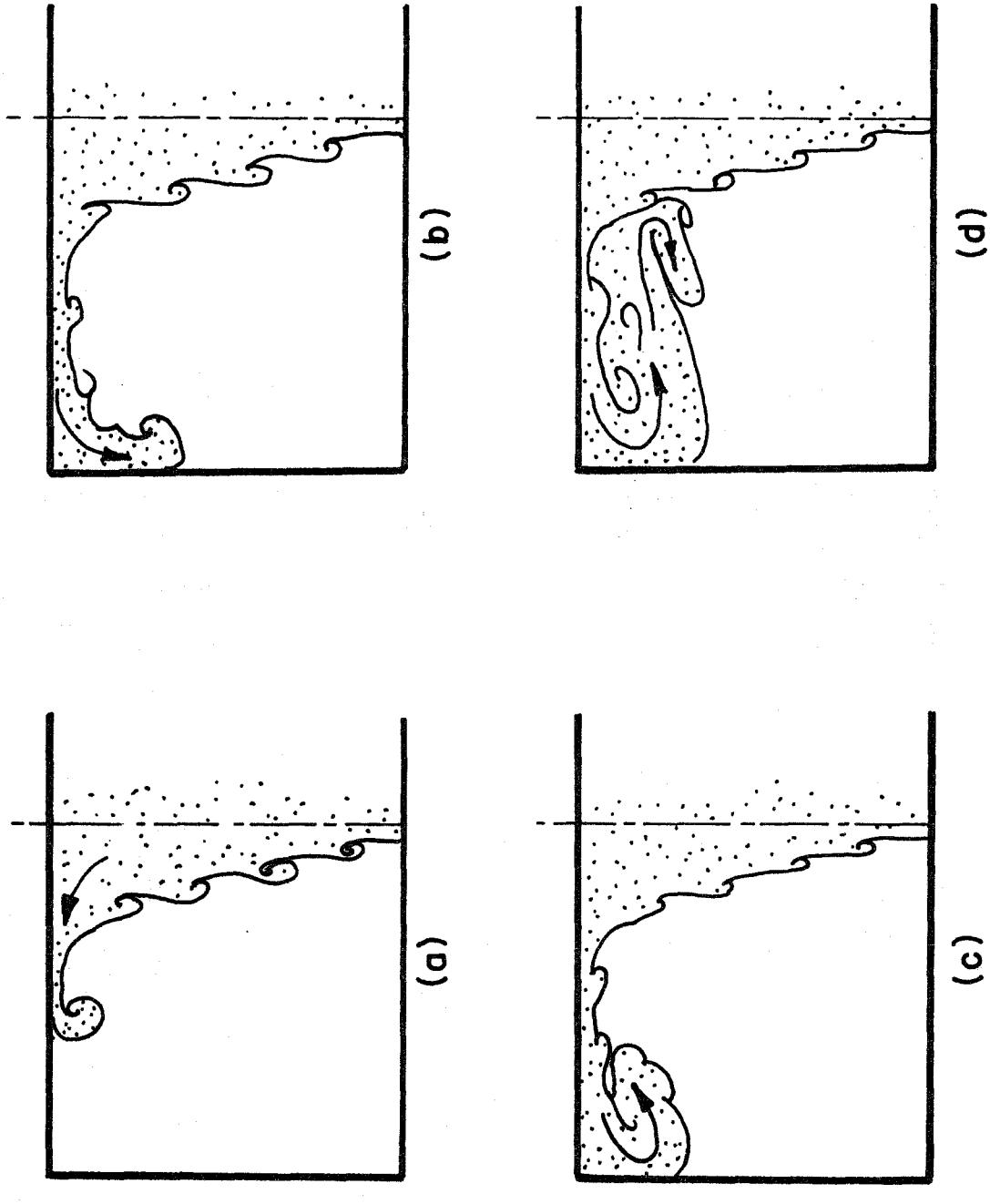

FIG. 35 STARTING TRANSIENT

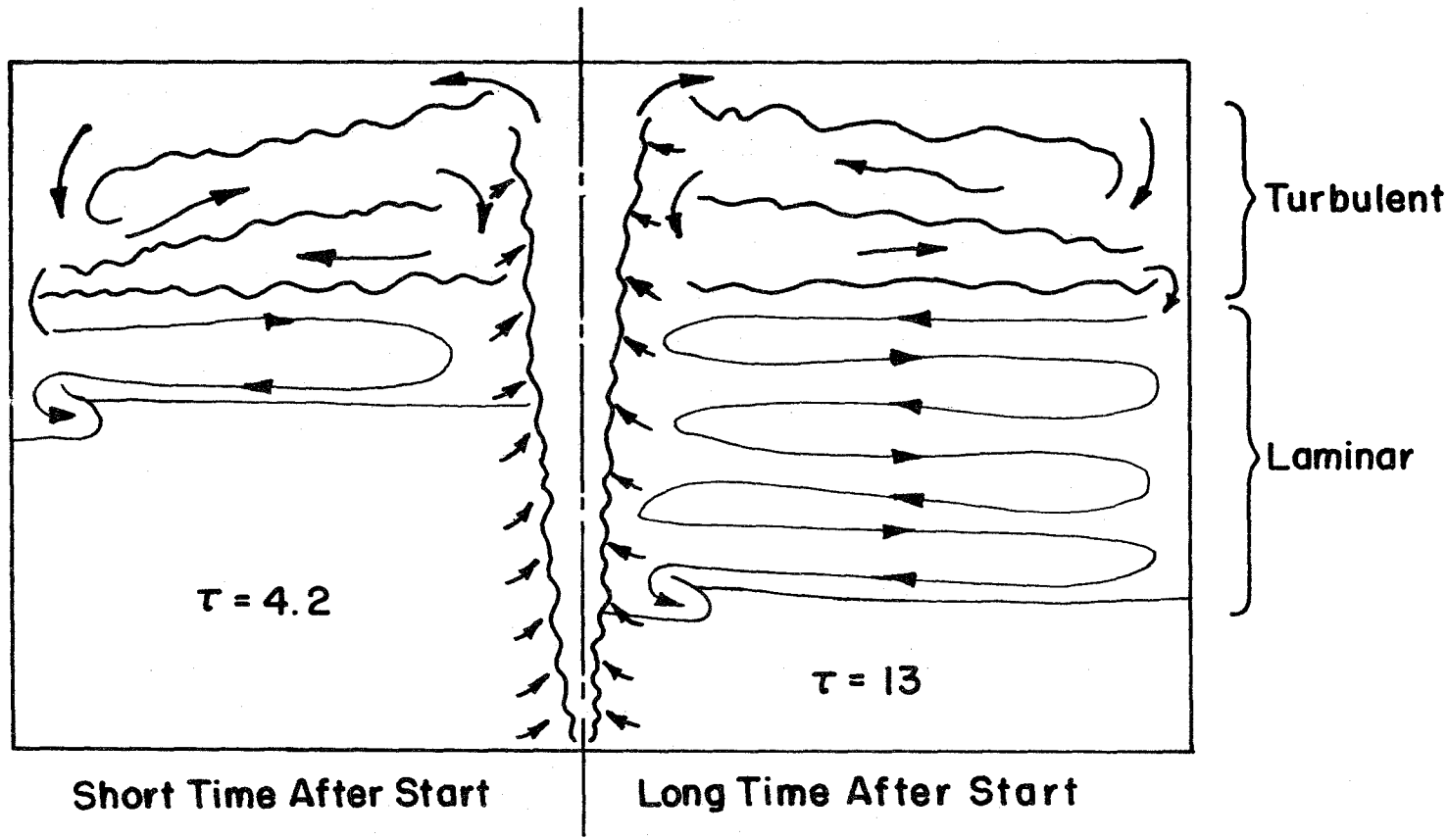

FIG. 36 FLOW FIELD IN CLOSED ROOM

Legend For Figures 37,39 and 41

Time; time in minutes

Density Ratio;

Symbol	Fractional Height From Bottom
□	0.10
○	0.20
△	0.30
+	0.40
×	0.50
◇	0.60
↑	0.70
X	0.80
Z	0.90

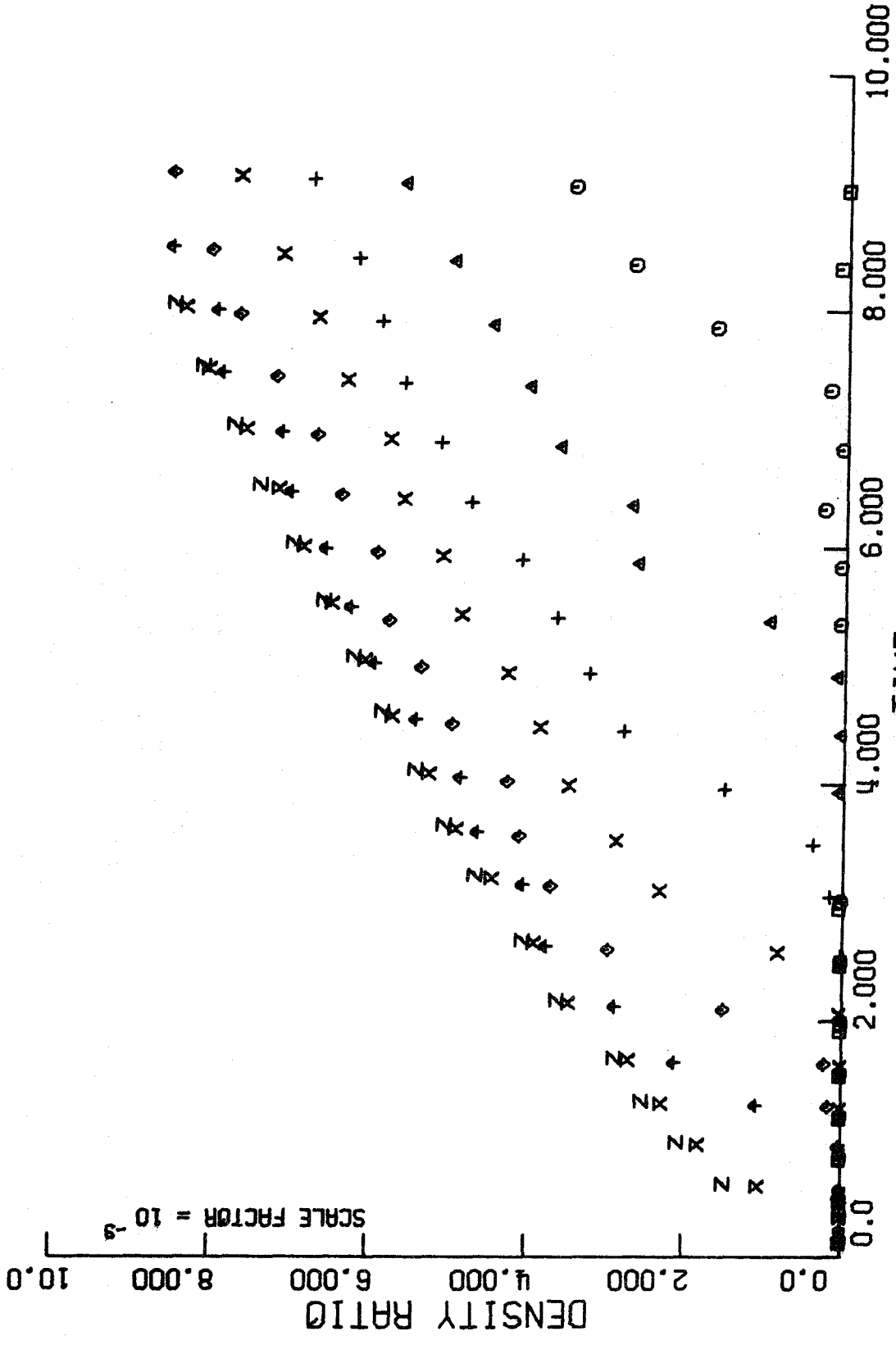

Figure 37 Density History for Center Fire in Closed Room

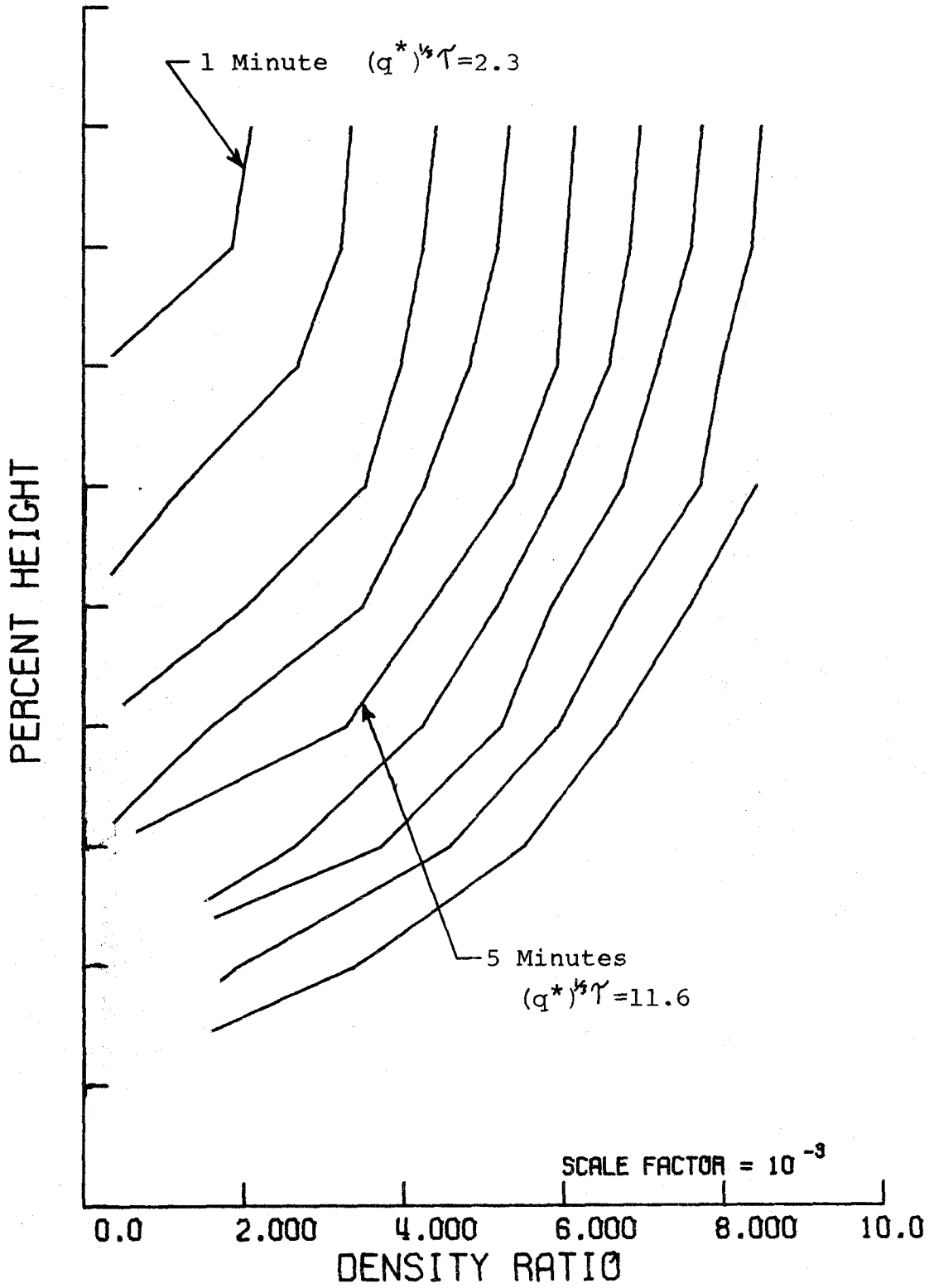

Figure 38 Density Profile for Center Plume in Closed Room

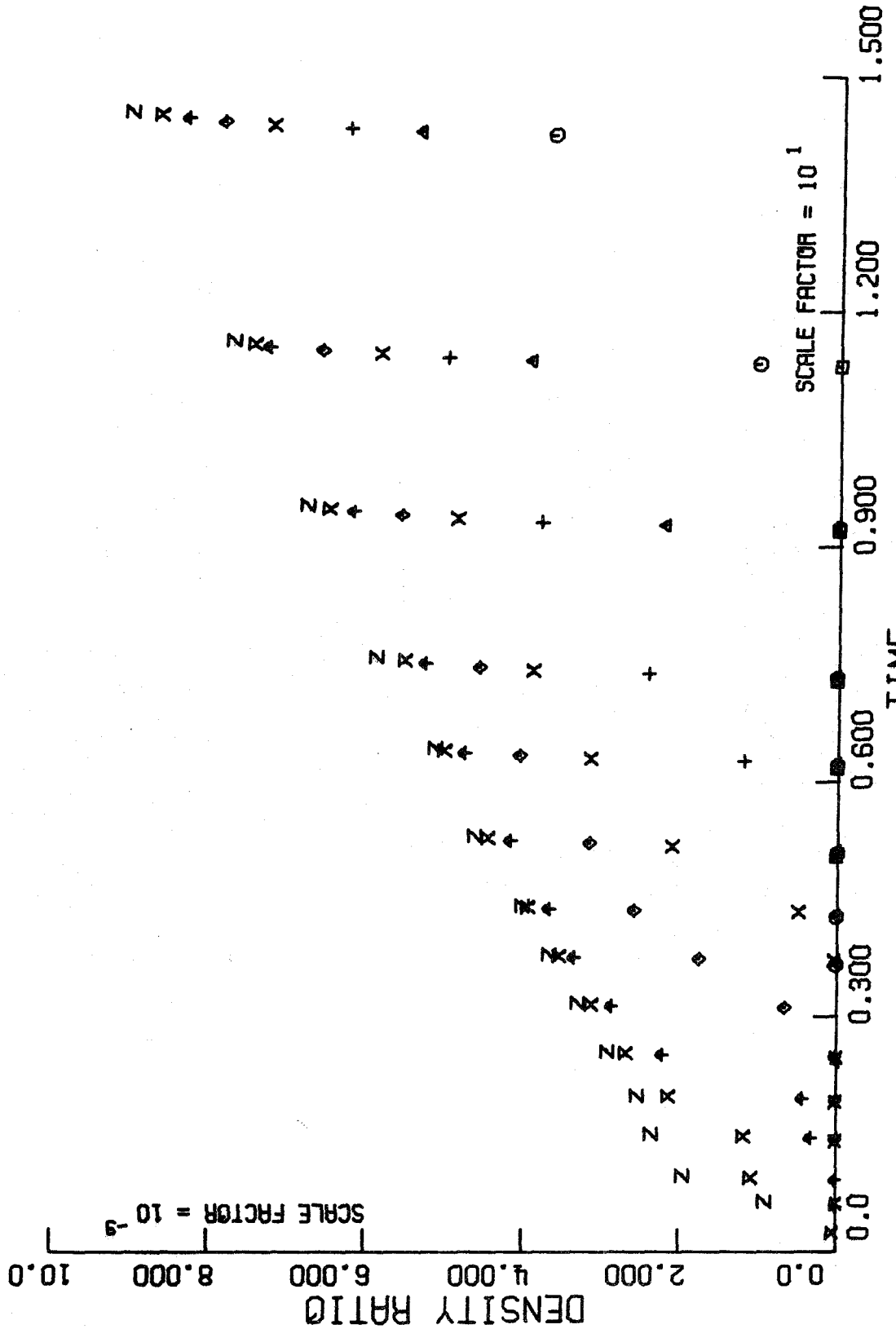

Figure 39 Density History for Wall Fire in Closed Room

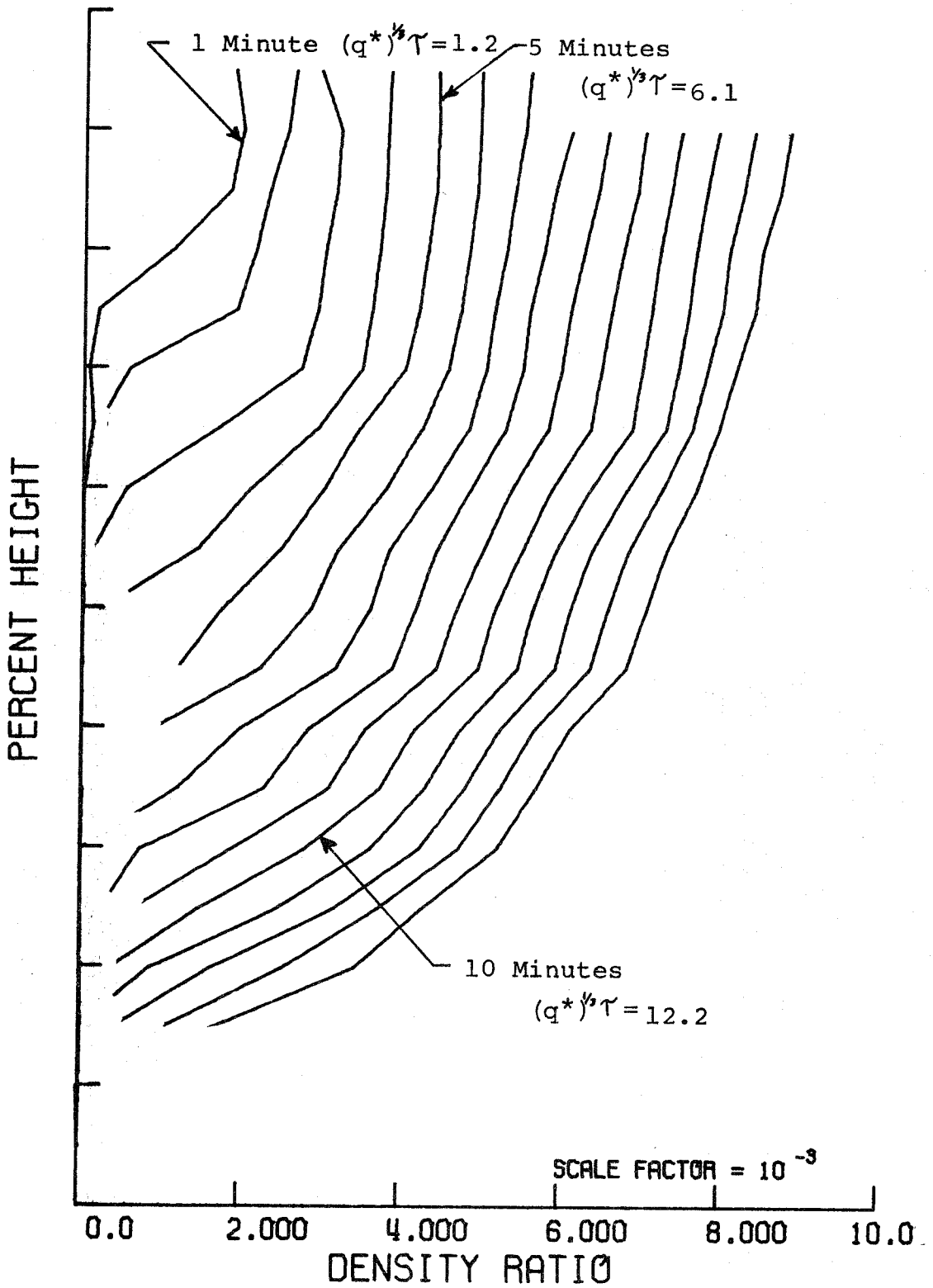

Figure 40 Density Profile for Wall Plume in Closed Room

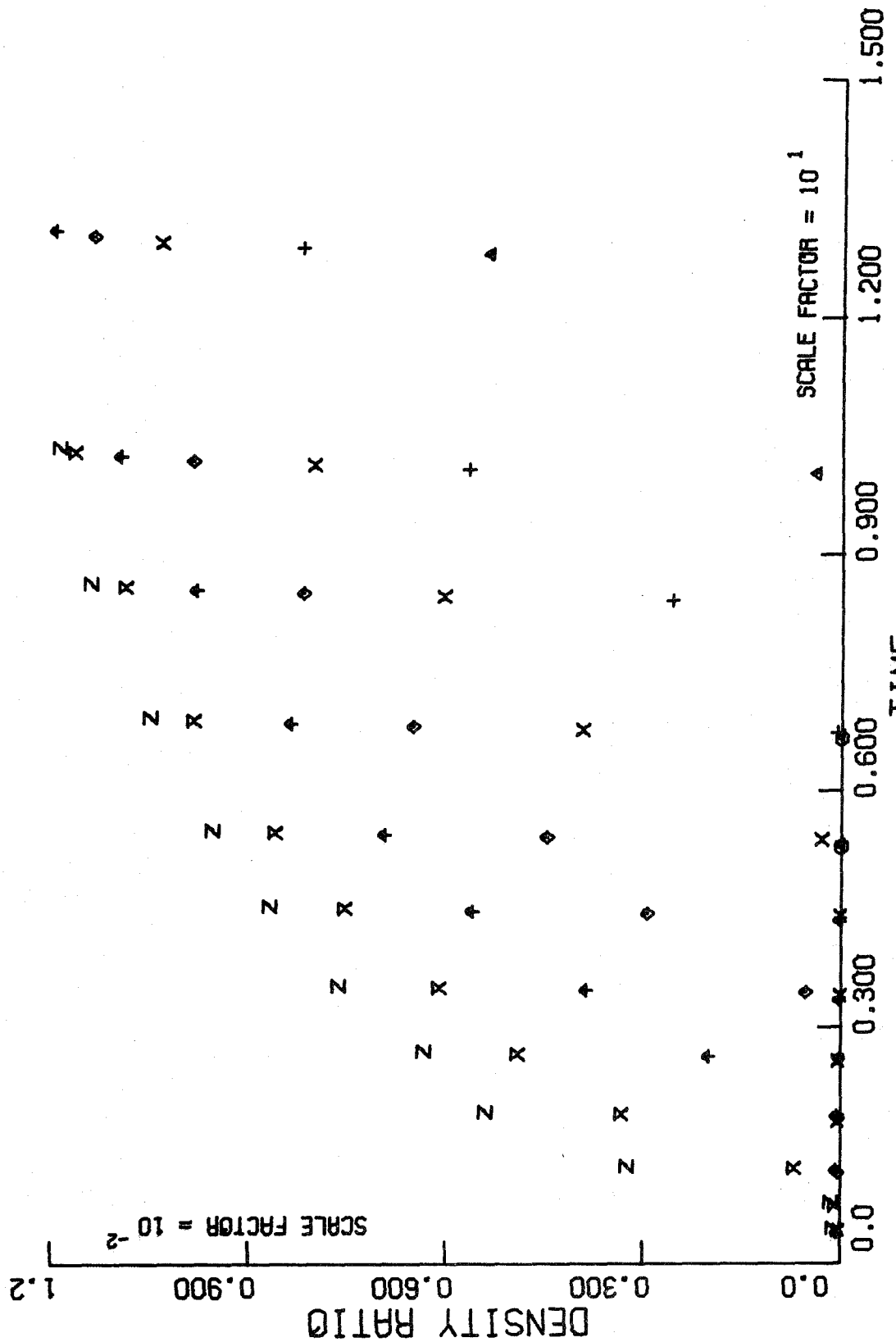

Figure 41 Density History for Corner Fire in Closed Room

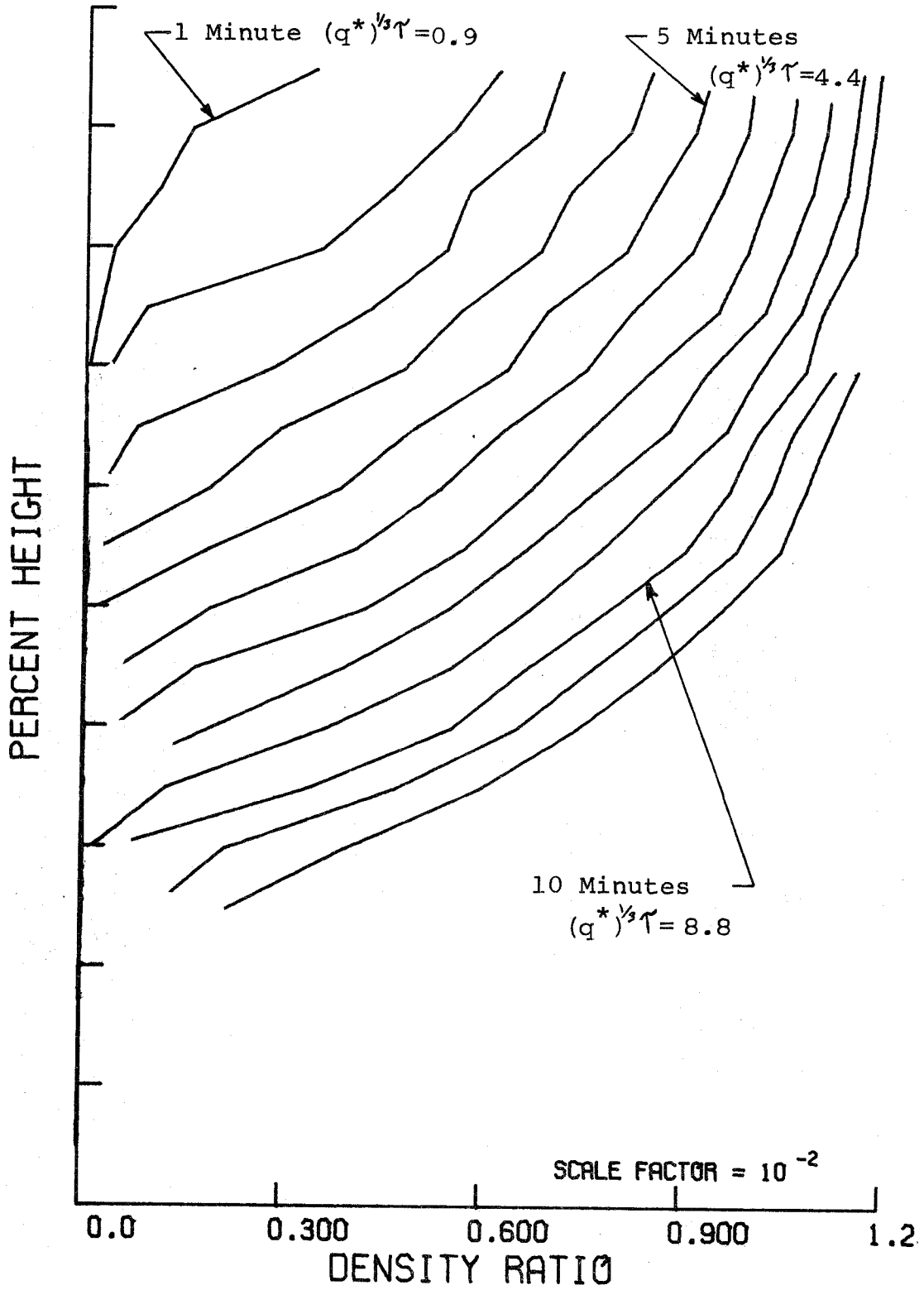

Figure 42 Density Profile for Corner Plume in Closed Room

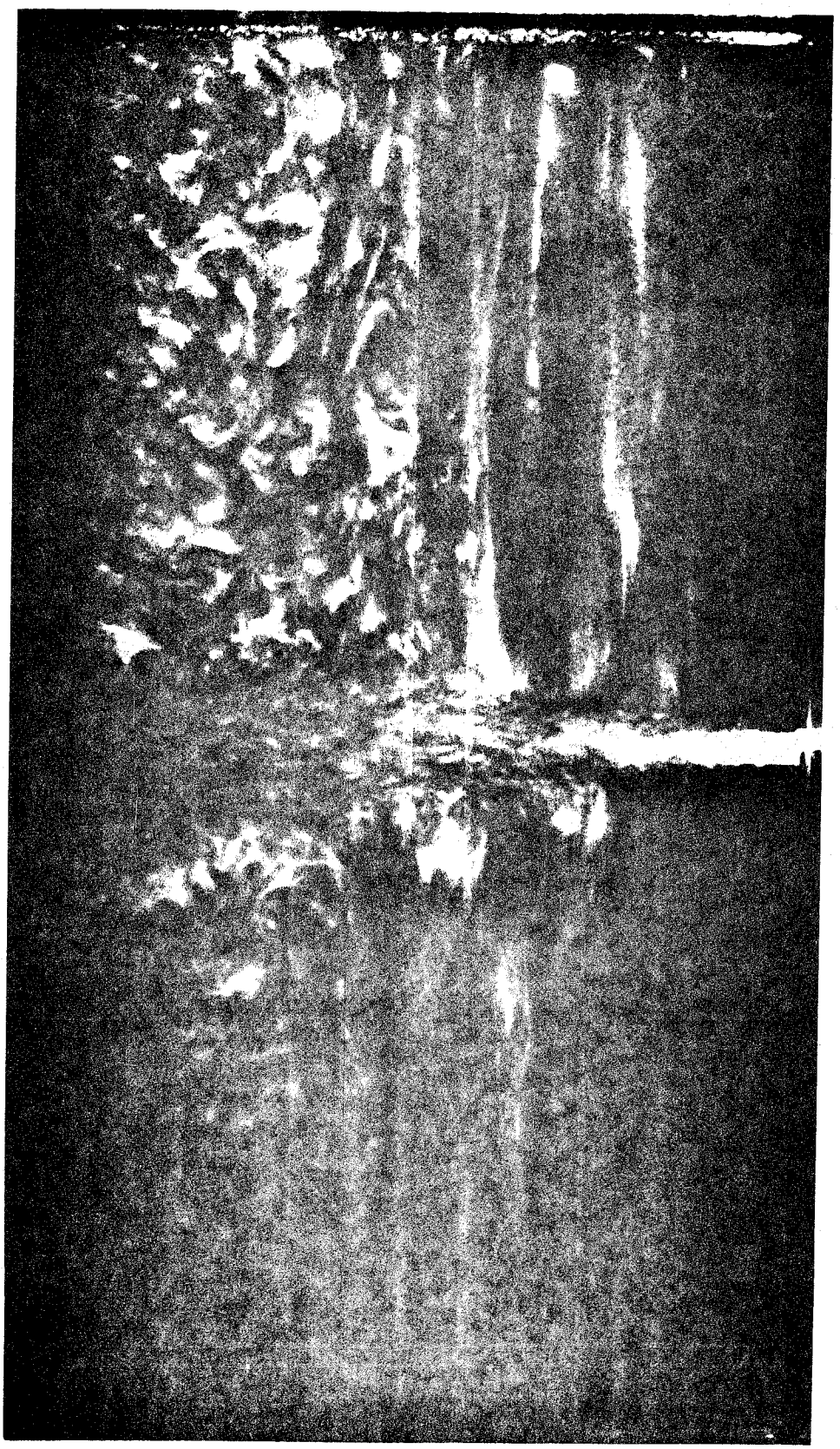

FIG. 43 CLOSED ROOM FLOW PHOTOGRAPH

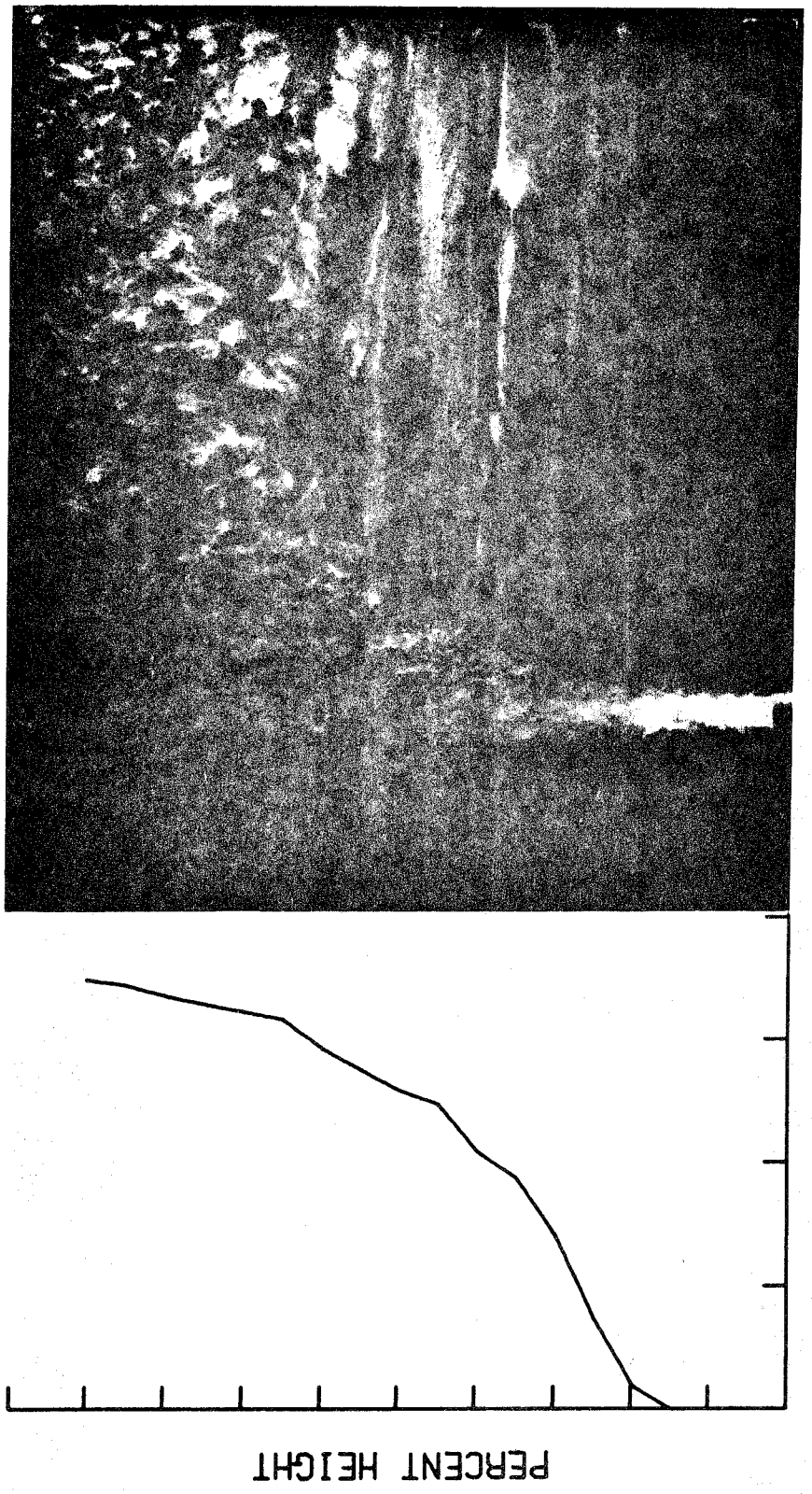

FIG.44 COMPARISON BETWEEN DENSITY PROFILE AND FLOW FIELD

APPENDIX A

Plume Properties and Mass Balance

The turbulent fire plume can be characterized by the following equations when density differences are small and when the elevation above the fire, Z, is large compared with the fire diameter:

$$\frac{\Delta T_m}{T_1} = \frac{\Delta \rho_m}{\rho_1} = C_T (q^*)^{2/3} \qquad C_T \approx 9.1 \qquad \text{(A1)}$$

$$\frac{w_m}{\sqrt{gZ}} = C_v (q^*)^{1/3} \qquad C_v \approx 3.8 \qquad \text{(A2)}$$

$$\frac{\ell_v}{Z} = C_\ell \qquad C_\ell = 1/8 \qquad \text{(A3)}$$

$$\frac{\ell_T}{T} = C_{\ell_t} \qquad \frac{C_{\ell_t}}{C_\ell} = 1.15 \qquad \text{(A4)}$$

and

$$\frac{\Delta T}{\Delta T_m} = \exp\{-(r/\ell_v)^2\},$$

$$\frac{w}{w_m} = \exp\{-(r/\ell_v)^2\}.$$

Here, ΔT_m and w_m are centerline temperature difference and velocity, and:

$$q^* = Q/(\rho_1 \sqrt{gZ}\, C_p T_1 Z^2) \qquad \text{(A5)}$$

is a dimensionless buoyancy parameter based on Q, which is the heat addition: $\Delta\rho \equiv (\rho_1 - \rho)$ is positive, and ℓ_v and ℓ_t are velocity and temperature scale lengths.

Given these approximations, we can show that the mass-averaged temperature and density in the plume are:

$$\frac{\overline{\Delta T}}{T_1} = \frac{\overline{\Delta \rho}}{\rho_1} = \frac{1}{\pi C_v C_\ell^2} (q^*)^{2/3} = \frac{Q}{\dot{m} C_p T_1} \tag{A6}$$

and mass flow in the plume at a height Z is:

$$\dot{m}_p = \rho_1 \, w_m \, \pi \, \ell_v^2 \tag{A7}$$

or

$$\dot{m}_p = \rho_1 \left(g \frac{\overline{\Delta \rho}}{\rho_1} \right)^{1/2} (\pi C_v C_\ell^2)^{3/2} (Z)^{5/2} \tag{A8}$$

In (A8), $(\overline{\Delta \rho}/\rho_1)$ was used to replace q^* (which enters through w_m via equation (7b) by use of equation (A6) and $\overline{\Delta \rho}$ is evaluated at Z.

APPENDIX B, LIST OF EXPERIMENTS

Experiment No.	Flow Rate (flow meter)	Source	Significant Geometry
1	8	2" pipe	
2	8	"	
3	16	"	
4	32	"	
5	64	"	
6	16	"	Short Door
7	16	"	
8	16	"	
9	16	"	
10	64	"	
11	8	"	
12	16	"	
13	8	"	
14	32	"	
15	64	"	
16	32	"	
17	32	"	
18	16	"	Denser Brine 1.1
19	32	"	Narrow Door 10 cm
20	32	"	" " 18.5 cm
21	32	"	" " 10 cm
22	32	"	Fire in Corner
23	32	"	Window 27 x 21 cm
24	32	"	Window 27 x 15 cm
25	32	"	Window 27 x 27 cm
26	32	"	
27	16	"	
28	16	"	
29	16	"	Window 18.9 x 29 cm
30	16	"	Window 18.9 x 16.4 cm
31	16	"	
32	16	"	Fire Near Door
33	16	"	Fire Near Door
34	16	"	Fire in Center
35	16	"	Fire in Corner
36	16	"	Fire Off Center
37	16	"	
38	32	"	Fire Near Door
39	32	"	Fire in Center
40	32	"	Fire in Center
41	32	"	
42	32	"	
43	24	"	Fire on Back Wall
44	32	"	Near Door Off Center

Experiment No.	Flow Rate (flow meter)	Source	Significant Geometry
45	24	"	Fire on Side Wall
46	24	"	Fire in Corner
47	24	"	Fire in Corner
48	32	2" Axisym.	
49	32	10 x 2 cm	Fire Perpendicular to Door Jet
50	32	10 x 2 cm	Fire Parallel to Door Jet
51	24	2 Axisym.	Transient Test
52	32	"	Door Open 30"
53	16	Line	Fire Across Center
54	16	Line	Fire Against Wall
55	32	6.4 x 3.2 cm.	
56	10	Line	Fire Across Center
57	24	Line	Fire Against Wall
58	8	1" Axisym.	
59	16	"	
60	32	"	
61	16	Line	Fire in Center
62	32	2" Axisym.	Fire 1/4 Way Down
63	16	"	Fire 1/4 Way Down
64	16	"	Fire 1/2 Way Down
65	16	1" Axisym.	Fire 1/2 Way Down
66	32	Perforated	
67	32	"	
68	16	1" Axisym.	Fire 1/2 Way Down
69	10	Line	2-D Room, Fire in Center
70	14	Line	2-D Room, Fire on Wall
71	16	Line	2-D Room, Short Door Fire in Center
72	24	Line	2-D Room, Short Door Fire on Wall
73	24	2" Pipe	Fire in Corner
74	32	2" Axisym.	Window 19 x 19 cm

Note: Expts. 1-25 were done in 130 x 108 room
Expts. 25-74 were done in 100 x 50 room

Flow meter calibration
8 - .02838 1/s
16 - .05863
32 - .1191
64 - .2382